BIOLOGICAL LIMITATIONS OF *SHEWANELLA ONEIDENSIS* MR-1 IN BIOELECTROCHEMICAL SYSTEMS

A Dissertation

Presented to the Faculty of the Graduate School

of Cornell University

In Partial Fulfillment of the Requirements for the Degree of

Doctor of Philosophy

by

Michaela Anne TerAvest

January 2014

BIOLOGICAL LIMITATIONS OF *SHEWANELLA ONEIDENSIS* MR-1 IN BIOELECTROCHEMICAL SYSTEMS

Michaela Anne TerAvest, Ph. D.

Cornell University 2014

Shewanella oneidensis MR-1 is a model microbe for use in bioelectrochemical systems (BESs) for several reasons, including its ability to produce electric current in the presence of oxygen and its use of endogenous electron shuttles for electron transfer. I performed in-depth studies on the growth and physiology of *S. oneidensis* to gain insight into BES performance with this microbe. In the first study, I analyzed changes in current production when oxygen was added to batch- and continuously-fed BESs with *S. oneidensis*. These experiments revealed that oxygen is more beneficial under continuously-fed conditions because it allows *S. oneidensis* to grow and produce flavins at a faster rate, and therefore decreases flavin washout. In the second study I optimized poised electrode potentials, because previous research suggested that electrodes poised at oxidizing potentials may cause a stress response in *S. oneidensis*. I grew *S. oneidensis* in continuously-fed BESs with potentiostatically poised electrodes at 5 different redox potentials and concluded that oxidizing electrode potentials do not cause a general stress response, but decrease current production by direct damage of biofilm cells at the electrode surface. In the third study, I compared the transcriptomes of *S. oneidensis* grown in a wide variety of conditions and used machine learning to discover genes important to anode- and iron-respiration in this organism. This meta-analysis revealed that some putative members of the electron transport chain, including an NADH dehydrogenase and a cytochrome oxidase, were important under anode- or Fe(III)-respiring conditions. Knockouts strains with these genes deleted confirmed their role in the anaerobic electron transport chain of *S. oneidensis*. Future work is needed to

better characterize the efficiency of the anaerobic electron transport chain in *S. oneidensis*. The overall finding of this work is that *S. oneidensis* is not appropriate for use in BES applications that require strict anaerobic conditions or quick exchange of medium (e.g., wastewater treatment), because it performs better when mediators and planktonic cells are not washed out of the system.

BIOGRAPHICAL SKETCH

Michaela TerAvest earned a B.S. in Biochemistry and Molecular Biology from Michigan State University in 2008 and began her Ph.D. studies in Biological and Environmental Engineering at Cornell University in 2009. During her study, she worked as a research assistant with Dr. Lars Angenent for 7 semesters and 4 summers, and as a teaching assistant in the department of Biological and Environmental Engineering for 1 semester. While pursuing her Ph.D. she received an Environmental Policy Fellowship from the Council of Women World Leaders and spent 3 months in Reykjavik, Iceland working with the Icelandic Ministry for the Environment. She also received the Cornell Provost's Diversity Fellowship. After graduation from Cornell University she will begin work as a postdoctoral researcher with Dr. Caroline Ajo-Franklin at the Lawrence Berkeley National Lab in Berkeley, CA.

I dedicate this dissertation to my husband, Andrew Myers, and to my family. Their unwavering support is the key to my confidence and success.

ACKNOWLEDGEMENTS

I thank my advisor, Dr. Lars Angenent for supporting my work, teaching me perseverance in research, and encouraging me to develop my writing skills. I also thank my special committee members, Dr. James Shapleigh, and Dr. Larry Walker for their support. All of the work described here was funded by the National Science Foundation through CAREER grant no. 0939882. Finally, I thank all members of the Angenent lab past and present for the knowledge, experience, and camaraderie that they have shared with me, especially, Dr. Miriam Rosenbaum, Dr. Matt Agler, Elliot Friedman, Dr. Zhongjian (Jimmy) Li, Devin Doud, Dr. Marianna Villano, Dr. Nina Hospodsky, Drs. Hanno and Lubna Richter, Juan Guzman, and Catherine Spirito.

TABLE OF CONTENTS

LIST OF FIGURES

LIST OF TABLES

CHAPTER 1

INTRODUCTRION: CENTRAL AIM AND SUMMARY OF EXPERIMENTS

1.1 Central aim

The study of bioelectrochemical systems (BESs) is an important research area because of possible applications in biosensing, biocomputing, bioenergy, and research on biogeochemical cycling in anaerobic sediments. *Shewanella oneidensis* MR-1 is a key model microbe for BESs because it engages in extracellular electron transfer (EET) by two major pathways; direct electron transfer (DET) and mediated electron transfer (MET). Other BES model microbes use only one of these mechanisms because they lack the ability to produce soluble electron shuttles or lack the machinery to transport electrons directly to solid surfaces. This is possible for *S. oneidensis* because it expresses outer membrane *c*-type cytochromes, which allow it to transfer electrons directly to the electrode, and it also secretes flavins into the culture medium, which act as electron shuttles to transport electrons from cells to the electrode. The use of both of these pathways is interesting because it better approximates mixed-culture BESs, which are important for waste treatment applications and environmental research. To date, *S. oneidensis* is the only BES model microbe that allows detailed investigation of the interplay of these two pathways in a pure-culture system. It is also a facultative aerobe, which allows study of the effects of oxygen on BES anodes. This is an important consideration because maintenance of anaerobic conditions can be difficult, especially in microbial fuel cells with oxygen based cathodes. Because of its importance as a model microbe, my work focused on investigating the biological limitations of *S. oneidensis* in BESs using engineering, molecular biology, and bioinformatics techniques. I investigated microbial limitations of electric current generation in BES anodes, specifically

regulation of EET mechanisms by oxygen, the possibility of increased protein turnover and a stress response caused by electrode respiration, and mined previously collected transcriptomic data to identify genes with supporting roles in extracellular respiration. Identification of these limitations will inform improvement of BESs that could be achieved through genetic modification of organisms, or by altering system parameters to reduce microbial stress and improve EET processes. Other implications of my research include improved understanding of EET processes in subsurface environments and development of bioinformatics approaches for analysis of BESs.

1.2 Introduction

This dissertation describes previous work on BESs and *S. oneidensis* and new work performed to further understanding of the limitations to current production by this microbe. Chapter 2 is a literature review introducing previous work on bioelectrochemical systems and *S. oneidensis*, with a focus on molecular biology and bioinformatics techniques. Chapters 3, 4 and 5 describe the three aims of my dissertation work, and experiments performed toward those aims. Chapter 3 describes experiments to determine the mechanism by which oxygen enhances current production by *S. oneidensis*. I used a 2 x 2 x 2 experimental design varying the feeding regime (batch or continuous), oxygen addition (present or absent), and strain used (wild-type or flavin deficient mutant). Chapter 4 describes experiments performed to determine whether electrode respiration induces a transcriptional stress response in *S. oneidensis*. I grew *S. oneidensis* at potentiostatically poised electrodes that were set at 5 different potentials, and found moderate potentials to be optimal for performance, and that higher potentials directly damage outer membrane cytochromes. Chapter 5 describes meta-analysis of transcriptomic data for *S. oneidensis* for discovery of genes that support extracellular respiration. I confirmed

bioinformatic findings from this analysis by observing the phenotypes of gene deletion strains. Appendices 1 and 2, and 3 contain supplementary information for chapters 3, 4, and 5, respectively. Appendix 4 is a related publication describing transcriptomic comparison of *Bacteroides thetaiotaomicron* biofilms and planktonic cells. The analysis used was similar to that used in chapter 5. Appendix 5 includes experimental protocols used in this work.

1.3 Summary of experiments

Aim 1: Determine the mechanism of enhancement in current production by *S. oneidensis* MR-1 in response to oxygen.

- *S. oneidensis* MR-1 was grown in batch- and continuously-fed BESs with and without addition of oxygen.
- Current production, coulombic efficiency, cell density, pH, biofilm formation, and heme content of the cells were measured. Cyclic voltammetry analysis was used to differentiate between DET and MET.
- The same experiments were performed with a strain of *S. oneidensis* incapable of excreting electron shuttles (Δ*bfe*).

Aim 2. Determine whether potentiostatically-poised electrodes induce damage or stress in *S. oneidensis* cells.

- *S. oneidensis* MR-1 was grown in continuously-fed BESs with graphite electrodes that were potentiostatically poised at 5 different potentials.
- Current production, coulombic efficiency, cell density, pH, and biofilm formation were measured. RNA was extracted from cells attached to the electrodes. Cyclic voltammetry analysis was used to investigate damage to biofilm cells.
- Expression levels of 4 genes were measured to investigate transcriptional changes in response to electrode potentials.

Aim 3: Discover supporting functions of extracellular respiration by *S. oneidensis* MR-1 through meta-analysis of transcriptomic data

- Previously collected transcriptomic data for *S. oneidensis* grown under a wide variety of conditions was downloaded from the NCBI GEO database, aggregated, and normalized by ranking.
- Principal component analysis and machine learning were used to discover genes important to extracellular respiration.
- Knockout strain analysis was used to confirm the importance of genes identified by the meta-analysis and elucidate their functions.

CHAPTER 2

INTRODUCTION TO BIOELECTROCHEMICAL SYSTEMS WITH A FOCUS ON *SHEWANELLA ONEIDENSIS* MR-1, EXTRACELLULAR ELECTRON TRANSFER, AND MOLECULAR BIOLOGY TECHNIQUES

2.1. Bioelectrochemical systems

2.1.1 Introduction and research directions

Generally, bioelectrochemical systems (BESs) are devices in which biological materials exchange electrons with inorganic circuitry (Logan, Hamelers et al. 2006). For example, the biological material can consist of whole bacteria that oxidize an organic electron donor and use an anode as a terminal electron acceptor for respiration through extracellular electron transfer (EET). There are also many other configurations that can include bacteria, yeast, or enzymes donating electrons in an anode or accepting electrons in a cathode. Microbial BESs are designed to exploit microbial EET for human gain. One application of BESs is energy recovery (electricity production) from wastewater with microbial fuel cells (MFCs) (He, Minteer et al. 2005; Rabaey and Verstraete 2005; Logan, Hamelers et al. 2006). Recently, however, there has been increased interest in alternative applications such as self-powered biosensors, electronic devices (e.g., robots) powered directly from organic substrates, biocomputers, microbial physiology and metabolism research tools, and generation of chemical products (Wilkinson 2000; Ieropoulos, Melhuish et al. 2003; Hamelers, Heijne et al. 2010; Li, Rosenbaum et al. 2011). Most of these systems are not focused on generating electricity for power grids, but consume energy to perform other useful functions. For example, microbial electrolysis cells (MECs) use a microbial anode to harvest electrons, and apply an exogenous potential to produce a valuable chemical product such as hydrogen gas or hydrogen peroxide (Liu, Grot et al. 2005; Rozendal, Leone et al. 2009). A

microbial 3-electrode cell (M3C) also uses electricity and can be used in EET research, biosensing, and biocomputing (TerAvest, Li et al. 2011). For these energy-consuming systems, a potentiostat or power supply is used to poise the electrode at a favorable potential for the desired reaction(s). This can improve the stability of the BES, drive reactions that are not favorable in traditional MFCs, and allow study of the anode or cathode without limitations from the other half cell. The study of BESs is branching out in many different directions, with some researchers focusing on engineering improved reactor designs, some on novel applications, and others on studying the biology of microbes that live in these systems and their unique respiratory pathways. This review focuses on the biological aspects of BES research, particularly on molecular biology techniques that can be applied to this area, with emphasis on the BES model microbe *Shewanella oneidensis* MR-1.

2.1.2 Methods and terminology

A BES typically consists of a two chambered system with an anode and a cathode separated by a cation or anion exchange membrane. These systems can be constructed from glass, plastic, or other materials, with electrodes often made from graphite materials (plates, rods, granules, brushes, etc.). External circuitry is used to connect the anode and cathodes. A typical lab-scale BES is shown in Figure 2.1. The anode and/or cathode chamber is inoculated with a mixed or pure culture of bacteria containing electrochemically active microbes. For MFCs, the cathode chamber often uses an abiotic process to allow specific study of anode processes. Abiotic cathodes may contain a platinum catalyst for oxygen reduction or a solution of potassium ferricyanide, which is easily reduced to potassium ferrocyanide.

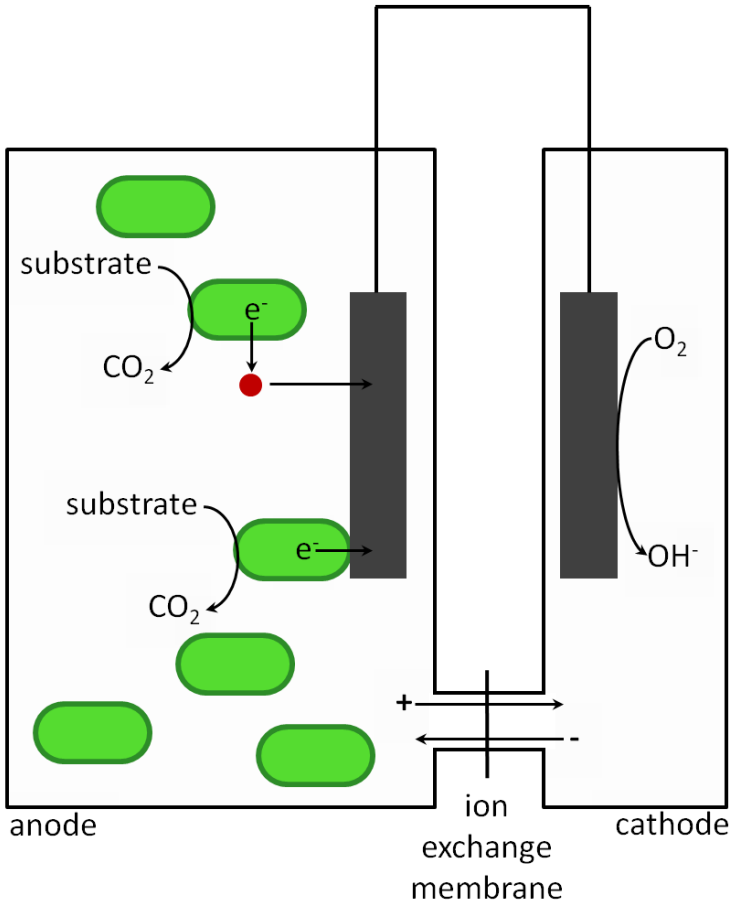

Figure 2.1. A schematic of a typical microbial fuel cell (MFC). Green ovals represent bacterial cells, the red circle represents a soluble electron shuttle molecule. An organic substrate is oxidized by microbes at the anode and metabolic electrons are transferred to the anode. The current passes through an external circuit and the electrons are released from the cathode through a reduction reaction, often catalyzed by platinum. Charge balance in the system is maintained by an ion exchange membrane. The potential difference between the anode and cathode maintains the current production.

Alternatively, a potentiostat may be used to control the potential of one electrode in an M3C. This instrument allows the user to control the potential of an electrode and measure the current passing through that electrode. The working electrode is controlled against a reference electrode with a known potential. A third electrode (the counter electrode) serves as a current drain for the system to ensure that the working electrode potential remains accurate while no current passes through the reference electrode. This is important because the flow of current

through the reference electrode changes its chemical properties, and alters its redox potential, thus rendering the potential control inaccurate. Controlling the working electrode potential allows the user to mimic bacterial respiration with solid electron acceptors, such as iron or manganese minerals, optimize the potential of the working electrode for maximum current production, or study EET mechanisms. Potentials in these systems are often reported with respect to the standard hydrogen electrode (SHE), which is assigned a value of 0.0 V; however, the most commonly used reference electrodes are the silver/silver chloride electrode (Ag/AgCl/sat'd KCl) at ca. +197 mV_{SHE} and the saturated calomel electrode (SCE) at ca. +244 mV_{SHE}. These electrodes are more common because they are simpler to construct and use than a hydrogen gas-based electrode. A schematic of a typical lab scale, continuously-fed M3C is given in **Figure 2.2**.

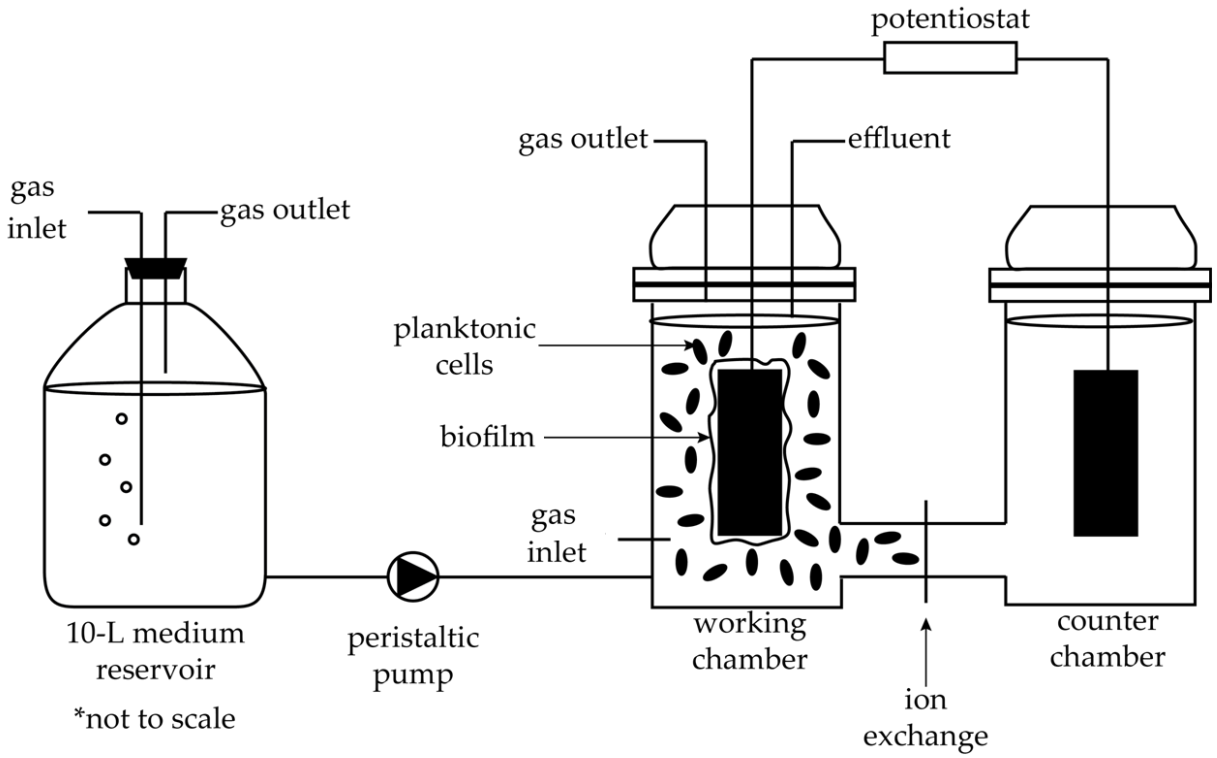

Figure 2.2. A schematic of a typical lab scale, continuous-flow, 2-chambered, microbial 3-electrode cell (M3C). Medium and gas (e.g., N_2) are fed into the working chamber continuously, while the counter chamber contains an electrolyte solution. Microbes are inoculated into the working chamber and may grow as biofilms for free-living planktonic cells.

For all types of BESs, electrochemical performance can be measured by current and power densities produced, which may be reported with respect to the projected electrode surface area (i.e., mA/m^2, mW/m^2) or with respect to the volume of the chamber (i.e., mA/m^3, mW/m^3). These are measured using a multimeter or potentiostat and are useful in calculations of scale-up possibilities and comparisons between different systems (Logan, Hamelers et al. 2006; Logan and Rabaey 2012). Another important measure of performance in BESs is the coulombic efficiency, which is the percentage of metabolic electrons that are captured by the electrode. The coulombic efficiency is calculated by performing a mass and energy balance on the system and dividing the number of electrons (coulombs) captured as electric current by the number released in the conversion of substrate to products (Liu and Logan 2004; Logan, Hamelers et al. 2006).

This measure provides one view of how efficiently the system converts the chemical energy in organic substrates into electric current. For some BES applications, such as wastewater treatment, it is also important to measure the percent removal of COD or pollutants of interest (He, Minteer et al. 2005; Li, Zhang et al. 2010). Other parameters may also be measured including microbial growth, biofilm formation, electron shuttle production, and product formation. Molecular biology techniques may also be used to identify bacterial species, quantify gene expression, or determine involvement of specific genes in EET pathways.

In addition to measuring the current production, a potentiostat is also useful for performing cyclic voltammetry analysis in BESs. Cyclic voltammetry is performed by sweeping the potential of the working electrode across a set range and recording the current production at each potential. Data from this analysis shows how the biological and chemical species react to different electrode potentials and can reveal electron shuttles in the system or the rate of electrode respiration at different potentials. Altering the parameters of the potential sweep allows the user to obtain different types of information. A cyclic voltammogram (CV) at a slow scan rate and with sufficient substrate provided to the organisms is termed a "turnover CV." This means that metabolic turnover is occurring under these conditions and the current recorded at each potential is indicative of the electrode respiration capacity of the organism at that potential. A CV at a very fast scan rate or with no substrate provided to the organism is a "nonturnover" CV. In this case the ability of chemical species in the system (such as electron shuttles or redox enzymes) to donate and receive electrons is measured in the absence of metabolic electron production by the organism. In this type of CV the presence of a chemical electron shuttle will cause characteristic current peaks, allowing for their detection by this method (Logan, Hamelers

et al. 2006; Rabaey 2010). See Figure 2.3 for an example of a turnover CV and interpretation for a *Shewanella oneidensis* biofilm.

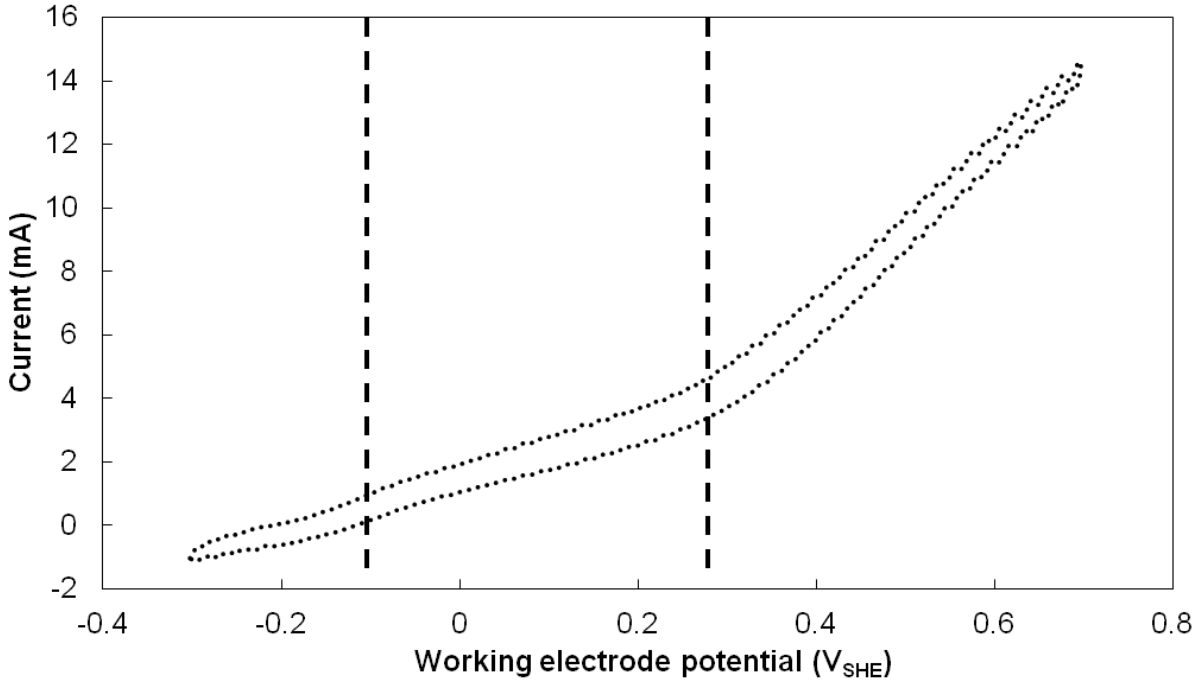

Figure 2.3. A turnover cyclic voltammogram (CV), of a biofilm of *Shewanella oneidensis* MR-1 performed at a scan rate of 2 mV per second. The dramatic changes in slope signal the onset potential of different microbial activities. In this biofilm two different electron transfer pathways (mediated electron transfer in the center, and direct electron transfer on the right) were at work, resulting in two catalytic waves.

2.1.3 Microbial fuel cells

A microbial fuel cell (MFC) is a specific type of BES in which no external potential is applied, and the potential difference required for current production is created by separating the oxidation of an organic substrate at the anode from a corresponding reduction at the cathode. MFCs have been built with a variety of configurations, including H-type, plate-type, and upflow-type (He, Minteer et al. 2005; Logan, Hamelers et al. 2006). Although there have been great improvements in power production in the last decade, a recent life cycle analysis and economic analysis revealed that applying MFCs to wastewater treatment will not result in environmental benefits

when compared with conventional anaerobic treatment (Foley, Rozendal et al. 2010; Fornero, Rosenbaum et al. 2010). This indicates that MFCs will not likely become important for domestic wastewater treatment and electricity production. However, there is evidence that some MFCs (such as benthic MFCs) could provide a useful power source for remote applications. Benthic MFCs take advantage of the natural redox gradient that occurs between anaerobic ocean sediments and the overlying oxygenated water and can be used to power remote oceanographic equipment for extended periods (Tender, Gray et al. 2008). A variant of this design (the microbial electrochemical snorkel) does not harvest (or consume) any electricity but allows microbes in the sediment to take advantage of the electrode as an electron acceptor for degradation of organic matter in the sediment. This can potentially speed the degradation of pollutants in anoxic sediments (Erable, Etcheverry et al. 2011).

In addition to the oxidation of municipal wastewater or benthic sediments, MFCs have been used to treat a number of other wastewaters and organic pollutants, and to convert recalcitrant substrates (such as cellulose) to electricity (Pant, Van Bogaert et al. 2010). MFC wastewater treatment studies have included swine, chocolate processing, and brewery wastes. Specific organic pollutants, such as phenol and azo dyes have also been treated (Luo, Liu et al. 2009). Organic removal efficiencies vary, but can reach values greater than 90%, although a large fraction of this removal may be due to methanogenic activity in mixed culture systems (He, Minteer et al. 2005). Although many types of wastewater have been treated in lab-scale MFCs, there is no evidence to date that they will be applicable for commercial treatment of any type of wastewater. To improve wastewater treatment (without electricity generation) the microbial electrolysis cell may prove more useful.

2.1.4 Microbial electrolysis cells

In a microbial electrolysis cell (MEC), electrons donated by anode microbes are transported through external circuitry to the cathode where they are used to form a valuable chemical product. For these reactions to occur, the potential difference between the anode and cathode is increased to the required value by a potentiostat or power supply. To date, products that are generated include hydrogen gas, hydrogen peroxide, and ethanol (Rozendal, Leone et al. 2009; Rosenbaum, Cotta et al. 2010). A recent life-cycle analysis of BESs applied to wastewater treatment showed no environmental benefit of using a traditional MFC versus a traditional anaerobic treatment design, however, an MEC producing hydrogen peroxide would have significant environmental benefits because the microbial anode reduces the energy required to generate the product and may concurrently treat a wastewater stream (Foley, Rozendal et al. 2010).

2.1.5 Microbial biocathodes and microbial electrosynthesis

Other types of BESs that consume electricity to perform useful functions are microbial biocathodes and microbial electrosynthesis systems. In both of these systems microbes accept electrons from a cathode. The goal of microbial biocathodes is to replace expensive precious metal catalysts that are often used in abiotic cathodes for the reduction of molecular oxygen to water. Because precious metal catalysts are nonrenewable, expensive and become poisoned easily, research efforts have moved toward finding microbial catalysts that are capable of catalyzing this cathodic reaction (He and Angenent 2006). Clauwaert, et al. (2007) constructed MFCs with bioanodes and biocathodes working together. The biocathodes were inoculated with a mixture of different sludges and were capable of catalyzing oxygen reduction. This system was able to produce electricity from an organic substrate without the addition of any chemical catalysts. Erable, et al. (2010) also enriched a biofilm capable of catalyzing cathodic reactions by

placing an electrode potentiostatically poised at a cathodic potential in aerobic seawater. This activity was reproduced when laboratory reactors with sterile seawater were inoculated from the same film, indicating that it is feasible to enrich or isolate microbes capable of cathodic activity from the environment.

Other researchers are growing microbes with cathodes for the purpose of fixing carbon dioxide rather than reducing oxygen. In microbial electrosynthesis, bacteria are grown at a cathode to catalyze the reduction of carbon dioxide to organic molecules (Nevin, Woodard et al. 2010; Rabaey and Rozendal 2010). In contrast with MECs, the microbes in these systems do not provide any of the energy for product formation, but are only used as renewable catalysts for this process. Thus far, only very small amounts of acetate and 2-oxobutyrate have been produced by pure culture acetogenic bacterial strains (e.g. *Sporomusa ovata*) at a high coulombic efficiency. Several organisms are capable of this activity, and some convert over 80% of the electrons received to products (Nevin, Woodard et al. 2010; Nevin, Hensley et al. 2011). Nevin et al. (2010) proposed that, with further development, this process could be used to store solar energy as liquid fuels. Although there are only two experimental publications on this subject to date, there has been much speculation on additional organisms and products that could useful in these systems, including analysis of the feasibility of using *S. oneidensis* (Rabaey and Rozendal 2010; Ross, Flynn et al. 2011). These processes are not yet well understood and several different mechanisms may be involved for the transfer of electrons into bacterial cells (Rosenbaum, Aulenta et al. 2011; Ross, Flynn et al. 2011).

2.1.6 Mechanisms of electron transfer

In microbial BESs, there are several known and proposed mechanisms of extracellular electron transfer (EET) between cells and electrodes. Understanding the mechanisms of electron transfer

in BESs is important because the different mechanisms have varying efficiencies and play a role in the overall performance of the system (Schröder 2007). In addition, a deep understanding of these mechanisms may suggest new functions and applications for BESs (Ross, Flynn et al. 2011). The capacity for electrode respiration requires specialized electron transport systems to convey electrons to the outer surface of the cell and is closely linked with the dissimilatory metal-reducing function of environmental bacteria that respire with solid iron and manganese minerals (Hernandez and Newman 2001). Indeed, model BES organisms have been found in anaerobic sediments where they participate in biogeochemical cycling by reducing solid metal oxides (Lovley 2002). To date, most known EET mechanisms of BESs fall into two general categories: direct electron transfer (DET) and mediated electron transfer (MET).

Within DET, the following mechanisms have been described: direct oxidation of membrane bound *c*-type cytochromes and longer distance transfer through conductive pili. In the direct oxidation of outer membrane *c*-type cytochromes (OMCs), cells must be attached to the electrode to create direct contact between the cytochrome and the solid surface (Schröder 2007). This mechanism has been especially well documented for *Geobacter sulfurreducens* which has many (>50) different, multiheme, *c*-type cytochromes, several of which are localized to the outer membrane (Methé, Nelson et al. 2003). Similarly, *S. oneidensis* has many (>40) *c*-type cytochromes, with many localized to the outer membrane (Meyer, Tsapin et al. 2004; Gao, Barua et al. 2010). It seems that there are a few of these OMCs that that are specialized for DET, such as OmcA and MtrC of *S. oneidensis* MR-1 and OmcS of *G. sulfurreducens* and although each organism has many OMCs, only a small subset are essential for DET (Mehta, Coppi et al. 2005; Coursolle, Baron et al. 2010; Coursolle and Gralnick 2010).

Some bacteria (*G. sulfurreducens*, *S. oneidensis*) may also use conductive pili to transport electrons to the electrode (Reguera, McCarthy et al. 2005; Gorby, Yanina et al. 2009; El-Naggar, Wanger et al. 2010). This mechanism was first proposed for *G. sulfurreducens* by Reguera et al. (Reguera, McCarthy et al. 2005), and the conductive structures were named bacterial nanowires. The pili were viewed with conductive-probe atomic force microscopy, which revealed their conductivity (Reguera, McCarthy et al. 2005). Gorby et al. (2009) used scanning tunneling microscopy to show that *S. oneidensis* nanowires (and also similar structures from other organisms) are also conductive. However, the specifics of this mechanism are not well understood and some have hypothesized that pilin proteins are conductive and may be involved in oxidation/reduction reactions, while others have speculated that the pili are only structural and are covered by some other redox active compound, possibly cytochromes (Reguera, McCarthy et al. 2005). Scanning tunneling microscopy of *S. oneidensis* nanowires found that they were poorly conductive when OMCs were absent (in OMC and type-II secretion mutants) (Gorby, Yanina et al. 2009). Leang et al. (2010) found the outer membrane cytochrome OmcS (which is necessary for current production in *G. sulfurreducens*) localized along the length of the *G. sulfurreducens* pili using immunogold labeling, suggesting that pilin proteins may be a scaffolding material for other redox active species. A broader scale study showed that *G. sulfurreducens* biofilms are conductive as a whole, and linked this conductivity to one of the pilin proteins. The suggested mechanism for this conductivity is pi bond stacking in adjacent aromatic amino acids, but this claim has not been substantiated (Malvankar, Vargas et al. 2011). Although the mechanism of electron transfer through these pili has not been determined, there is general evidence to show that nanowires are important for EET in *G. sulfurreducens*, while similar analyses for *S. oneidensis* have been inconclusive (Reguera, Nevin et al. 2006; Bouhenni, Vora et al. 2010).

This issue is clouded by the role of these pili in biofilm formation, which is an important factor for EET in BESs (Reguera, Pollina et al. 2007). However, Franks et al. (2010) found evidence that the nanowires are directly involved in EET by measuring the metabolic activity in different layers of a thick *G. sulfurreducens* biofilm attached to an electrode. Analysis showed that cells in all layers were metabolically active, indicating that cells at the outer edge of the biofilm have some connection to the electrode (the sole electron acceptor in the system). This topic remains under close scrutiny and further research is under way to determine the specific role of these conductive pili in both *G. sulfurreducens* and *S. oneidensis*.

In contrast to direct electron transfer, mediated electron transfer can occur through the use of exogenous or endogenous electron shuttles. Exogenous shuttles include methylene blue, neutral red, methyl viologen, AQDS and others, although their use in BES research has declined because addition of synthetic chemicals to such systems is not sustainable (Park and Zeikus 2000; Ringeisen, Henderson et al. 2006; Aulenta, Catervi et al. 2007; Schröder 2007). Endogenously produced mediators include flavins and phenazines (Marsili, Baron et al. 2008; Venkataraman, Rosenbaum et al. 2010). The finer points of MET differ in various organisms. For example, work by Coursolle et al. (2010) revealed that in *S. oneidensis,* OMCs are required for use of MET, indicating that endogenously produced flavins are reduced by EET, not through diffusion into the cell. In contrast, *Pseudomonas aeruginosa* is able to transfer electrons electrodes using phenazine mediators, although it has no known OMCs (Rabaey, Boon et al. 2005; Venkataraman, Rosenbaum et al. 2010). Addition of redox mediators can allow a wide range of organisms (including fermenters) to reduce solid electron acceptors and the EET mechanism for many of these organisms is not known, indicating that there are different forms of MET which have not yet been fully elucidated (Venkataraman, Rosenbaum et al. 2011).

Proposed EET mechanisms that do not fit into the categories of DET and MET include electrokinesis (which could involve some of the previous mechanisms), redox-active membrane vesicles, and OMC-mediator complexes (Gorby, McLean et al. 2008; Okamoto, Nakamura et al. 2009; Harris, El-Naggar et al. 2010; Okamoto, Nakamura et al. 2011). Electrokinesis is a process in which bacteria build up metabolic electrons, then periodically swim to and touch a solid electron acceptor for a short time to release these electrons (Harris, El-Naggar et al. 2010). A microscope video recording of this process was made by Harris et al. (2010) with *S. oneidensis* respiring with a solid manganese mineral. This mechanism could be important for EET by planktonic cells in the absence of soluble electron shuttles. Another mechanism that could enhance EET at a distance is the use of membrane vesicles that act as electron shuttles. Gorby et al. (2008) found membrane vesicles produced by *S. oneidensis* that are electrochemically active, and proposed that they could be involved in EET. Protein purification showed that these vesicles contained OMCs and it is possible that they also contained flavins, although these compounds were not measured (Gorby, McLean et al. 2008). The importance of the interactions between OMCs and flavins are currently under study, and one group has suggested that riboflavin and selected OMCs may form a complex with improved DET characteristics (Okamoto, Nakamura et al. 2011). These mechanisms are not yet well studied, but may become an important part of the understanding of EET in the future (Okamoto, Nakamura et al. 2009).

The relative efficiencies of different EET mechanisms were discussed in a review by Schröder (2007). Theoretically 54% of the energy liberated from the complete oxidation of glucose could be captured by an external circuit *via* a DET mechanism involving OMCs with a theoretical reduction potential of ca. 0.0 V_{SHE}. No similar value was calculated for MET, although the coulombic efficiency of MET processes should be considerably lower than for DET

processes because of losses in the diffusion process. While DET has this advantage, it also has the disadvantages that it is limited to only the cells directly attached to the surface and the energy gain from each electron transferred is small (Schröder 2007). The method of EET and the interaction between different mechanisms is important to the function of BESs and should be the subject of further research.

2.1.7 BES model microbes

BES studies are performed with a variety of organisms, including pure cultures, defined mixed cultures, and undefined mixed cultures (He, Minteer et al. 2005; Logan, Hamelers et al. 2006; Nevin, Richter et al. 2008; Rosenbaum, Bar et al. 2011; Venkataraman, Rosenbaum et al. 2011). Mixed communities are important for BES applications, such as wastewater treatment, and environmental applications, such as benthic MFCs. Although current production with a pure culture of *G. sulfurreducens* can reach levels as high as those for mixed-culture anodes, pure-cultures are limited to a much narrower substrate range and cannot be fed with nonsterile wastewaters or sediments (Nevin, Richter et al. 2008). Community sequencing analysis of MFC anodes has not shown enrichment of any specific genus of bacteria, but rather a general presence of proteobacteria (Rabaey, Boon et al. 2004). Pure culture research is required for improving understanding of the mechanisms of EET and the microbial limitations of BES applications, as well as for production of high-value products. Several pure-cultures for BES research have been isolated from several different environments, but two major model microbes for pure-culture BES anode research have emerged—*G. sulfurreducens* and *S. oneidensis* MR-1—which are both dissimilatory metal-reducing proteobacteria. *G. sulfurreducens* produces the greatest power and current densities of any pure culture in BES systems, forms thick (~50 μm) *c*-type cytochrome rich biofilms, and is an obligate anaerobe (Holmes, Bond et al. 2004). *S. oneidensis* is a

facultative aerobe that secretes flavins as electron shuttles and forms *c*-type cytochrome rich biofilms, and engages in both DET and MET (Marsili, Baron et al. 2008; Baron, LaBelle et al. 2009). Because *S. oneidensis* uses both types of electron transfer it is an important model for how these two types of EET may interact in mixed community BESs, which have complex mixtures of mechanisms contributing to the total EET. *Geobacter* and *Shewanella* species can both be found in anaerobic sediments and have also been found in community sequencing analyses of mixed-culture anodes (Logan and Regan 2006).

2.2. Shewanella oneidensis *MR-1*

2.2.1 Shewanella oneidensis *MR-1 as a model microbe for BESs*

S. oneidensis MR-1 is a metal-reducing bacterium originally isolated from sediments of Lake Oneida, New York, USA (Myers and Nealson 1988). This organism and others like it are important in the biogeochemical cycling of iron, manganese, and other metals in anaerobic sediments (Nealson and Myers 1992). *S. oneidensis* is the most metabolically diverse of the BES model microbes and is capable of reducing a wide variety of soluble and insoluble electron acceptors, including DMSO, TMAO, Fe(III), Mn(VI), Cr(VI), U(VI), nitrate, thiosulfate and others (Beliaev, Thompson et al. 2002). Conversely, possible electron donors are more limited, because *S. oneidensis* favors lactate as carbon source and electron donor, although it can also use ethanol and some sugars under certain environmental conditions (Biffinger, Byrd et al. 2008).

Because *S. oneidensis* is a facultative aerobe it is also useful for studying the effects of oxygen intrusion on BES anodes, which results in competition between the anode and oxygen for metabolic electrons (Biffinger, Byrd et al. 2008; Biffinger, Ray et al. 2009). Dissolved oxygen at the anode has long been considered a detriment to MFC performance, and indeed it can decrease current production and coulombic efficiency (Ringeisen, Ray et al. 2007). However, recent studies have shown performance benefits from oxygen in an anode chamber with *S. oneidensis*

(Biffinger, Byrd et al. 2008; Biffinger, Ray et al. 2009; Rosenbaum, Cotta et al. 2010). One group has suggested (with a different *Shewanella* species) that the higher redox potential of oxygen compared to the electrode results in increased NADH production, and the concomitant increase in metabolic electrons causes the increased current production even while the coulombic efficiency is lower (Li, Freguia et al. 2010). In another study, increased fuel diversity was cited as a major advantage (Biffinger, Byrd et al. 2008). In the publications cited above, oxygen was a detriment in experiments where biofilm growth was not observed and increased current production when biofilm growth was observed. This indicates that oxygen limitation and other biofilm characteristics may also be important factors in this effect and warrant further research.

Another interesting aspect of BESs with *S. oneidensis* is that they often contain populations of both biofilm and planktonic cells, whereas *G. sulfurreducens* grows only in biofilms at BES anodes because of its limitation to DET (Franks, Malvankar et al. 2010). Operating conditions can have an effect on this aspect with some *S. oneidensis* anodes having mostly planktonic cells and others mostly biofilm cells (Biffinger, Pietron et al. 2007; Lanthier, Gregory et al. 2008). This is likely due to the diversity of EET mechanisms used by *S. oneidensis* allowing cells to grow at different locations with respect to the electrode surface.

2.2.2 EET mechanisms of S. oneidensis *MR-1*

DET of *S. oneidensis* occurs through the use of several outer membrane *c*-type cytochromes, which have electrochemical activity both *in vivo* and *in vitro*. Early research on this organism revealed that 80% of its membrane bound cytochromes are localized to the outer membrane under anaerobic conditions (Myers and Myers 1992). Analysis of 36 *c*-type cytochrome knockout strains showed various important functions of these proteins in both aerobic and anaerobic respiration. Seven of these knockouts completely eliminated the ability of the cells to

respire with solid manganese minerals, suggesting a complex pathway for solid mineral reduction (Gao, Barua et al. 2010). Recent work has also illustrated the importance of DET through the OMCs (Okamoto, Nakamura et al. 2009; Okamoto, Nakamura et al. 2011). Selective inhibition of *c*-type cytochromes with nitric monoxide again confirmed the importance of these proteins in EET for *S. oneidensis*. The interaction of a few of these cytochromes with electrodes has been directly characterized in the absence of bacteria *via* protein film voltammetry, revealing their capability to catalyze EET (Hartshorne, Jepson et al. 2007; Meitl, Eggleston et al. 2009).

DET by bacterial nanowires has not been studied as intensively for *S. oneidensis* as for *G. sulfurreducens*, but there have been some studies on the subject. Gorby et al. first proposed this mechanism for *S. oneidensis* in 2005 and measured the conductivity of these pilus-like structures with scanning tunneling microscopy. However, this conductivity was only measured in the z-plane, perpendicular to the length of the pilus, so the possibility that they transfer electrons along the length of the structure was still unsure. In addition, *omcA* and *mtrC* knockouts produced nonconductive surface structures, suggesting that these OMCs play a critical role in any conductive structures produced by this organism (Gorby, Yanina et al. 2009). The conductance along the length was only recently shown through the use of nanofabricated electrode arrays that could measure the conductance of a single nanowire (El-Naggar, Wanger et al. 2010). Unlike *G. sulfurreducens*, there has been no study yet to show that these structures influence current production or EET in *S. oneidensis*, and therefore the importance of this mechanism for *S. oneidensis* is currently unknown. Studies of pilin knockouts of this organism have not been conclusive because during incubations of several days these knockouts sometimes produced more and sometimes produced less current than the wild type (Bouhenni, Vora et al. 2010).

MET by *S. oneidensis* was first explored by culturing it with iron oxides sequestered in porous glass beads as the sole electron acceptor. This approach showed that *S. oneidensis* is capable of reducing solid iron oxides without direct contact, precluding DET mechanisms (Lies, Hernandez et al. 2005). The mediator responsible for this activity was not immediately identified, but eventually two research groups showed that *S. oneidensis* excretes flavins into the culture medium, including riboflavin and flavin mononucleotide (FMN) up to 500 nM (Marsili, Baron et al. 2008; von Canstein, Ogawa et al. 2008). They also showed that the excreted flavins are important for EET in this organism by manipulating the amount of riboflavin in the culture medium. When the reactor medium was replaced with fresh (flavin free) medium current production dropped to 20% of the previous value. When the original medium (minus the planktonic cells) was replaced the current returned to the original value and when additional riboflavin was added the current increased further (Marsili, Baron et al. 2008).

In an effort to understand this process better, Covington et al. (2010) produced a transposon mutant library of *S. oneidensis* and screened for mutants deficient in riboflavin excretion. These mutants lacked the ability to convert flavin adenine dinucleotide (FAD) to FMN in the periplasm, thus, demonstrating that this organism excretes FAD, which is then converted to FMN and riboflavin in the periplasm. This was an important finding for understanding flavin production in this organism, but because FAD is also an efficient electron shuttle this mutant cannot be used to exclude the effects of MET for *S. oneidensis* (Covington, Gelbmann et al. 2010). Recently, the same approach was used to discover a gene necessary for flavin export from *S. oneidensis*, which has been termed “bacterial flavin exporter” or *bfe* (Kotloski and Gralnick 2013). Deletion of this gene results in an *S. oneidensis* strain incapable of excreting electron shuttles.

An interesting aspect of the MET and DET pathways of *S. oneidensis* is that they overlap. The OMCs responsible for reducing electrodes directly are also those responsible for reduction of flavins. It was recently shown that each mechanism accounts for approximately 50% of total EET under some experimental conditions (Carmona-Martinez, Harnisch et al. 2011). However, other methods have indicated that MET accounts for 70-80% of electron transfer, indicating that culture conditions may have a strong influence on the distribution of electrons between DET and MET (Marsili, Baron et al. 2008; Kotloski and Gralnick 2013). The overlap of these pathways makes *S. oneidensis* an especially important model microbe because the interplay of DET and MET is important in mixed-culture BESs and cannot be studied with any other pure culture (Rabaey, Boon et al. 2004; Logan 2009).

2.2.3 The Mtr pathway of S. oneidensis *MR-1*

Although it has multiple EET mechanisms, it has been clearly demonstrated that the Mtr (metal reduction) respiratory pathway is essential for appreciable EET from *S. oneidensis*. This system transports electrons from the menaquinone pool to the OMCs, allowing *S. oneidensis* to overcome the insulating properties of the membrane and use solid electron acceptors. MtrA and MtrC are the two major cytochromes in this pathway, although some of its other extracellular *c*-type cytochromes may have overlapping functions, because many OMC knockouts can survive with an electrode as the sole electron acceptor (Beliaev, Saffarini et al. 2001; Myers and Myers 2001; Coursolle and Gralnick 2010). A number of studies have been performed to elucidate the structure and location of this pathway. The current working model shows that CymA transports electrons across the inner membrane, where they are accepted by MtrA, which then donates them to MtrC or OmcA, with the help of the outer membrane-spanning protein MtrB (Figure 2.4) (Carmona-Martinez, Harnisch et al. 2011).

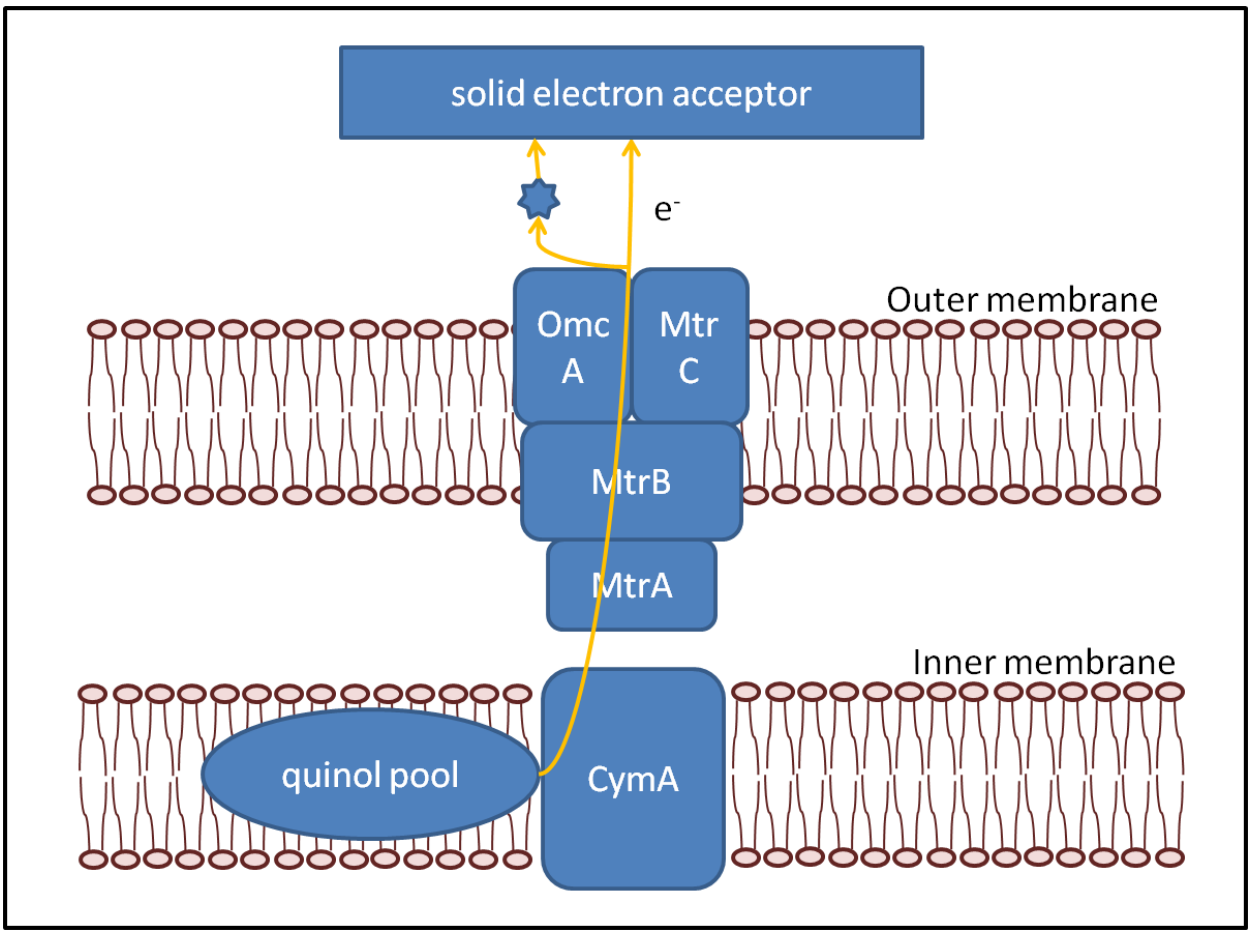

Figure 2.4. This figure depicts the current working model of the Mtr pathway of MR-1 based on protein function and localization studies. Arrows indicate both direct electron transfer from outer membrane cytochromes (e.g., MtrC) to the electron acceptor, and mediated electron transfer with flavins (blue star). Adapted from Ross et al. (2011).

The location of this pathway at the outer membrane of the cell has been confirmed by antibody-recognition force microscopy, its translocation and assembly is dependent on type II secretion (Shi, Deng et al. 2008; Lower, Yongsunthon et al. 2009). Shi et al. (2006) also found evidence of the interaction of MtrC and OmcA through pull-down experiments. Recent bacterial two-hybrid experiments also confirmed this model and showed that there are several periplasmic proteins involved in shuttling electrons from CymA to MtrA (Borloo, Desmet et al. 2011). Ross et al. (2007) used cross-linking experiments to find that MtrA, MtrB, and MtrC form a complex

with 1:1:1 ratios. With the knowledge gained and biological model of the Mtr pathway built from these studies, this electron conduit has been successfully reconstituted in *E. coli*. The genes *mtrA*, *mtrB*, *mtrC* were cloned into *E. coli* along with a cytochrome maturation plasmid. This modification resulted in a strain that could reduce solid metal oxides at a rate ca. 8 times faster than the parent strain, demonstrating that these three proteins constitute an "electron conduit" for transport of charges to the cell surface (Jensen, Albers et al. 2010). Recent work has improved current production from *E. coli* with the Mtr pathway by optimizing promoter strengths (Goldbeck, Jensen et al. 2013).

Recent studies of the EET capabilities of several *S. oneidensis* knockout strains combined with more advanced electrochemical analysis for biological systems have not only improved our understanding of the EET mechanisms of *S. oneidensis*, but also brought to light how complicated its network of EET systems is. Future work should focus on the isolation of these pathways to understand what their individual roles are and how they interact. Currently, our inability to consistently parse out the contributions of riboflavin is a severe disadvantage to understanding electricity production with this organism (Covington, Gelbmann et al. 2010).

2.2.4 Biofilm development in S. oneidensis

Another factor in electricity production by *S. oneidensis* is biofilm formation. *S. oneidensis* forms biofilms, and after extended growth forms the mushroom structures characteristic of other biofilm formers, such as *P. aeruginosa* (Thormann, Saville et al. 2004). They progress in a standard fashion, with a few cells adhering first and producing microcolonies that grow to cover the entire surface, followed by tower and channel formation. Time course images of several mutant biofilms show that type IV pili are important for initial attachment, while flagella are involved in biofilm structure maturation. The structure and stability of these biofilms is

influenced by nutrient availability and an imaging study has shown that *S. oneidensis* grown in LB medium forms flatter, more fragile biofilms, compared to the highly structured, robust biofilms formed in more nutrient limited media (Thormann, Saville et al. 2004). In contrast to biofilm *formation*, it seems that biofilm *detachment* is controlled by the concentration of oxygen, rather than carbon source. Lies et al. (2005) found that 80% of an *S. oneidensis* biofilm detached when flow was arrested in a hydrodynamic culture system. Exchanging the medium with one containing no carbon source (without stop of flow) revealed that substrate limitation did not cause biofilm detachment. Only oxygen limitation could reproduce this level of detachment under flow-through conditions. The remaining cells could be induced to detach by resuming flow for 45 min and arresting it again, indicating that they were metabolically active and changed behavior after exposure to the biofilm surface (Thormann, Saville et al. 2005). Real-time imaging with strains expressing fluorescent protein markers for ribosome and *mtrB* expression show that even in the center of large structures, cells are metabolically active and display increased expression of the *mtr* operon in response to oxygen limitation (Teal, Lies et al. 2006). Structural studies of strictly anaerobic biofilms have not been performed, perhaps due to the requirement of molecular oxygen for GFP fluorescence. Future studies of anaerobic biofilm processes are necessary to improve understanding of anaerobic respiration in *S. oneidensis*.

2.3. Molecular biological analysis of BESs

2.3.1 Introduction

Molecular biology techniques can be a useful tool for understanding microbial behavior in BESs. Understanding which proteins are involved, how they are regulated, and how they function could yield insight into BESs and increase productivity of biological electricity generation. Techniques that have been of central importance for understanding BESs, thus far, are 16S rRNA gene

community characterization, transcriptional analysis, proteomic analysis, gene knockout studies, and crystallographic analysis of important BES proteins.

2.3.2 Community Characterization of BES microbiomes

Because research on BESs for wastewater treatment is often performed using undefined mixed cultures, community sequencing analyses are necessary to determine which bacterial species become enriched in BESs. MFC anodes may be inoculated from a variety of sources including municipal wastewater sludge and anaerobic sediments, and the community changes over time as it adapts to the environment at the anode. A 2006 review by Logan and Regan shows that across several studies, laboratory MFC anodes have contained highly diverse communities with no bacterial phylum dominating, and that there can be a high proportion (20-30%) of unidentified clones. Communities in different systems had some similar characteristics, such as a high proportion of proteobacteria, but the community was observed to vary depending on inoculum and substrate (Logan and Regan 2006). In contrast, benthic MFCs are usually dominated by Geobacteraceae, with some electrode communities showing up to 70% of sequences from *Geobacter* species. This may be due to the strict anaerobic nature of the sediments compared with laboratory MFC anodes, where there may be oxygen diffusion from the cathode (Logan and Regan 2006).

Community characterization can be a useful tool beyond simple identification of microbes present because it can lead to elucidation of specific microbial interactions in BESs. For example, a study by Venkataraman et al. (2011) found a large percentage of proteobacteria, and within the proteobacteria many sequences for *Pseudomonas* and *Enterobacter* species after a 3 month operation of an upflow, continuous MFC. This is a curious result, considering that *Enterobacter* species are fermenters, not known to participate in EET, and because previous

work has suggested that *Pseudomonas* spp. should be more common in batch-fed MFCs than in continuously-fed reactors (Logan and Regan 2006). However, subsequent co-culture experiments indicated that together these two organisms could produce more than ten times higher current than either culture alone due to increased mediator production by *P. aeruginosa* in the presence of *Enterobacter aerogenes* (Venkataraman, Rosenbaum et al. 2011). More in depth analysis of defined co-cultures, suggested by community characterization, will provide deeper insight into the relationships between bacteria and how they affect mixed culture current production.

2.3.3 Global transcriptomic analysis

While determining relationships between organisms in a BES is more relevant to real world applications, such as wastewater treatment, there is a need for deeper understanding of EET by pure cultures. Because the microbial physiology and mechanisms of EET in pure culture BESs are still poorly understood, many researchers have used gene expression studies to discover genes that are important for EET and other factors affecting BES performance, such as biofilm formation. Previous analyses have confirmed important aspects of BES physiology, such as the upregulation of genes for outer membrane cytochromes in *G. sulfurreducens* and *S. oneidensis* under electrode-respiring conditions.

One interesting finding from two studies is the upregulation of ribosomal proteins under electrode respiring conditions. Rosenbaum et al. found a dramatic increase in expression of ribosomal proteins in *S. oneidensis* cells grown with anodes, compared to soluble Fe(III)-citrate, or oxygen (Rosenbaum, Bar et al. 2012). This could indicate that there are changes in protein turnover under these growth conditions, or it may be a result of the biofilm status of these cells (Lazazzera 2005). Franks, et al. (2010) also found ribosomal proteins to be upregulated in the portion of a *G. sulfurreducens* biofilm closest to an electrode, with respect to cells farther from

the electrode surface. Neither group has yet provided an explanation for this behavior, but other evidence shows that it may not be limited to electrode respiration. Data from a study of *S. oneidensis* grown with a wide variety of electron acceptors (but not with an electrode) showed ribosomal protein expression positively correlated with the reduction potential of the electron acceptor (Beliaev, Klingeman et al. 2005). Similarly, Rosenbaum et al. (2012) and Franks et al. (2010) also found increased expression of stress response genes in cells grown nearer to the electrode possibly due to a lower local pH close to the electrode. This is a possibility for *G. sulfurreducens* biofilms, which experience pH gradients with low pH near the electrode (Franks, Nevin et al. 2009). This is unlikely to occur in *S. oneidensis* because its biofilms grown on anodes show little or no pH difference between inner and outer layers (Babauta, Nguyen et al. 2011).

Global transcriptomic analysis has also been used to characterize the gene expression of mutants, such as knockout strains, that are of interest to BES researchers. When combined with performance data from these mutants, transcriptional analysis can aid in parsing direct and indirect effects of mutations on performance. For example, Kim et al. (2008) found that an *omcF* knockout in *G. sulfurreducens* generated less current not because OmcF was directly involved in EET but because it also affected expression and localization of other proteins important for current production. As is common in transcriptomic studies there are also many results that cannot yet be interpreted, such as differential expression of hypothetical proteins. Further analysis of hypotheses generated from these global transcriptomic approaches is necessary.

2.3.4 Expression analysis by qRT-PCR

In contrast to the global approach of microarrays, quantitative, reverse transcription polymerase chain reaction (qRT-PCR) is a method whereby the amount of transcription of a single, specific

gene can be measured. This method can be used to validate microarray results, by comparing the normalized expression values calculated from both techniques (Dallas, Gottardo et al. 2005). While there can be variation between the results of the two methods, they generally correlate well with each other and this type of validation is widely accepted (Morey, Ryan et al. 2006). This type of validation has previously been used in BES and EET research. Franks et al. (2010) successfully used qRT-PCR to validate microarray results from different layers of a *G. sulfurreducens* biofilm, and Beliaev et al. (2005) used a similar approach in a study of *S. oneidensis* under different EET conditions. This method can also be used for rigorous testing of hypotheses developed through global transcriptomic analyses. For example, Nevin et al. (2009) used microarray analysis to choose genes of interest for current production in *G. sulfurreducens,* then used qRT-PCR on that subset of 6 genes to compare transcript levels with current production under different experimental conditions. Analysis showed that expression of 5 out of 6 correlated positively with current production.

2.3.5 Knockout studies in BESs

Further evidence that a specific gene is involved in the EET process can be attained through a gene knockout study. If the gene of interest is disrupted or deleted from the organism and current production decreases, it is likely that the gene is important for EET. Numerous knockout studies have been performed on BES model microbes, some with success, and others with less clear outcomes. Knockouts of several components in the Mtr pathway have displayed a greatly decreased ability to reduce solid metal oxides and electrodes (Beliaev and Saffarini 1998; Beliaev, Saffarini et al. 2001; Bretschger, Obraztsova et al. 2007; Gorby, Yanina et al. 2009). Coursolle et al. (2010) demonstrated that this pathway is necessary for the reduction of flavins by this organism, particularly the transmembrane segment composed of MtrA and MtrB. Deleting

the outer membrane cytochromes OmcA and MtrC also decreased flavin reduction, but to a lesser extent, because of their redundant function with each other and other outer membrane cytochromes (Coursolle, Baron et al. 2010). Although the Mtr pathway is responsible for a very large percentage of EET in this organism, some researchers are also interested in the roles of other surface structures (bacterial nanowires) in EET (Coursolle, Baron et al. 2010). Two studies investigated current production in a number of *S. oneidensis* MR-1 strains with mutated genes for outer surface structures, such as OMCs, pili, and flagella (Bouhenni, Vora et al. 2010; Carmona-Martinez, Harnisch et al. 2011). These studies confirmed the importance of OMCs and the Mtr pathway in DET, but the results for other surface structures were less clear.

Bouhenni et al. (2010) found that flagellin deletion mutants produced nearly twice the maximum current of the wild-type *S. oneidensis* (although this behavior wasn't explained). Conversely, it appears that pilin cluster deletion had little effect on current production. Biofilm formation was implicated in these results, but the evidence is not clear, since the flagellin mutant produced the highest maximum current with no detectable biofilm formation (Bouhenni, Vora et al. 2010). Carmona-Martinez et al. (2011) investigated the same set of mutants, but with a focus on using cyclic voltammetry analysis of the mutants to determine whether DET or MET was the dominant EET mechanism in each case. Results showed that these outer surface structure mutations did not change the DET:MET ratio, except perhaps in the case of the flagellin mutant which shifted slightly toward MET. The reasons for the changes in current production in these mutants remains unclear and should be the subject of deeper electrochemical analysis (Carmona-Martinez, Harnisch et al. 2011).

These results can be difficult to interpret and such knockouts may sometimes have unintended consequences. For example, a *pilD* mutant of *S. oneidensis* MR-1 produced much

less current than the wild type due to a disruption in OMC secretion caused by this mutation, rather than the loss of pilin structures (Bretschger, Obraztsova et al. 2007; Bouhenni, Vora et al. 2010). In addition, gene expression comparison between one *S. oneidensis* knockout and the wild type show that even when the function of the knockout strain appears similar, there are many gene expression changes occurring which are not easily observed (Thompson, Beliaev et al. 2002). This indicated that mutant studies should be interpreted very carefully and mechanistic studies of individual proteins should be used as corroborating evidence. Indeed, a Tn7-based insertion of GFP into the genome causes a loss of motility in *S. oneidensis*, indicating that even seemingly simple genetic modification can have complex unintended effects (Thormann, Saville et al. 2004).

2.3.6 Protein structure and localization studies relevant to BESs

Studies on the structure and location of OMCs have been performed in an effort to understand how they conduct electrons across the membrane. Recently, structures for two multi-heme cytochromes relevant to BESs have been solved by x-ray crystallography. Pokkuluri et al. (2011) determined the structure of a dodecaheme c-type cytochrome of *G. sulfurreducens*, finding a long, thin protein with a nanowire-like organization of the twelve heme groups. Clarke et al. (2011) reported a high-quality structure for the outer-membrane, decaheme, *c*-type cytochrome MtrF of *S. oneidensis*. They also suggested a possible binding site for donation of electrons to MtrF from MtrE and a possible site of electron exit from the protein and suggested that the structure may be conducive to flavin binding. However, flavin was not found in the structure, and protein crystals did not form in the presence of exogenous FMN. In both cases the positions of all heme groups were resolved, showing that they are all at a close enough distance to transfer electrons efficiently with their nearest neighbor (Clarke, Edwards et al. 2011). This is the first

structural documentation of an "electron conduit" through an OMC relevant to bioelectrochemical systems.

Before the structures of these cytochromes were solved, the location of related OMCs at the cell surface was determined. Lower et al. (2009) used antibody recognition force microscopy to visualize the localization of OmcA and MtrC at the outer surface of *S. oneidensis* MR-1 cells. Likewise, Leang, et al. (2010) used immunogold labeling to show the localization of OmcS on the surface and pili of *G. sulfurreducens*. Nevin, et al. (2009) took a simpler approach by washing loosely bound proteins from the cell surface, and staining them with heme stain. Several of the bands visualized were identified as OMCs by LC-MS.

These localization studies imply an EET mechanism for OMCs, yet they do not prove that these proteins are capable of interacting with solid electrodes in oxidation and reduction reactions. To understand the direct interaction between these proteins, there have been several direct electrochemical studies of purified OMCs. For example, a study by Hartshorne et al. (2007) revealed that MtrC from *S. oneidensis* MR-1 can participate in redox reactions with carbon electrodes between ca. +100 mV_{SHE} and -500 mV_{SHE}. This confirms that DET from *S. oneidensis* is a viable mechanism, although it also uses flavin mediators.

3.7 Challenges for molecular biology study of BESs

There are several caveats to applying the previously mentioned molecular biology tools to BESs; most notably the heterogeneity of biofilm microenvironments, and therefore gene expression in biofilms (Franks 2010). In some cases, this problem can be avoided by microdissection of bacterial biofilms and separate transcriptomic analysis of cells at different levels of the biofilm. Franks et al. (2010) demonstrated this approach with thick biofilms of *G. sulfurreducens* grown on anodes. This study showed increased expression of 146 genes in the cells closest to the anode

surface, including a number of ribosomal proteins, indicating that proximity to the electrode may indeed be a driving force in the expression of these genes. This approach may be useful in the study of other BES systems, although not all organisms produce a thick (>50 μm) biofilm similar to that of *G. sulfurreducens*. Differences between mRNA expression levels and corresponding protein expression levels due to translational regulation can also cause problems. For example, simultaneous proteomic and transcriptomic analysis of *S. oneidensis* MR-1 grown under different anaerobic conditions by Beliaev et al. (2002) showed consistent results for some genes, but different results for other genes.

2.4. Conclusions

Bioelectrochemical systems are a valuable research topic for their potential applications in bioenergy, biosensing, and biogeochemical research. Using molecular biology tools to study pure cultures in BESs can improve understanding of environmental processes and possibly lead to improvements in BESs for bioenergy. *S. oneidensis* MR-1 is an important model microbe for this research because it uses multiple extracellular electron transport pathways. Improving the understanding of the extracellular electron transport mechanisms of this organism is important for BES research, as well as understanding how different EET mechanisms may be important in environmental settings.

CHAPTER 3

OXYGEN ALLOWS *SHEWANELLA ONEIDENSIS* MR-1 TO OVERCOME MEDIATOR WASHOUT IN A CONTINUOUSLY-FED BIOELECTROCHEMICAL SYSTEM

Adapted from: TerAvest, Rosenbaum, Kotloski, Gralnick, and Angenent. Submitted to *Biotechnology and Bioengineering*, July 2013.

3.1 Abstract

Many bioelectrochemical systems (BESs) harness the ability of electrode-active microbes to catalyze reactions between electrodes and chemicals, often to perform useful functions such as wastewater treatment, fuel production, and biosensing. A microbial fuel cell (MFC) is one type of BES, which generates electric power through microbial respiration with an anode as the electron acceptor, and typically with oxygen reduction at the cathode to provide the terminal electron acceptor. Oxygen intrusion into MFCs is typically viewed as detrimental because it competes with anodes for electrons and lowers coulombic efficiency. However, recent evidence suggests it does not necessarily lead to lower performances—particularly for the model microbe *Shewanella oneidensis* MR-1. Because flavin-mediated electron transfer is important for *Shewanella* species, which can produce this electron shuttle endogenously, we investigated the role of flavins in the performance of pure-culture BESs with *S. oneidensis* MR-1 with and without oxygen. We found that oxygen increases current production more than 2-fold under continuously-fed conditions, but only modestly increases current production under batch-fed conditions. We hypothesized that oxygen is more beneficial under continuously-fed conditions because it allows *S. oneidensis* to grow and produce flavins at a faster rate, and thus lowers flavin washout. Our conclusions were supported by experiments with a flavin-deficient mutant of *S. oneidensis*.

3.2 Introduction

Microbes interact with solid-state electrodes through oxidation or reduction reactions in bioelectrochemical systems (BESs). BESs are under development for several applications, including wastewater treatment, biosensing, biocomputing, and chemical or fuel production (He, Minteer et al. 2005; Logan, Hamelers et al. 2006; Logan, Call et al. 2008; Rozendal, Leone et al. 2009; Li, Rosenbaum et al. 2011; Friedman, Rosenbaum et al. 2012). Many of these applications involve the production of electric current at anodes as a product or output signal. A commonly studied BES is a microbial fuel cell (MFC) that simultaneously treats wastewater and generates electric power. For MFCs, oxygen intrusion is considered detrimental to performance because oxygen competes with anodes for electrons, and therefore lowers coulombic efficiency (*i.e.*, the percentage of metabolic electrons that are captured by the external circuit) (Liu and Logan 2004; Logan, Hamelers et al. 2006; Fan, Hu et al. 2007; Quan, Quan et al. 2012). Oxygen can also be a problem because some important electrode-active bacteria (*e.g.*, *Geobacter sulfurreducens*) are only minimally aerotolerant, and may be inhibited by higher concentrations of oxygen (Lin, Coppi et al. 2004; Freguia, Rabaey et al. 2008).

Indeed, in batch-fed experiments without substrate addition in stationary phase, oxygen caused a decrease in current production with lactate as the electron donor for *S. oneidensis* MR-1 (Ringeisen, Ray et al. 2007). However, several researchers have documented the opposite—an increase in current production when BESs with *S. oneidensis* MR-1 were supplemented with oxygen. For example, in semi-batch experiments performed with periodic lactate addition after initial substrate depletion, an increase in maximum current production was observed in response to oxygen (Biffinger, Ray et al. 2009). In continuously-fed BESs, oxygen addition resulted in a sustained 3-fold increase in current production (Rosenbaum, Cotta et al. 2010). In summary, results on oxygen addition to batch-fed BESs with pure cultures of *Shewanella* sp. have been

mixed, while results for continuously-fed BESs have shown a prominent increase in current in response to oxygen. Although the proteins necessary for electrode reduction are downregulated under aerobic conditions (Rosenbaum, Bar et al. 2012), anaerobic micro-environments (e.g., lower biofilm layers) may allow *S. oneidensis* to produce these proteins in generally aerobic environments.

A key difference between batch- and continuously-fed modes is that cells and metabolites are washed out of the latter system by constant medium replacement. Because *S. oneidensis* is capable of both direct electron transfer (DET) and mediated electron transfer (MET) (Marsili, Baron et al. 2008; Coursolle, Baron et al. 2010; Carmona-Martinez, Harnisch et al. 2011), medium washout is particularly important because it influences which electron transfer mechanism is used by this organism. Both mechanisms involve the Mtr pathway, which transports electrons to the outer surface of the cell and transfers them to electrodes, flavins, or other electron acceptors (Coursolle, Baron et al. 2010). DET occurs when the Mtr pathway transfers electrons directly to electrodes or other solid-state electron acceptors, and MET occurs when electrons are transferred to flavins or other electron shuttles. Riboflavin and flavin mononucleotide are the main electron shuttles that transfer electrons between *S. oneidensis* and external electron acceptors. *S. oneidensis* not only uses flavins as electron shuttles, but also produces and secretes them at concentrations up to 250 nM (Marsili, Baron et al. 2008; von Canstein, Ogawa et al. 2008).

Previous modeling efforts and thermodynamic calculations have indicated that MET may cause lower efficiencies and higher cellular energy losses than DET (Mahadevan, Bond et al. 2006; Schröder 2007), and therefore MET has been reflected on less favorably than DET for BES applications (Lovley 2006). In addition, electron shuttles can be washed out in the effluent

of continuous-flow systems, which is particularly problematic for exogenously added mediators (Rabaey, Rodriguez et al. 2007; Read, Dutta et al. 2010). Even for endogenously produced mediators, the ability of cells to produce the compound faster than the washout rate would be a limiting factor (Schröder 2007). This effect has been shown to reduce current production from *Pseudomonas aeruginosa* in continuously-fed BES (Read, Dutta et al. 2010). However, if electrostatic interactions between electron shuttles and electrodes are accounted for, models predict higher favorability of MET compared to previous calculations (Rabaey, Rodriguez et al. 2007). Further, riboflavin adsorbs to graphite, which is a common electrode material in BESs (Miyawaki and Wingard 1984; Sun, Kong et al. 1996), making retention of this mediator in BESs more likely. Adsorbed flavins may possibly desorb when flavin concentrations in the bulk liquid drop to increase electron transfer from planktonic cells or improve electron transfer rates at the cell-electrode interface.

Flavins are important for several reasons. First, flavins influence extracellular electron transfer from *S. oneidensis* by increasing the specific electron transfer rate for each cell (Marsili, Baron et al. 2008; von Canstein, Ogawa et al. 2008). They are predicted to interact with outer membrane cytochromes *via* specialized binding sites (Clarke, Edwards et al. 2011), and are reduced by the same electron conduit responsible for reduction of insoluble electron acceptors in *S. oneidensis* (Coursolle, Baron et al. 2010). Second, flavins give direction to each *S. oneidensis* cell through taxis. *S. oneidensis* migrates toward soluble and insoluble electron acceptors (Nealson, Moser et al. 1995; Bencharit and Ward 2005), and Li et al. (Li, Tiedje et al. 2012) have shown that taxis toward electron acceptors is enabled by redox gradients of flavin molecules, which are sensed by the cells. Therefore, flavins are crucial to *S. oneidensis* not only for electron transfer but also for making initial contact with insoluble electron acceptors.

Early experiments using medium replacement showed that flavin-based MET could account for up to 80% of electron flux from *S. oneidensis* (Marsili, Baron et al. 2008). This number was confirmed by using an *S. oneidensis* MR-1 lacking a flavin exporter to find that MET accounted for 75% of electron flux (Kotloski and Gralnick 2013). Electrochemical analyses have estimated that DET and MET are each responsible for *ca.* 50% of electron flux (Carmona-Martinez, Harnisch et al. 2011). The difference between these numbers may be due to errors associated with the electrochemical measurement, and differences in the culture conditions. This analysis used cyclic voltammetry to distinguish between DET and MET taking advantage of the fact that electron transfer occurs at a different electrochemical potential for each mechanism. For *S. oneidensis,* DET has an onset of *ca.* +0.3 V_{SHE}, while MET has an onset of *ca.* -0.1 V_{SHE} (closer to -0.2 V_{SHE} in our system) due to the differing redox potentials of *c*-type cytochromes and flavins, respectively. The magnitude of current production in each potential range provides an indication of the importance of each mechanism under the given conditions (Carmona-Martinez, Harnisch et al. 2011). Cyclic voltammetry has provided important insights into the electrochemical behavior of *S. oneidensis*, however, to date it has only been used on cultures in batch-fed mode, and the balance between DET and MET in continuously-fed mode is unknown. Considering that a large portion of electron flux goes through MET in all previously tested conditions, it is important to determine how this balance changes when flavins are washed out by medium replacement. Because the influence of oxygen and the interplay of DET and MET are poorly understood in continuously-fed BESs with *S. oneidensis*, we combined electrochemical techniques with a comparison between wild-type (WT) *S. oneidensis* MR-1 and a flavin-secretion-deficient mutant (Δ*bfe* strain) (Kotloski and Gralnick 2013) to determine the

relative importance of DET and MET under anaerobic and micro-aerobic, and batch- and continuously-fed conditions, in a 2 x 2 x 2 experimental design (**Table 3.1**).

Table 3.1. Summary of the 2 x 2 experimental design that was utilized for each of the 2 strains (*i.e.*, WT and *Δbfe S. oneidensis*) in 250 mL anode chambers.

batch-fed anaerobic sparged with N_2	**batch-fed micro-aerobic** used passive air diffusion
continuously-fed anaerobic fed medium at 15 mL/h sparged with N_2	**continuously-fed micro-aerobic** fed medium at 15 mL/h bubbled air at 1/s

3.3 Materials and methods

3.3.1 Bioreactor setup and sampling

We used two-chambered glass bioelectrochemical reactors, with an anion exchange membrane (Membranes International, Ringwood, NJ) separating the two chambers. A three-electrode system consisting of working, counter, and reference electrodes was used to maintain a consistent and defined electrochemical environment in the bioreactors. The working electrode consisted of a 9 cm x 9 cm piece of carbon cloth (PANEX ® 30 - PW06, Zoltek Corp, St Louis, MO) affixed to a carbon rod with carbon cement (CCC Carbon Adhesive, EMS, Hatfield, PA). The working electrode was poised at +0.2 V *vs.* Ag/AgCl/sat'd KCl (+0.397 V_{SHE}) using a potentiostat (VSP, BioLogic USA, Knoxville, TN). This potential was chosen because it allows

S. oneidensis to use both DET and MET. The counter electrode consisted of a carbon block affixed to a carbon rod (Poco graphite, Decatur, TX) with conductive carbon cement and the counter chamber was filled with 300 mL PBS (100 mM phosphate buffer, 50 mM NaCl).

The working chamber was filled with 250 mL of a modified M4 medium containing per liter deionized water: 0.221 g K_2HPO_4; 0.099 g KH_2PO_4; 0.168 g $NaHCO_3$; 1.189 g $(NH_4)_2SO_4$; 7.305 g NaCl; 1.192 g HEPES; 0.5 g yeast extract; 0.5 g tryptone; 10 mL trace mineral solution; 10 mL $CaCl_2$ stock solution; and 20 mM sodium L-lactate (added from filter sterilized stock solution after autoclaving). The trace mineral solution consisted of per liter deionized water: 2.26 g Na_2EDTA; 24.89 g $MgSO_4 \cdot 7H_2O$; 0.029 g $MnSO_4 \cdot 4H_2O$; 0.058 g NaCl; 0.068 g $FeCl_2$; 0.065 g $CoCl_2$; 0.029 g $ZnSO_4 \cdot 7H_2O$; 0.005 g $CuSO_4 \cdot 5H_2O$; 0.35 g H_3BO_3; 0.08 g Na_2MoO_4; 0.119 $NiCl_2 \cdot 6H_2O$; and 0.028 Na_2SeO_4. The $CaCl_2$ stock consisted of 7.13 g $CaCl_2 \cdot 2H_2O$ dissolved in 1 liter deionized water. Chemicals were purchased from Sigma Aldrich or VWR and used as provided. For continuously-fed reactors, the medium was fed at a rate of 10-15 mL per h with a peristaltic pump (Cole-Parmer, Vernon Hills, IL) from a 10-L reservoir, resulting in a hydraulic retention time of 20 h. The entire system was sterilized by autoclaving at 121^{o}C for 1 h. The working chamber was maintained at 30^{o}C using a water jacket and a recirculating water heater (Model 1104, VWR Scientific, Radnor, PA) and the working chamber was mixed by a magnetic stir bar at *ca*. 200 rpm. Anaerobic reactors were constantly sparged with sterile N_2 gas (high purity gas, used as provided). Batch-fed, micro-aerobic reactors received oxygen through passive air diffusion, while continuously-fed, micro-aerobic reactors were slowly bubbled (1 bubble/s) with sterilized room air to offset the continuous feeding of anaerobic medium and to manage similar oxygen availability compared to the batch-fed reactors. The oxygen content of the micro-aerobic reactors was measured using a battery-powered dissolved oxygen probe (DO110,

Oakton, Vernon Hills, IL) to prevent electric short-circuiting. We maintained low oxygen provision rates such that prior to inoculation typical DO values ranged from 85-95% saturation, but within 12 h of inoculation they decreased to levels below the detection limit. Dissolved oxygen remained below the detection limit for the remainder of the experiments due to rapid utilization by the bacteria, and therefore we did not perform detailed analyses on DO concentrations. We replicated each experimental condition three times (WT batch-fed) or four times (mutant batch-fed; WT continuous-fed; mutant continuous-fed).

The reactors were sampled daily, and pH and OD_{600} were measured. After 5 h of background current measurement, the reactors were inoculated with 3 mL of an overnight culture of *S. oneidensis* MR-1 that was diluted to an OD_{600} of 0.1 in LB. *Shewanella oneidensis* MR-1 (WT) and the Δ*bfe* strain (mutant) were grown in LB medium and on LB agar plates for maintenance. Plates were periodically streaked from stocks stored in 50% glycerol at -80^{o}C. Current was recorded by the potentiostat and the reactors were sampled for 7 days. Samples (1.5 mL) were centrifuged at 10,000 rpm for 10 min and the pellets and supernatants were stored separately at -20^{o}C. Protein was extracted from the pellets by adding 1.0 mL of 0.2 M NaOH and incubation at 96^{o}C for 1 h. At the end of each experiment, the working electrode was removed and stored at -20^{o}C. Biofilm protein was extracted by adding 25 mL of 0.2 M NaOH and incubation at 96^{o}C for 1 h.

3.3.2 Analytical methods

Lactate and acetate concentrations in the samples were measured by HPLC (600 HPLC, Waters, Milford, MA). We used an Aminex HPX-87H column (Bio-Rad, Hercules, CA) at a temperature of 65^{o}C, and a 5 mM sulfuric acid eluent at a flow rate of 0.6 mL/min. Metabolites were detected *via* an RI (refractive index) detector (410 Differential Refractometer, Waters,

Milford, MA). Protein was measured in the pellet and biofilm NaOH lysed extracts using a BCA assay, following the instructions of the manufacturer (Thermo Scientific, Waltham, MA). Heme was measured in the same extracts by absorbance at 420 nm using hematin as a standard (Appaix, Minatchy et al. 2000). Both measurements were performed using a 96-well plate reader (Synergy 4, BioTek Instruments, Winooski, VT). ANOVA was performed using standard functions in R. Unless otherwise stated, two-tailed t-tests were used to test significance.

3.4 Results and Discussion

3.4.1 Results for WT S. oneidensis *MR-1*

We utilized both batch- and continuously-fed BESs with *S. oneidensis* MR-1 to investigate the relative importance of DET and MET in BESs with oxygen. We used a 2 x 2 x 2 experimental design varying the strain used, hydrodynamic condition, and oxygen level (**Table 3.1**). Micro-aerobic BESs with WT *S. oneidensis* achieved significantly higher maximum current production than anaerobic BESs ($p<0.05$, two tailed t-test) under both batch-fed and continuously-fed conditions (**Figure 3.1**). The increase was modest with the WT strain for the batch-fed BESs (31.9%) and considerable for the continuously-fed BESs (254.8%). For batch-fed mode, we reported the absolute maximum current reading, which typically occurred ~20 h or ~36 h after inoculation for the WT and mutant, respectively. For the continuously-fed mode, we report the maximum current production *after* a short peak and subsequent drop on the 2nd day. This maximum typically occurred on the 7th day of operation (**Figure 3.2**). The early peak was caused by high microbial growth in the startup phase before lactate concentration and pH reached equilibrium values (**Figure A1.1**). The feeding rate in the continuously-fed reactors was chosen such that excess substrate was always available. Substrate utilization at maximum current production ranged from 0 to 24% (residual lactate 20 to 15.2 mM) for anaerobic reactors and 30

to 90% (residual lactate 14 to 2 mM) for micro-aerobic reactors (0% indicates that the change in lactate concentration was within the error of our measurement).

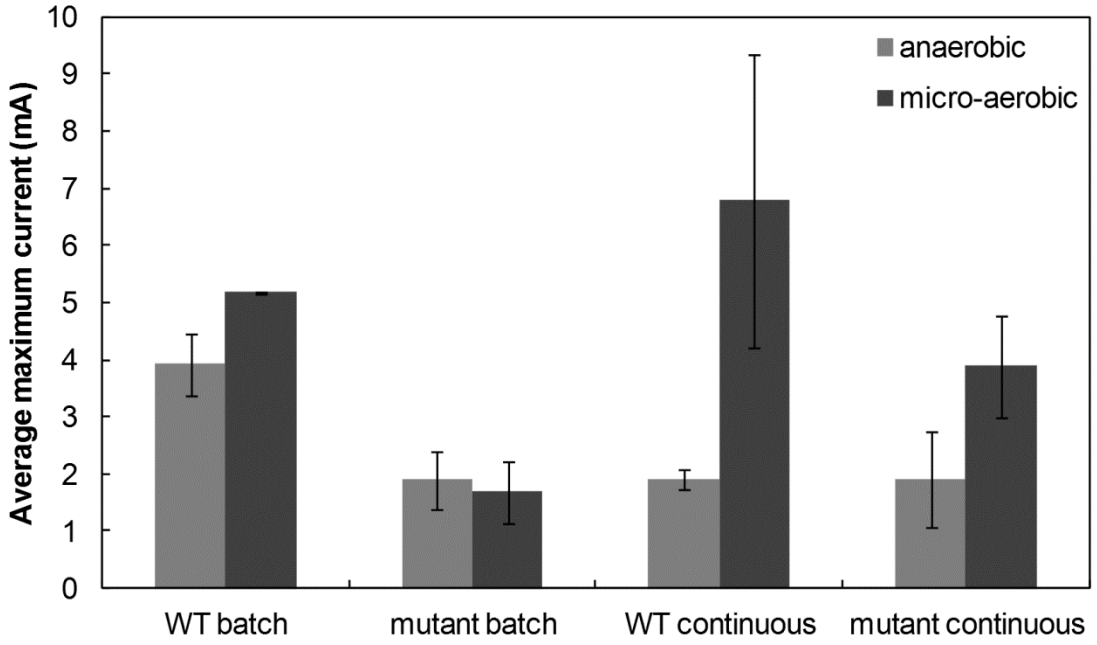

Figure 3.1. Average maximum current production from bioelectrochemical systems with *S. oneidensis* grown in micro-aerobic or anaerobic conditions (n=3 or n=4). For batch-fed conditions this represents absolute maximum and for continuously-fed conditions this represents the maximum (~7 days) after an initial current spike (~2 days).

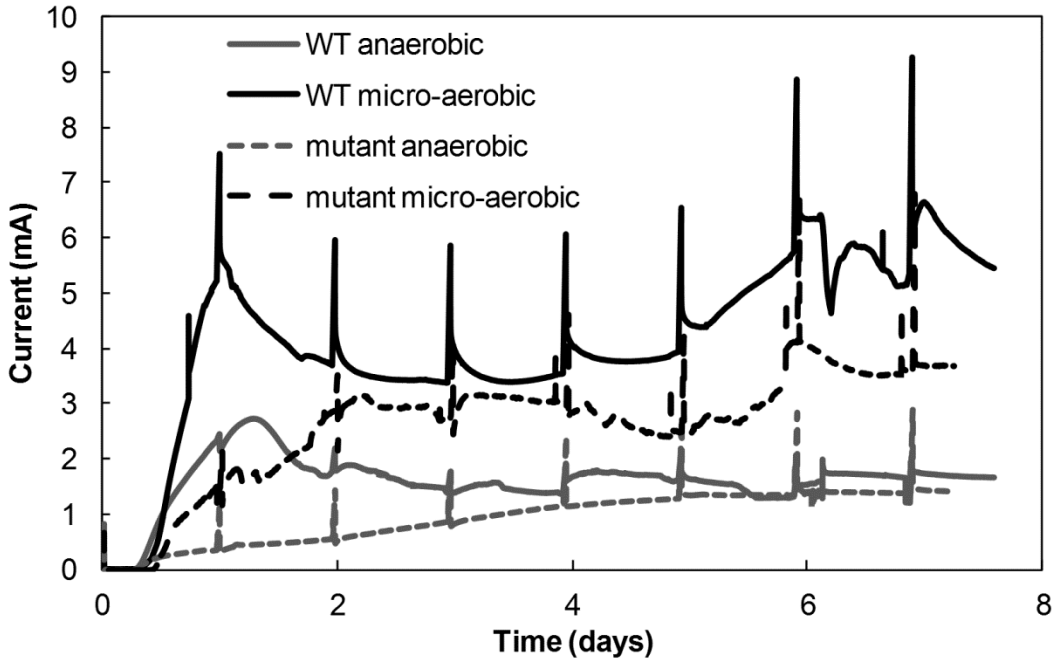

Figure 3.2. Current production over time in continuously-fed bioelectrochemical systems with WT *S. oneidensis* grown under micro-aerobic or anaerobic conditions. Each current profile is the average from four experiments. The current was recorded by a potentiostat at a working electrode poised at +0.397 V_{SHE}. Gray lines represent anaerobic conditions and black lines indicate micro-aerobic conditions. Solid lines represent WT *S. oneidensis* MR-1 and dashed lined represent its flavin-secretion-deficient mutant (Δ*bfe* strain) (Kotloski and Gralnick 2013). The daily current spike is an artifact of switching between chronoamperometry and cyclic voltammetry methods.

The current enhancement in batch-fed mode is within the range seen in previous studies (Ringeisen, Ray et al. 2007; Biffinger, Ray et al. 2009), and the enhancement in the continuously-fed system is very similar to a previous study performed with the same bioreactors, indicating that the methods used here are consistent with previous research on WT *S. oneidensis* BESs with oxygen (Rosenbaum, Cotta et al. 2010). Increased planktonic cell density and biofilm formation have been implicated as causes for the increase in current density associated with oxygen addition to BESs with WT *S. oneidensis* MR-1 (Rosenbaum, Cotta et al. 2010). Oxygen addition increased biofilm biomass (mg of protein attached to the electrode) in the reactors under batch-fed and continuously-fed conditions by ~4- and ~2-fold, respectively. Planktonic biomass increased by ~3-fold for both batch-fed and continuously-fed conditions (**Table 3.2**). Three-

factor ANOVA for measurements of biofilm and planktonic biomass indicated that oxygen significantly increased both planktonic and biofilm biomass (**Table 3.3**). Although previous work demonstrated that removal of oxygen from *S. oneidensis* biofilm may cause rapid detachment, it is unclear how this phenomenon would affect our biofilm measurements because biofilms were grown and maintained either under micro-aerobic or anaerobic conditions, and never switched from one condition to the other (Thormann, Saville et al. 2005).

Table 3.2. This table includes average OD_{600} and biofilm biomass values, and number of replicates for each experimental condition. OD_{600} is reported for the day of maximum current production and biofilm biomass values are mg of total protein attached to the electrode at the end of the experiment.

	OD_{600} mean	**OD_{600} std deviation**	**biofilm mean**	**biofilm std deviation**	**# of samples**
WT - batch					
anaerobic	0.13	0.04	3.30	0.96	3
micro-aerobic	0.36	0.03	14.60	1.52	3
mutant - batch					
anaerobic	0.13	0.02	6.72	1.35	4
micro-aerobic	0.49	0.28	15.56	2.43	4
WT - continuous					
anaerobic	0.21	0.05	7.69	4.90	4
micro-aerobic	0.75	0.30	29.59	10.20	4
mutant - continuous					
anaerobic	0.18	0.03	7.96	1.82	4
micro-aerobic	0.52	0.10	36.90	37.51	4

To gain a more detailed picture of the changes caused by oxygen addition, we performed turnover cyclic voltammetry analysis daily. We scanned the potential from -0.303 V_{SHE} to +0.697 V_{SHE} and back at a scan rate of 2 mV/s (in duplicate). We intended to use the method of Carmona-Matinez et al. (Carmona-Martinez, Harnisch et al. 2011) to separate direct and mediated electron transfer, but differences in pH (pH varied between 5.7 and 7.0 throughout the operating periods of all experiments) and other variables between different experimental

conditions and time points made quantitative analysis of the cyclic voltammograms difficult. However, qualitative visual analysis of the voltammograms was informative. We compared the voltammograms for each of the reactors with the WT strain and found that within batch systems oxygen mainly enhanced DET (attributed to increased biofilm growth), while in continuous systems oxygen mainly enhances MET (attributed to an increase in flavin concentrations; **Figure 3.3**).

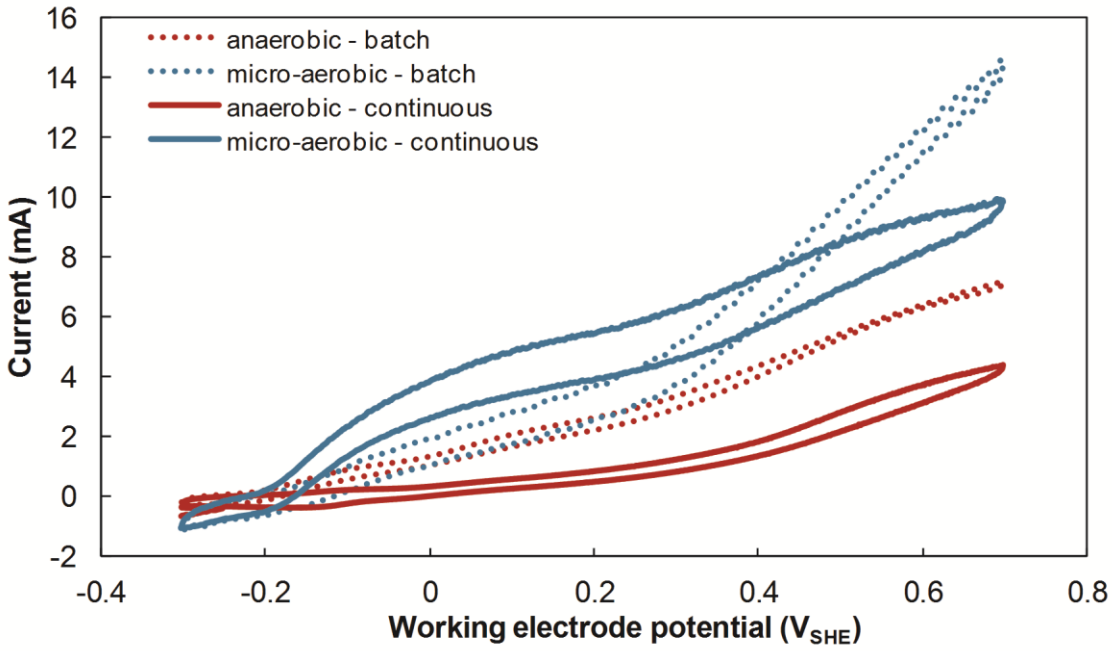

Figure 3.3. Representative cyclic voltammograms from the day of maximum current production for WT *S. oneidensis* MR-1 under each experimental condition. Cyclic voltammetry was performed using a potentiostat scanning from -0.303 V_{SHE} to 0.697 V_{SHE} at a scan rate of 2 mV/s.

Prominent flavin-mediated catalytic waves were observed in all reactors (at an onset of close to -0.2 V_{SHE}), except in the continuously-fed, anaerobic BES. This indicates that under batch-fed conditions flavins were accumulated to electrochemically relevant rates whether or not oxygen was present, but under continuously-fed conditions only the micro-aerobic BES produced flavins at a sufficient rate to overcome washout and accumulate to electrochemically

relevant concentrations. Flavins have previously been shown to increase electron transfer rates from *S. oneidensis* in BESs (Marsili, Baron et al. 2008), and therefore we expected that the increased presence of flavins could account for some of the current enhancement seen in continuously-fed BESs with oxygen. We attempted to confirm the results of our cyclic voltammetry analysis by measuring flavin concentrations by LC/MS/MS, but we were not able to obtain quantitative results. The peak areas for flavins in samples from continuously-fed reactors were small, and in some samples flavins were not detected at all. Because the concentrations were close to the detection limit of the LC/MS/MS method, we chose to use biological methods to investigate the influence of flavins in this system.

3.4.2 Analysis of a flavin-secretion deficient mutant strain of S. oneidensis

To further elucidate the links between oxygen, flavins, and current production, we sought to eliminate the effect of flavins. This was possible through the use of an *S. oneidensis* mutant strain that is incapable of excreting flavins (Δ*bfe* strain) (Kotloski and Gralnick 2013). We repeated all the experiments described for the WT strain using this mutant strain and compared electrochemical and other measurements. For all experimental conditions this mutant produced less current than the WT (under corresponding conditions). In batch-fed reactors with this mutant, oxygen *decreased* maximum current production by 11.5% (consistent with expectations for electron acceptor competition); and in continuously-fed reactors, oxygen *increased* maximum current production by 102.2% (**Figure 3.1**). This is in sharp contrast to the reactors containing WT *S. oneidensis*, which showed a much larger increase in current production in response to oxygen addition and this alteration in the *difference* between micro-aerobic and anaerobic conditions reveals the importance of the Δ*bfe* mutation (**Figure 3.1**). We performed three-factor ANOVA on maximum current production values and found significant interaction ($p<0.05$)

between presence of oxygen and presence of flavins (*i.e.*, WT *vs.* mutant). This indicates that flavin concentration was a significant factor in the difference between anaerobic and micro-aerobic conditions. Although oxygen addition caused many changes in the reactor, this statistical result indicates that flavin production was, indeed, a significant factor in the current increase caused by oxygen. We cannot conclude whether this was due to increased flavin production on a per cell basis, or simply increased flavin production by increased biomass, however, in either case oxygen allows *S. oneidensis* to functionally maintain MET as a viable extracellular electron transfer pathway under continuous flow conditions.

Planktonic cell densities and quantitative biofilm biomass levels in reactors with the mutant strain were not significantly different (three-factor ANOVA, **Table 3.3**) from WT *S. oneidensis* (**Figures A1.2 and A1.3**). The only exception (found by individual, two-tailed, t-tests) was in the batch-fed, anaerobic condition, wherein the mutant produced significantly more biofilm biomass than WT ($p<0.05$). However, this did not result in higher current production for the mutant compared to WT. Because we did not observe consistent or statistically significant differences in biomass production between the WT and mutant strains, we did not consider the biomass concentration to be a major factor causing differences in current production between the two strains. Therefore, we relate the difference in current production between the WT and mutant strains to the effect of flavin secretion rather than a growth defect of the mutant (which we did not observe).

Table 3.3. This table includes p-values for three ANOVA tests (each three-factor), for current production, planktonic growth (OD_{600}) and biofilm biomass values. The three factors used were the strain (WT or mutant), flow conditions (batch or continuous), and oxygen (present or absent). Significance codes: * ≤ 0.05, ** ≤ 0.01, *** ≤ 0.001. p-values for the significance of each factor, and interaction between factors are included).

Factor	current production	planktonic growth	biofilm growth
A: WT *vs.* Δ*bfe*	$9.91x10^{-5}$***	0.078	0.670
B: batch *vs.* continuous	0.220	0.003**	0.060
C: anaerobic *vs.* micro-aerobic	$1.36x10^{-4}$***	$2.98x10^{-7}$***	0.002**
A:B	0.129	0.213	0.885
A:C	0.018*	0.228	0.154
B:C	0.007**	0.045*	0.662

Similar to the reactors with WT *S. oneidensis*, cyclic voltammetry analysis was performed on the reactors with the mutant strain. As anticipated, the BESs with the mutant strain did not show a visible catalytic wave for flavin-based MET, except for in the micro-aerobic, continuous condition (**Figure 3.4**). This could be due to some flavin buildup from lysed cells. Although the growth medium used contained 0.5 g/L yeast extract, flavin use was not visible in most conditions for the mutant strain, indicating that flavins in the yeast extract were not in high enough concentrations to support significant MET. In contrast to the WT strain, the shapes of the anaerobic and micro-aerobic voltammograms were very similar for the flavin-deficient strain. For both batch-fed BESs, there was a slight *increase* in the DET-based wave during micro-aerobic conditions, and for continuously-fed BESs there was an *increase* in the DET-based wave during micro-aerobic conditions. The changes in the DET-based wave mirror the changes in total current production, indicating that cell growth and *c*-type cytochrome content were the major

drivers of differences between the anaerobic and micro-aerobic conditions for the flavin-deficient mutant. By comparing the current increases for the WT and flavin-deficient mutant strains, we inferred that for the WT *ca.* 40% of the current increase due to oxygen is related to increased growth and *ca.* 60% is due to increased flavin concentrations, because the increase for the mutant strain is 40% as large as the increase for the WT strain.

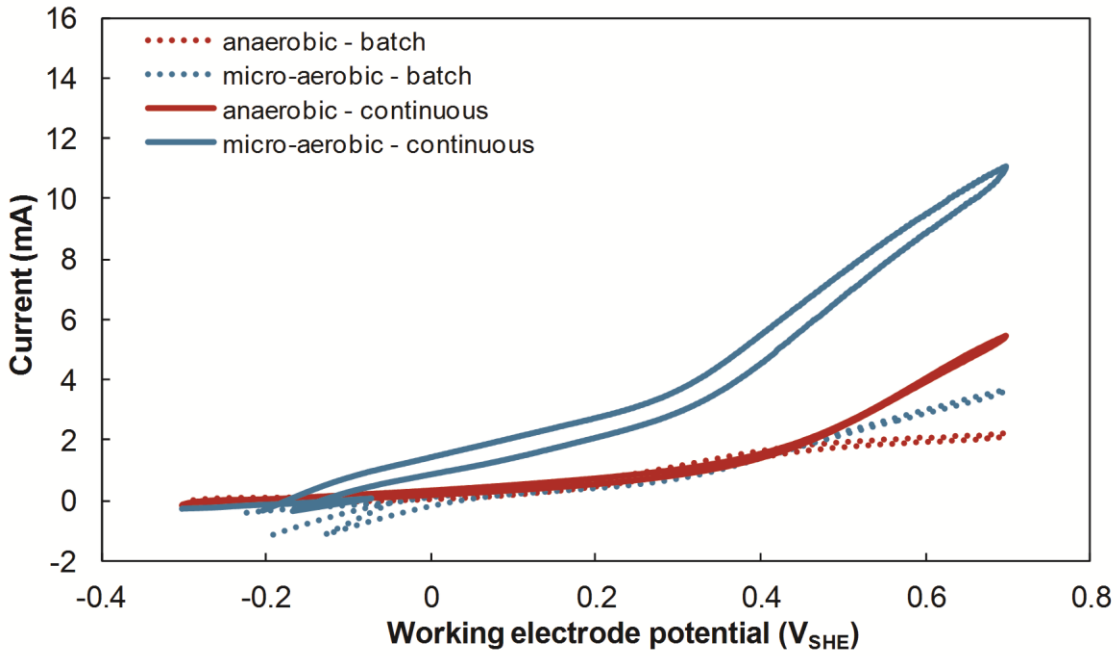

Figure 3.4. Representative cyclic voltammograms from the day of maximum current production for the *S. oneidensis* Δ*bfe* strain under each experimental condition. Cyclic voltammetry was performed using a potentiostat scanning from -0.303 V_{SHE} to 0.697 V_{SHE} at a scan rate of 2 mV/s.

3.4.3 c-*type cytochrome content in continuously-fed BESs*

After we determined that the relative importance of DET and MET changed depending on our experimental conditions, we examined cell physiology more closely for the continuously-fed BESs. Cytochrome content is an important parameter for electrode respiring bacteria, because outer membrane cytochromes are important for extracellular electron transfer. In these experiments, cytochrome content was estimated by measuring heme concentration (Appaix,

Minatchy et al. 2000), resulting in levels between 0.08 and 1.57 μmol hematin per mg of protein. The heme concentration was normalized to protein measurements taken for the same extracts. For the WT, the heme content of the cells was significantly lower ($p<0.05$) under micro-aerobic conditions than under anaerobic conditions (**Figure 3.5**).

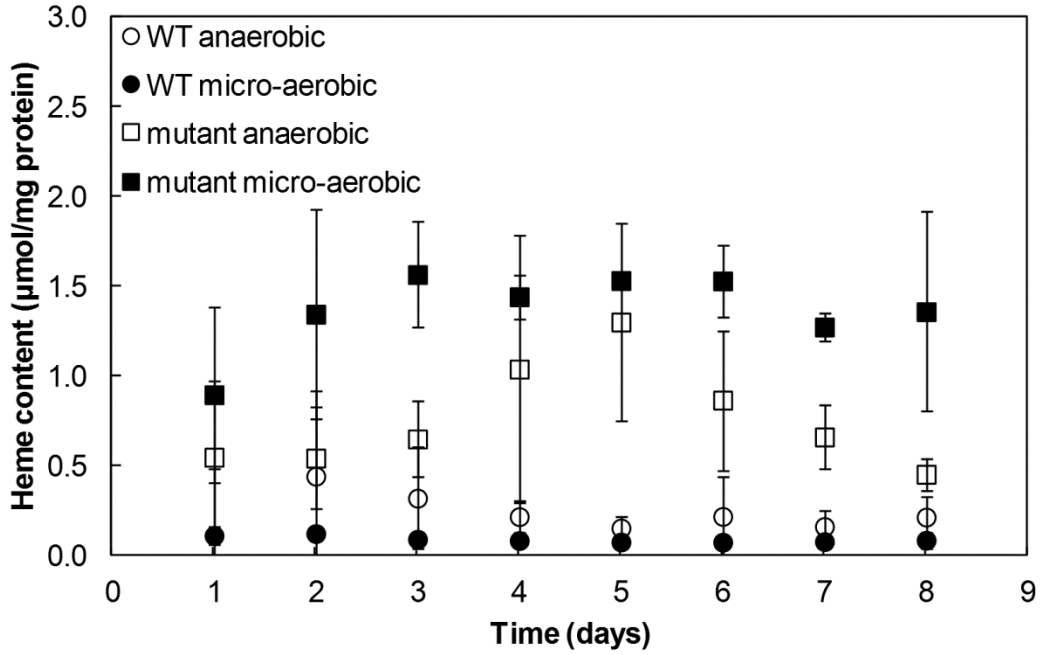

Figure 3.5. Heme content of planktonic cells over the course of the experiments (continuously-fed bioreactors only).

Heme concentrations were consistent with the hypothesis that flavins enhance the specific electron transfer rate for extracellular cytochromes, because micro-aerobic cells exposed to increased flavin concentrations would require fewer cytochromes to maintain the same electron transfer rate. Conversely, the mutant cells accumulated more heme per cell under micro-aerobic conditions, indicating that additional cytochromes are necessary to support the increased metabolic rate with oxygen in the absence of excreted flavins. This may constitute a compensatory mechanism, whereby the Δ*bfe* strain balances the lack of flavins by increasing cytochrome expression. As yet, a sensing system that could regulate these changes is unknown,

and further work would be necessary to address the possible expression changes caused by the Δ*bfe* mutation in BESs.

3.5 Conclusions

The results presented here confirm that oxygen improves current production by *S. oneidensis* in continuously-fed mode and further our understanding of the complex interplay between competing electron acceptors and extracellular electron transfer mechanisms. Cyclic voltammetry analysis provided qualitative evidence for a role of flavins in the increase in current production, and the use of a flavin deficient mutant established a statistically significant link between flavin production and increased current production under micro-aerobic conditions. At this point, it is not clear whether flavin production on a per cell basis is altered by oxygen levels, but we have confirmed that oxygen addition allows MET to be viable method of extracellular electron transfer for *S. oneidensis* under continuous-flow conditions. Functionally, this means that oxygen allows *S. oneidensis* to overcome mediator washout caused by hydrodynamic conditions, and this finding may be applicable to other hydrodynamic BES applications with aerotolerant microbes.

3.6 Acknowledgements

We thank Dr. Daniel Bond (University of Minnesota) for helpful comments on the experiments. We thank Elliot Friedman, Devin Doud, and Dylan Webster (Cornell University) for helpful comments during experimentation and preparation of the manuscript. This work was supported by the National Science Foundation through CAREER grant no. 0939882 to L.T.A.

CHAPTER 4

OXIDIZING ELECTRODE POTENTIALS DECREASE CURRENT PRODUCTION AND COULOMBIC EFFICIENCY THROUGH CYTOCHROME *C* INACTIVATION IN *SHEWANELLA ONEIDENSIS* MR-1

Adapted from: TerAvest and Angenent. In preparation for *Biosensors and Bioelectronics*.

4.1 Abstract

Shewanella oneidensis MR-1 is a model microbe for use in bioelectrochemical systems for several reasons, including its ability to produce electric current in the presence of oxygen and its use of endogenous electron shuttles for electron transfer. However, previous transcriptomic profiling has suggested that electrode respiration may induce a general cellular stress response (similar to a heat shock response) in *S. oneidensis*. Analysis of this organism grown with a wide variety of electron acceptors indicated that general stress may be related to the redox potential of the terminal electron acceptor. To test this hypothesis in a strictly controlled manner, we grew *S. oneidensis* at potentiostatically poised electrodes at five redox potentials from -3 and +797 mV_{SHE} and measured current production, coulombic efficiency, and transcription levels of marker genes for stress and protein turnover. We found that current production was maximal at +397 mV_{SHE} and coulombic efficiency was maximal at +197 mV_{SHE}. Both decreased at more positive (oxidizing) potentials, indicating that there is an optimal potential, which is sufficient to allow electron flow, but not high enough to cause stress or damage. Transcript measurements of stress and protein turnover marker genes confirmed that changes in transcription occurred in response to the applied potential, but were not consistent with previous findings of changes in ribosomal protein and general stress expression. We found that transcription of a gene coding for a ribosomal protein, correlated with current production rather than electrode potential, and that

outer membrane cytochrome and protease expression were more closely related to the electrode potential. Cyclic voltammetry revealed that the activity of *c*-type cytochromes was reduced at the higher potentials, indicating that oxidizing electrode potentials decrease current production by directly damaging *c*-type cytochromes at the electrode surface.

4.2. Introduction

Shewanella oneidensis MR-1 is an important model microbe for bioelectrochemical systems (BESs) because it is the only BES model microbe that is capable of both mediated and direct electron transport to solid electron acceptors. It produces and secretes its own mediators (flavins), thus negating the requirement of exogenous mediators (Marsili, Baron et al. 2008; von Canstein, Ogawa et al. 2008). Further, the well-understood extracellular electron transfer pathway of *S. oneidensis* makes it an ideal candidate for generation of biological logic gates and biosensors with electrical output *via* genetic modification (TerAvest, Li et al. 2011; Golitsch, Bücking et al. 2013). Briefly, electrons are transported from the menaquinol pool to the Mtr pathway by CymA, and MtrA and MtrC conduct electrons to the outer surface of the cell, while stabilized by MtrB (Coursolle, Baron et al. 2010; Shi, Rosso et al. 2012). Each enzyme in this pathway has multiple paralogs that have similar functions and may be optimized for interaction with specific electron acceptors (Coursolle and Gralnick 2010).

Although *S. oneidensis* has several advantageous characteristics that support its use in BESs, it converts substrates to electric current at a low coulombic efficiency under continuous flow conditions (Rosenbaum, Cotta et al. 2010). This may be due, in part, to the fact that *S. oneidensis* does not generate ATP using ATP synthase under anaerobic conditions and relies on substrate-level phosphorylation, although an external electron acceptor is still necessary to maintain redox balance, resulting electric current in BESs (Hunt, Flynn et al. 2010). Continuous medium flow may also cause difficulties for *S. oneidensis* because it does not form thick,

conductive biofilms similar to those of *Geobacter sulfurreducens*, and is, therefore, more likely to be washed out of systems with continuous flow conditions (Franks, Malvankar et al. 2010). Further, under typical laboratory conditions, 75-80% of extracellular electron flux goes through the flavin-mediated pathway in *S. oneidensis*, which may decrease performance under continuous flow conditions, with flavins being washed out of the system (Marsili, Baron et al. 2008; Carmona-Martinez, Harnisch et al. 2011; Kotloski and Gralnick 2013). Cell and mediator washout may be overcome by addition of oxygen to BESs, although this occurs at the expense of coulombic efficiency (TerAvest et al., manuscript under review for *Biotechnology and Bioengineering*). Overall, the previously described impediments to current production from *S. oneidensis* in continuously-fed BESs can be summarized as cell and mediator washout and inefficient metabolic pathways.

Another possible reason for the low coulombic efficiency may be that electrode respiration causes a stress response in *S. oneidensis*. Transcriptomic comparison of *S. oneidensis* grown with oxygen or potentiostatically-poised graphite electrodes revealed significant upregulation of both ribosomal proteins and proteases, indicating that protein turnover may be increased under electrode respiring conditions (Rosenbaum, Bar et al. 2012). It is unclear why protein turnover would be increased, but this process is likely to raise maintenance energy costs for *S. oneidensis* (Russell and Cook 1995). Rosenbaum et al. (2012) also found some markers of general stress, such as *dnaK*, were upregulated under electrode-respiring conditions. DnaK is a chaperone protein involved in the heat shock response and is involved in both protein and DNA repair (Schröder, Langer et al. 1993; Goldfless, Morag et al. 2006). Rosenbaum et al. (2012) proposed that this was due to a general stress response in cells grown at electrodes, but did not discover a mechanism for stress induction.

Another study comparing transcriptomes of *S. oneidensis* grown with different natural electron acceptors found significant variation in ribosomal protein expression in response to terminal electron acceptors, although the experimenters attempted to equalize the growth rate (and therefore protein production rate) of all samples by limiting the exposure time to the electron acceptors (Beliaev, Klingeman et al. 2005). Ribosomal protein expression was very similar for soluble and insoluble forms of the same metal, but varied between different metals. Considering that soluble forms are likely to be more toxic than insoluble forms of heavy metals, the redox potential of the metal, rather than toxicity or another property was likely responsible for the changes in ribosomal protein expression. However, no conclusion can be drawn from this data and future work must use better control of experimental parameters (e.g., growth rate, and toxicity of terminal electron acceptor) to elucidate the relationship between the redox potential of the electron acceptor and ribosomal protein expression.

The relationship between oxidizing potentials and cellular stress has already been demonstrated by several research groups. A study on sterilization *via* electrochemical methods indicated that potentials of +920 mV_{SHE} or more decreased the respiratory capability of *Escherichia coli* and *Bacillus subtilis* cells by oxidizing cofactors in the cell membrane (Matsunaga, Namba et al. 1984). A later study concluded that 99% of *E. coli* cells could be killed by a 5-h treatment with +900 mV_{SHE} on granular activated carbon (Matsunaga, Nakasono et al. 1992). A study on electrochemical sterilization *via* reactive oxygen species indicates that cell damage by this mechanism can only occur at much higher potentials, meaning that damage occurring at lower potentials likely occurs through direct oxidation of cell constituents, rather than production of toxic species, indicating that biofilm cells would be more vulnerable than planktonic cells to damage at lower potentials (Jeong, Kim et al. 2006). Sterilization of *S.*

oneidensis cultures by either of these methods has not been reported; therefore we can make no conjecture about the influence of the electrode potential on cell viability based on previous data.

While microbial fuel cells (which produce electric current *via* natural potential differences) are an important BES application, potentiostatically controlled BESs are becomingincreasingly important in new BES research in the areas of biosensing and biocomputing. As potentiostatically poised electrodes become an important tool in BES applications, it is essential to determine optimal potentials for cell growth, current production, and other parameters. Because previous research has suggested that oxidizing electrode potentials change the physiology of *S. oneidensis* in a manner that would inhibit BES performance, we chose to further study cellular stress and damage at electrodes poised at various oxidizing potentials. Our hypothesis was that more strongly oxidizing potentials would decrease BES performance because of either: i) an increase in general cellular stress, similar to a heat-shock response, or; ii) direct damage of proteins or cofactors at the electrode surface. To test this hypothesis, we grew *S. oneidensis* in continuous-flow, potentiostatically-poised bioreactors and measured current production, coulombic efficiency, and transcription of genes coding for ribosomal proteins and stress responses. We compared *S. oneidensis* biofilms grown on electrodes poised at different potentials to determine whether the redox potential of the terminal electron acceptor induces a general cellular stress response in *S. oneidensis*. A poised electrode in a BES is the ideal electron acceptor for this purpose, because its other properties (e.g., toxicity) remain constant while the potential changes.

4.3. Materials and methods

4.3.1 Cell culture and bioreactor operation

S. oneidensis was routinely cultured in liquid lysogeny broth (LB) medium or on solid LB (1.5% agar) at 30^{o}C. After 2 to 3 plate transfers, a new culture was prepared from a glycerol

stock that was maintained at -80^{o}C. During experiments, *S. oneidensis* was cultured in potentiostatically-controlled, two-chambered bioelectrochemical systems. The working electrode consisted of an 8 x 3 cm piece of graphite paper (AvCarb P50, FuelCellStore, Boulder, CO), which was affixed to a graphite rod with conductive carbon cement (CCC Carbon Adhesive, EMS, Hatfield, PA). Ag/AgCl/sat'd KCl electrodes were prepared in house. The working chamber was filled with 250 mL of a modified M4 medium (Rosenbaum, Cotta et al. 2010). Medium was constantly fed to the working chamber at ~10 mL/h, and effluent was removed by a multi-channel peristaltic pump (Cole Parmer, Vernon Hills, IL). The working chamber was stirred by a magnetic stirbar at ~200 rpm and maintained at 30^{o}C by a recirculating water heater (VWR, Radnor, PA) and a water jacket. The counter chamber was filled with PBS (100 mM phosphate buffer, 50 mM NaCl, pH 7.0), and was not exchanged over the course of the experiment, and the counter electrode was a graphite block affixed to a graphite rod. The potential was maintained by a potentiostat (VSP, Bio-Logic, Knoxville, TN) at -3, +197, +397, +597, or +797 mV_{SHE} (one potential in each of 5 different runs). In one set of reactors the electrodes were not connected to the potentiostat, and oxygen was provided by passive diffusion as the electron acceptor. After 5 h of background electrochemical measurements, the working chambers were inoculated with 3 mL of an overnight culture of *S. oneidensis* MR-1, which was diluted to an OD_{600} of 0.1 in fresh LB. Each condition was performed in triplicate, with three reactors fed from the same medium tank by the same multichannel pump, and maintained under constant conditions for 10 days.

4.3.2 Sampling and analytical methods

Medium flow rate, pH, and OD_{600} were measured daily. Liquid samples were collected from the effluent lines, centrifuged for 10 min at 10,000 x g, and the cell-free supernatants were

stored at -20^{o}C for subsequent HPLC analysis. Medium flow rate was adjusted when it fell below 8 mL/h or rose above 12 mL/h. The pH was measured *via* a standard pH meter (UB-10, Denver Instrument, Bohemia, NY) and OD_{600} was measured using a spectrophotometer with a 1-cm path length in plastic cuvettes (Spectronic 1201, Milton-Roy, Ivyland, PA). After 10 days of growth, working electrodes were removed from the reactors and placed immediately into 5 mL of RNAprotect Bacterial solution (Qiagen, Germantown, MD) in a sterile petri dish and stored at -80^{o}C until RNA extraction. Concentrations of lactate and acetate in the reactor samples were measured by HPLC (600 HPLC, Waters, Milford, MA), which was equipped with an Aminex HPX-87H column (Bio-Rad, Hercules, CA) and a refractive index (RI) detector (410 Differential Refractometer, Waters, Milford, MA). The HPLC was operated at an isocratic flow of 5 mM sulfuric acid at 0.6 mL/min, with a column temperature of 65^{o}C for 20 min per sample. Peaks were integrated *via* PeakSimple software (SRI Instruments, Las Vegas, NV) and quantified using a 5-point calibration curve. Coulombic efficiency was calculated from HPLC data using a standard protocol, and accounting only for lactate consumption and acetate production (Logan, Hamelers et al. 2006). Total electron capture was measured by integrating current *vs.* time in EC-lab software. All statistical analyses were performed using basic functions in Microsoft Excel.

4.3.3 RNA extraction and purification

For extraction, the graphite paper was sliced into ~1 cm wide strips with a sterile razor blade and homogenized with the RNA protect solution in a sterile plastic centrifuge tube. Mechanical homogenization was performed with a sterile serological pipette, and the paper was further broken up by vortexing at maximum speed (Fisher Scientific, Hampton, NH). The resulting slurry was centrifuged at 7,000 x g for 10 min. The pellet was used as the starting material for a MoBio PowerBiofilm RNA extraction kit (MoBio, Carlsbad, CA) and the rest of the extraction

was performed according to the manufacturer's instructions. After extraction, RNA samples were treated with Ambion RNAse-free DNAse according to the manufacturer's instructions (Life Technologies, Carlsbad, CA). Two rounds of treatment were necessary to remove all DNA contamination. RNA was checked for DNA contamination by PCR using GoTaq Flexi polymerase (Promega, Madison, WI) with qRT-PCR primers designed for this study and standard cycling conditions (60^{o}C annealing temperature). RNA concentration in the extracts was quantified using a Quant-iT Ribogreen assay and a single reading of a plus/minus assay on an ABI 7000 instrument (Life Technologies, Carlsbad, CA).

4.3.4 RT-qPCR

Primers for RT-qPCR were designed using Primer3 and synthesized by IDT (Rozen and Skaletsky 2000). A list of primers used in this study is given in **Table A2.1**. RT-qPCR was performed using the SuperScript™ III One-Step RT-PCR System (Life Technologies, Carlsbad, CA) and an ABI 7000 instrument (Life Technologies, Carlsbad, CA). The reaction volume was 25 µL and each measurement was performed in triplicate reactions. The cycling parameters were as follows: 50^{o}C for 3 min; 95^{o}C for 5 min; 40 cycles of: 95^{o}C for 15 s, and 60^{o}C for 30 s. Fluorescence measurements were collected each cycle during the 60^{o}C step. Threshold C_t values were chosen automatically using the instrument software. A dissociation analysis was performed to check product purity using standard instrument settings. Fold-change values were calculated using the $\Delta\Delta C_t$ method, using glycerate kinase (SO_1770) as the reference gene and aerobic respiration as the reference condition (Schmittgen and Livak 2008).

4.4. Results and discussion

4.4.1 Moderate electrode potentials are optimal for current production and coulombic efficiency

All of the anode cultures grown in this study reached stable current production after a few days of operation, and continued to produce current until the electrodes were harvested after 10 days.

Stable current production readings were taken as the maximum current production in the final hour of anode operation. Significant differences between cells that were grown at different potentials were observed in the stable electric current production. Stable current increased linearly from 0.07 to 0.99 mA between -3 mV_{SHE} and +397 mV_{SHE} and subsequently dropped to 0.45 mA at +797 mV_{SHE} (**Figure 4.1A**). This indicates that higher potentials were not advantageous for current production, although they theoretically afford more energy for respiration. This is consistent with our hypothesis that strong oxidizing potentials would decrease current production.

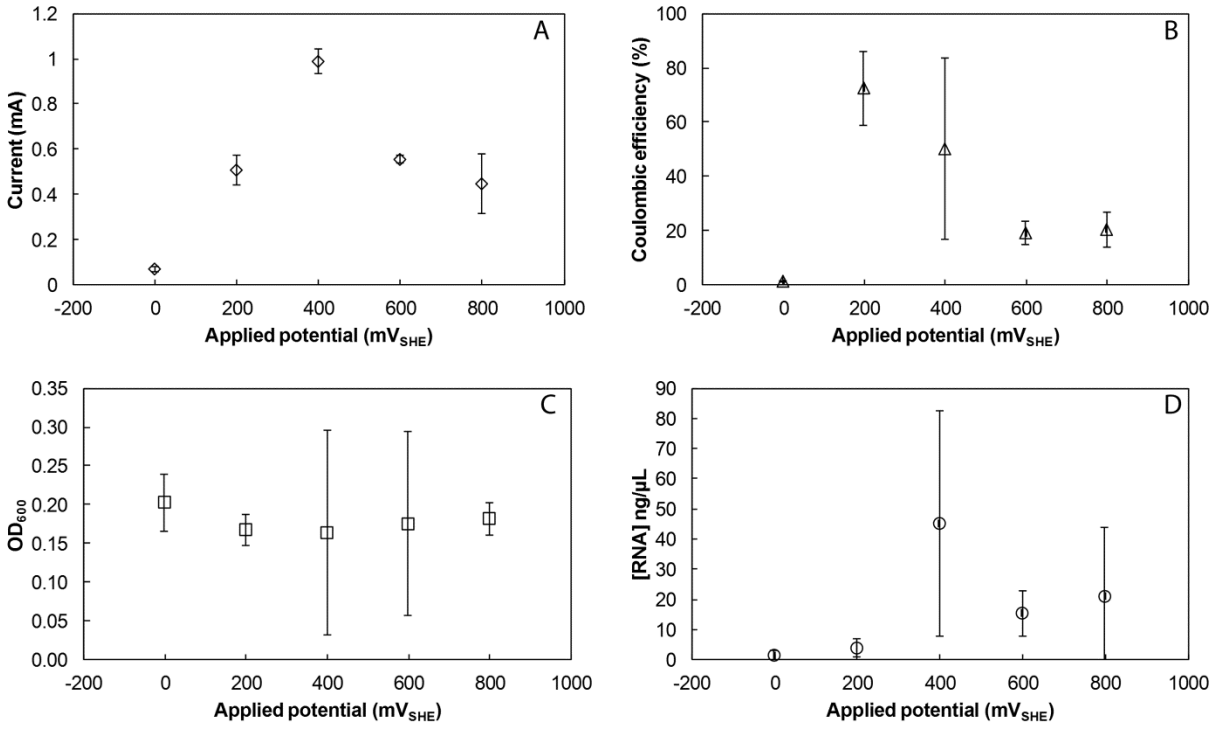

Figure 4.1. Measurements taken on the final day of operation of continuously-fed BESs with *S. oneidensis* for each set potential: (A) maximum current production; (B) coulombic efficiency; (C) OD_{600}; and (D) RNA concentration extracted from the electrode. Values are the average of 3 biological replicates, and error bars represent standard deviation. Standard deviations were generally higher in reactors poised at +397 mV_{SHE} for unknown reasons.

While current production provides a direct measurement of the respiratory rate of the cells, coulombic efficiency (the percentage of metabolic electrons captured by the electrode) is

also an important parameter for the metabolism of anode-respiring cells. Similar to electric current production, coulombic efficiency peaked at intermediate potentials, and decreased at more oxidizing electrode potentials, again, indicating a detrimental effect of high anode potentials. Coulombic efficiency peaked at a lower potential (+197 mV_{SHE}) than current production (+397 mV_{SHE}), although the difference in coulombic efficiency between cells grown at +197 mV_{SHE} and +397 mV_{SHE} was not statistically significant (**Figure 4.1B**). We theorize that the difference in optimal potentials occurred because cells at +397 mV_{SHE} experienced stress or damage, which lowered coulombic efficiency, but also benefited from improved electron transfer kinetics driven by the greater potential difference between the cytochromes and the electrode. At potentials higher than +397 mV_{SHE}, the further improvement in electron transfer kinetics was not great enough to compensate for increased stress or damage.

Although there were clear trends in current production and coulombic efficiency, the electrode potential did not greatly affect OD_{600} at the anodes, and generally, the planktonic cell density was low (OD_{600}<0.30), indicating that this was not a contributing factor to the changes in electrochemical activity, and electrode potentials did not alter planktonic growth (**Figure 4.1C**). Biofilm growth could not be measured directly because the entire electrode was used for RNA extraction. However, because all RNA extractions were performed using the same kit and procedure the RNA concentration in the extracted samples serves as an indirect measurement of biofilm growth. RNA concentrations extracted from the electrodes followed the same trend as current production, where the maximum amount of RNA was extracted from the electrode poised at +397 mV_{SHE} and RNA concentrations decreased at both higher and lower potentials (**Figure 4.1D**). The variability in the RNA concentrations was higher than the variability in current production, likely because RNA extraction is sensitive to small differences in procedure (e.g.,

accidental collection of pellet fragments when cell debris is precipitated). Although the variability in RNA concentration is large within some of the conditions, the similarity of trends between the current production and RNA concentration supports the conclusion that biofilm formation and current production are directly correlated under these experimental conditions. Comparison of trends in RNA concentration and OD_{600} across the electrode potentials indicates that biofilm growth was more important to current production than planktonic growth. Plotting OD_{600} and RNA concentration *vs.* current production reveals a statistically significant correlation for RNA but not for OD_{600}, further verifying the importance of the biofilm (**Figure 4.2**).

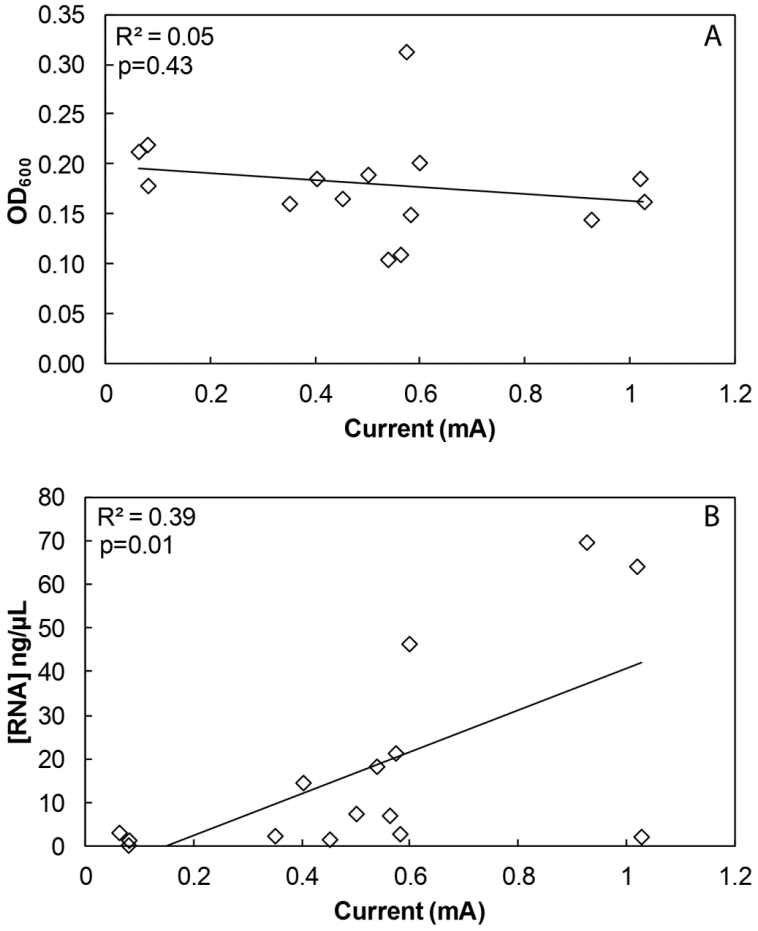

Figure 4.2. Correlation between current production, and OD_{600} in liquid samples from the continuously-fed BESs with *S. oneidensis* with electrodes poised at a range of potentials (A) and current production and RNA concentration in the extractions from the electrodes (B). Each biological replicate was plotted separately, however, these trends hold when values for biological replicates are averaged.

4.4.2 Strong oxidizing potentials did not cause general cellular stress

Previously, a general cellular stress response was proposed to occur in response to electrode respiration, and we hypothesized that this could be one factor contributing to decreased current production and coulombic efficiency at more oxidizing electrode potentials (Rosenbaum, Bar et al. 2012). A major part of this hypothesis was that ribosomal protein expression increased in response to extracellular respiration because oxidative damage of proteins or membrane constituents required an increase in protein turnover rate. A study by Beliaev et al. (2005) also indicated changes in ribosomal protein expression in response to extracellular respiration. We analyzed data from the study by Beliaev et al. (2005) further to better understand the relationships between the redox potential of the terminal electron acceptor and ribosomal protein expression. Analysis revealed a significant ($p=0.005$) correlation between the redox potential of metallic electron acceptors and ribosomal protein expression (**Figure 4.3**). The relationship between redox potential and ribosomal protein expression did not hold for not nonmetallic electron acceptors ($p>0.05$), indicating that potential-correlated changes in gene expression only occur for extracellular electron acceptors, and therefore may involve the Mtr pathway.

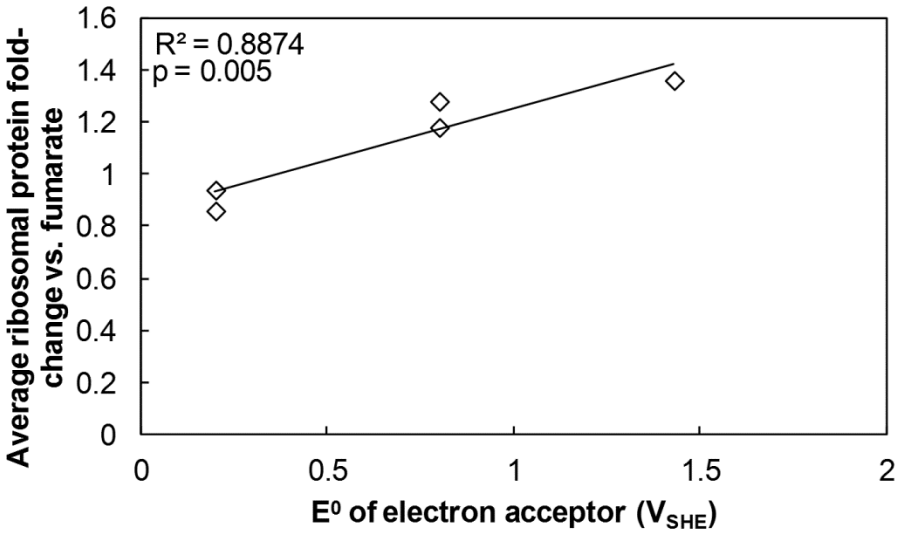

Figure 4.3. Correlation between average ribosomal protein expression in *S. oneidensis* (measured by transcript levels of a cluster of genes coding for ribosomal proteins) and the standard reduction potential of the electron acceptor for three metallic electron acceptors: iron (solid and soluble), cobalt (soluble only), and manganese (solid and soluble). Data were re-analyzed from a previous study (Beliaev et al. 2005).

This result supported the hypothesis that ribosomal protein expression and general cellular stress (caused by strongly oxidizing electron acceptors) may be linked; however, further work was necessary to confirm this in the absence of confounding variables. We investigated further by choosing a subset of stress and reference genes and measuring their expression during respiration with electrodes poised at different potentials and with oxygen. Our study differed from previous measurements of transcriptional responses to electron acceptors in three ways: i) we used specific detection of genes of interest *via* RT-qPCR, rather than whole-transcriptome profiling; ii) we carefully controlled the redox potential of the electron acceptor using potentiostatically poised electrodes; and iii) redox potential was the only experimental variable that was altered (i.e., growth form, and other terminal electron acceptor characteristics were constant). We included aerobic respiration as a reference condition, and to compare our results with those of previous studies.

Three genes were chosen as markers of protein turnover and general stress response: *rplK* (ribosomal protein L11), SO_0220; *dnaK* (a heat-shock protein involved in enzyme and DNA repair), SO_1126; and *clpP* (an ATP-dependent protease), SO_1794. We also measured expression of *omcA* (outer membrane *c*-type cytochrome involved in extracellular respiration), SO_1779 to infer the electrochemical activity of the cells. These genes were chosen based on observed upregulation during extracellular respiration relative to aerobic respiration in previous studies (Beliaev, Klingeman et al. 2005; Rosenbaum, Bar et al. 2012). Glycerate kinase was chosen as a reference gene (i.e., a gene that is expected to have equal transcript abundances across all conditions) because it had very similar expression in all conditions tested by Rosenbaum et al. (2012). Transcript levels for each gene were measured in three separate reactions for each sample, and for three biological replicates for each condition except +197 mV_{SHE}. Expression of the reference gene was not detected for one of the samples in this treatment group; and therefore it was excluded from expression analysis. Analysis was performed using the $\Delta\Delta C_t$ method with glycerate kinase as the reference gene (which normalizes for the amount of template RNA in the reaction) and aerobic growth with an unpoised electrode as a surface for biofilm attachment as the reference condition (to compare all other conditions against a single standard).

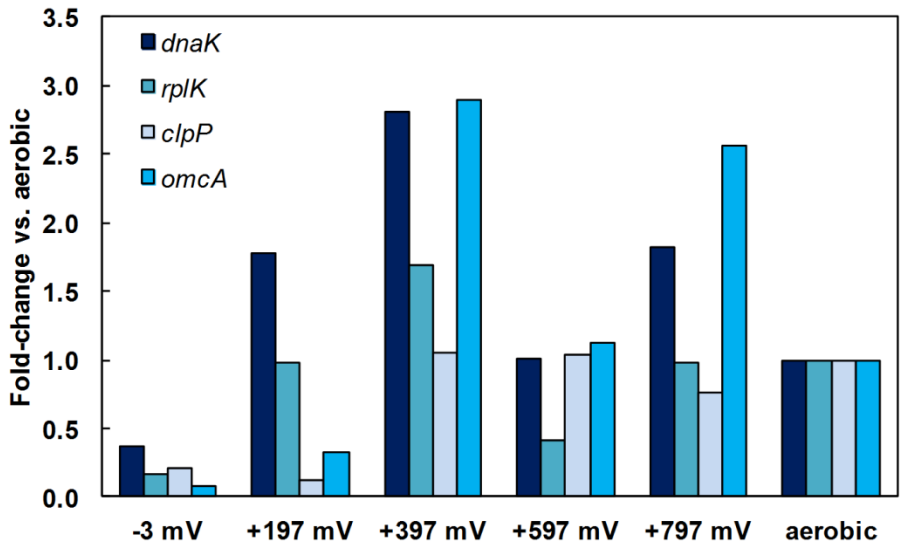

Figure 4.4. Fold-change values *vs*. aerobic conditions for 4 genes calculated using the $\Delta\Delta C_t$ method with glycerate kinase (SO_1770) as the reference gene. Genes measured were: ribosomal protein L11, SO_0220; *dnaK*, SO_1126; *omcA*, SO_1779; *clpP*, SO_1794. Labels indicate the potential set at the working electrode, (relative to the standard hydrogen electrode) in the continuously-fed BESs wherein the *S. oneidensis* samples were grown. The aerobic condition was used as the reference condition, therefore, all values given for this condition are equal to 1.

There was variation in transcript levels for all genes tested across the various electrochemical conditions (**Figure 4.4**). In contrast to our hypothesis, and unlike what we found in the data collected by Beliaev et al. (2005), we did not find that ribosomal protein expression positively correlated with redox potential (R^2=0.12, p=0.23), but that it correlated positively with growth and current production (**Figure 4.5**). Although there was high variability within biological replicates, the correlation between each of these two genes and current production was statistically significant ($p<0.05$).

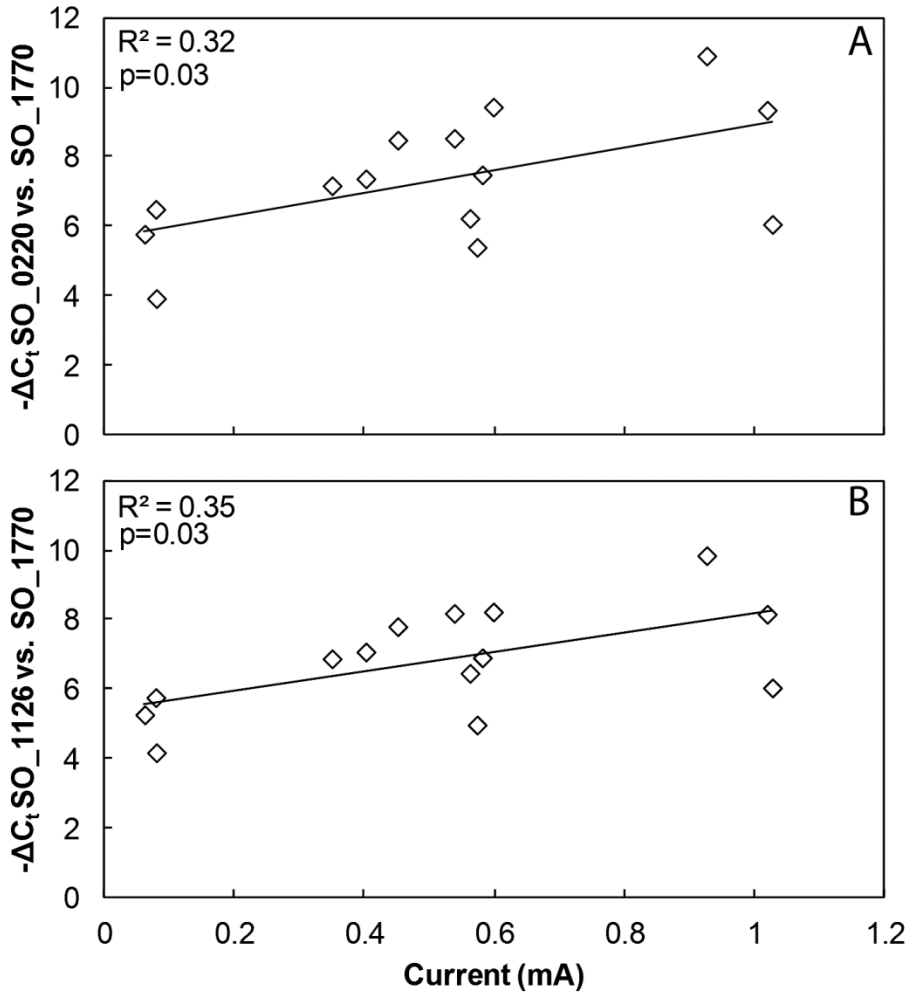

Figure 4.5. Correlation between current production and (A) *rplK* expression and (B) *dnaK* expression in *S. oneidensis* grown in continuously-fed BESs with working electrodes poised at a range of potentials.

The correlation analysis indicates that expression of *rplK* and *dnaK* was not specifically upregulated in response to the higher electrode potentials, and was rather related to biofilm biomass (which was correlated to current production). Both expression trends are very similar, indicating that these two genes may both be controlled by the same regulatory system, possibly a major growth-related regulator. The difference between our results and those of Beliaev et al. (2005) are likely due to differences in growth rate of the cells in the latter study. Although in the study by Beliaev et al. (2005) cells were only exposed to the terminal electron acceptors for 3.5

h, this time period may have been long enough to alter growth and protein production rates of the cells. This indicates that the correlation between redox potential and ribosomal protein expression seen in **Figure 4.3** is an artifact of changes in growth rate caused by the redox potentials. It is not surprising that the growth rates would correlate to redox potential, because higher redox potentials yield a greater thermodynamic advantage for respiration, and this would cause the correlation between redox potential and ribosomal protein expression.

In contrast to *rplK* and *dnaK*, *omcA* and *clpP* had qualitatively different expression profiles. Although the overall profile was different, *omcA* expression was also correlated to current production ($p=0.01$), since outer membrane cytochromes are essential to current production. Unlike all other genes tested, *clpP* expression was not significantly correlated with current production ($p>0.05$). Cells grown at more oxidizing potentials (+397 mV_{SHE} and above) had increased expression of *omcA* and *clpP* compared with cells grown at lower potentials (two-tailed t-test, $p<0.05$, performed at the ΔC_t level), while this was not true for *dnaK* and *rplK* ($p>0.05$). The increase in protease and cytochrome expression beginning at +397 mV_{SHE} aligns with the decrease in coulombic efficiency. The fact that cytochrome *c* and protease expression remained high, even as growth decreased, indicates that *S. oneidensis* directly or indirectly senses the potential at the working electrode and modulates gene expression in response. The increased expression of *omcA* at more strongly oxidizing potentials indicates that *S. oneidensis* cells sensed a favorable environment for extracellular respiration and increased expression of outer membrane cytochromes in response, while the increase in protease expression may signal an increase in protein damage during respiration with strongly oxidizing electrodes.

Our in-depth investigation of protease expression adds detail to the findings of Rosenbaum et al. (2012), and shows that the Clp complex is regulated in response to electrode

potential. ClpP is a proteolytic enzyme, which can associate with two different chaperones for protein degradation to form ClpAP or ClpXP (Gottesman 1996). Although the Clp-type proteases are not specialized for outer membrane protein degradation, previous study of MtrC turnover suggests reuptake and intracellular proteolysis, making the ClpXP complex a possible player in this function (Xiong, Chen et al. 2011). One possible reason for the ClpP upregulation is simply upregulation of the Mtr pathway. The cytochromes of this pathway are notoriously difficult to mature and produce high levels of immature peptides which must be degraded, possibly resulting in a concomitant increase in protease expression when expression of the Mtr pathway increases (Goldbeck, Jensen et al. 2013). Based on the transcript measurements obtained here, it is impossible to discern whether the increases in outer membrane cytochrome and protease expression would cause an overall increase or decrease in electrochemical activity of the cells, necessitating direct measurement of outer membrane cytochrome activity.

4.4.3 Cyclic voltammetry revealed outer membrane cytochrome damage at oxidizing potentials

Both *omcA* and *clpP* expression were high at the upper potentials, and the products of these two genes could potentially have opposing effects on outer membrane cytochrome accumulation. Therefore, we used additional electrochemical analysis to measure the amount of active outer membrane cytochromes at the electrode surface. Cyclic voltammetry analysis can be used to measure relative activity of direct and mediated electron transfer in BESs with *S. oneidensis* by comparing catalytic waves at -100 mV_{SHE} (mediated electron transfer) and +300 mV_{SHE} (direct electron transfer) (Carmona-Martinez, Harnisch et al. 2011). Although the biofilms grown at +397 mV_{SHE} (optimal current production) resulted in more extracted RNA, and likely contained more biomass, cyclic voltammetry analysis shows that the biofilm grown at +197 mV_{SHE} (optimal coulombic efficiency) contained more active cytochromes (**Figure 4.6**).

The electrodes poised at +197 mV_{SHE} and +597 mV_{SHE} fell on either side of the current production maximum, and had similar current production during normal operation. However, cyclic voltammograms indicate lower cytochrome *c* activity in electrodes poised at +597 $mV_{SHE,}$ indicating that outer membrane cytochromes were deactivated by the strong oxidizing potentials, but enhanced electron transfer kinetics due to the greater driving force mitigated this effect during normal operation. Activity of cytochromes as measured by cyclic voltammetry did not follow the same trend as *omcA* expression, indicating that factors other than transcription (e.g., maturation, export, denaturation, and degradation) control the activity of outer membrane cytochromes under these conditions.

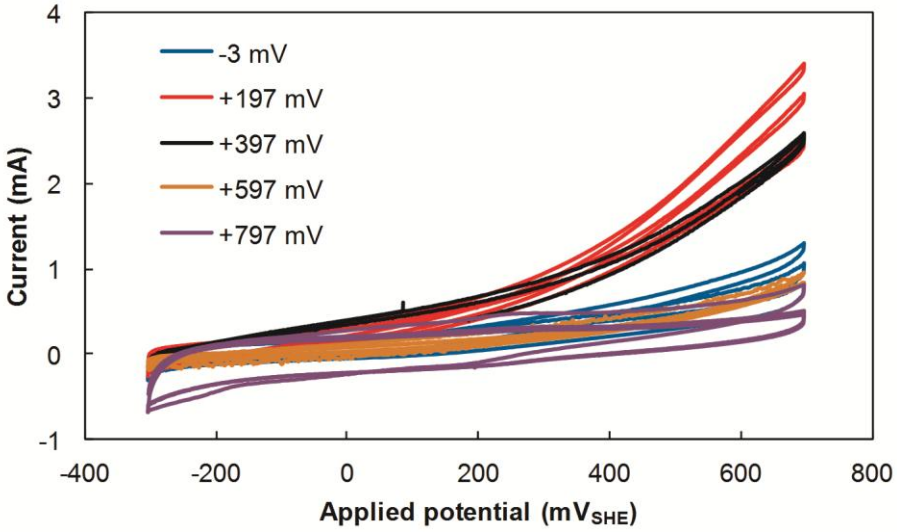

Figure 4.6. Cyclic voltammograms collected on the same day as biofilm sampling for each anode at a scan rate of 2 mV/s. Anodes were poised at a range of potentials and colonized by *S. oneidensis* in continuously-fed BESs. For each condition one representative scan is shown. The scans shown are the second of two replicate scans. The legend indicates the poised potential of the electrode during current production.

4.4.4 Comparison with other studies reveals that cytochrome c *damage occurs in biofilm cells*

Our study is not the first to investigate *S. oneidensis* grown with electrodes poised at different potentials. Cho and Ellington (2007) also performed a study comparing current production by *S.*

oneidensis at electrodes poised at various potentials, ranging from +197 mV_{SHE} to +697 mV_{SHE} (Cho and Ellington 2007). They found a slight decrease in maximal current production at higher set potentials, but the difference was small and was not confirmed by statistical analysis. In contrast, we saw a large and statistically significant decrease in current production at potentials above +397 mV_{SHE}. A major difference between the two studies is that Cho and Ellington (2007) used batch-fed anodes to perform their experiments, while we used continuously-fed anodes. Hydrodynamic conditions (i.e., continuous flow *vs.* batch feeding) alter the mechanism of electron transfer in BESs with *S. oneidensis* because continuous replacement of medium greatly reduces the ability of the cells to use mediated electron transfer (TerAvest et al., manuscript under review for *Biotechnology and Bioengineering*). In the present study with continuous flow, cyclic voltammetry analysis confirmed that there was little activity of mediated electron transfer in the anodes (**Figure 4.6**). We interpret the difference between these studies to mean that higher potentials negatively impact biofilm cells, which use direct electron transfer, and have relatively little impact on planktonic cells, which use mediated electron transfer. This provides evidence that higher electrode potentials damage cells at the electrode surface *via* direct damage of proteins, rather than by causing general stress in all cells in the bioreactor. Previous work has confirmed that proteins can be denatured by electric fields at electrodes, indicating that membrane proteins (e.g., *c*-type cytochromes) could be denatured by strong oxidizing potentials in our system, and thus lose activity (Palecek and Ostatna 2009).

A similar study was performed by Carmona-Martinez et al. (2012), using the closely related organism *S. putrefaciens* in a fed-batch system wherein medium was periodically replaced. In contrast to the results of both Cho and Ellington (2007) and the present study, they found a distinct linear increase in maximum current production with increasing anode potential.

This could have been due to the difference in strain or the periodic addition of fresh medium, which could have encouraged higher planktonic cell density and flavin production. Both previous studies indicate that poised electrodes do not have a damaging effect on planktonic *Shewanella* spp. in bioelectrochemical systems. This supports the conclusion that in our study current production and coulombic efficiency decreased because of damage to cells (e.g., direct denaturation of outer membrane cytochromes) directly at the electrode surface, rather than general stress occurring in both biofilm and planktonic cells.

4.4.5 Sources of variability and possible amendments

Gene expression measurements taken by analyzing transcript abundance are often subject to high variability, and should be checked against data generated by other researchers when possible. Inclusion of cells grown with oxygen as the electron acceptor was useful for comparing our expression results with those from other studies to validate the gene expression results. Overall, our results were consistent with previous measurements for differences between electrode- and oxygen-respiration, although differences between electrode respiration and aerobic respiration were not as pronounced as those found by Rosenbaum et al. (2012). This was likely due to the increased similarity between the electrode- and oxygen-respiring samples in our study. Most importantly, we sampled only biofilm cells, rather than comparing biofilm and planktonic cells. The similarity of our results to previous findings validates our RT-qPCR method, but further improvements could be made to his method in the future.

High variability made it difficult to test differences between individual sample groups, although we were able to make statistically significant comparisons using correlation or comparison of low potentials *vs.* high potentials. Future work could improve upon this study by including more biological replicates and improving sampling techniques to reduce variability.

The relatively high variability in gene expression observed here is surprising, considering the lower variation in current production and coulombic efficiency. It is possible that our sampling procedure produced some of this variability, because although the cultures were grown under strict anaerobic conditions (except for the aerobic samples) it was not possible to remove the electrodes under anaerobic conditions. The electrodes were placed directly into RNAprotect solution after removal from the reactor, but each one was exposed to oxygen for a few seconds. It is possible that for some of these electrodes this time period was long enough to cause some changes in transcript levels. Further, proteomic analysis of membrane fractions is necessary to confirm the direct damage of *c*-type cytochromes and determine the type of damage that is induced by the electrode. This could lead to strategies for mitigation of damage (e.g., utilization of different electrode materials or introduction of chemical protectants). Modeling of different types of damage and their putative effects on electron transfer and metabolism would also be a useful approach to specify likely forms of damage prior to experimentation.

4.5. Conclusions

In our experiments, *S. oneidensis* produced electric current at anodes poised at a wide range of potentials, but the optimal potential for current production in continuously-fed BESs was +397 mV_{SHE}. The optimal potential with regard to coulombic efficiency, however, was lower than the optimal for current production (+197 mV_{SHE}). In contrast to a previous hypothesis, this was not due to a general stress response caused by oxidizing electrode potentials; rather, our data supports the conclusion that the decrease in current coulombic efficiency is due to direct protein degradation by the electrodes poised at higher potentials. Cyclic voltammetry indicated a greater abundance of active *c*-type cytochromes on the electrode poised at +197 mV_{SHE} than that poised at +397 mV_{SHE} (more oxidizing potential), although it contained less biomass overall and produced less electric current during normal operation. We observed a trade-

off between increasing electron transfer rates by increasing the applied potential and damaging redox proteins with strong oxidizing potentials. Comparison with other studies shows that this effect is mitigated by slowing or stopping medium replacement to encourage mediated electron transfer and planktonic growth, which indicates that *S. oneidensis* may be better suited to bioelectrochemical applications involving little or no flow as opposed to applications with continuous flow conditions.

4.6. Acknowledgements

We acknowledge Dr. Miriam Rosenbaum (RWTH Aachen) for helpful comments in developing the study. This work was supported by the National Science Foundation through CAREER grant no. 0939882 to L.T.A.

CHAPTER 5

META-ANALYSIS OF TRANSCRIPTOMIC DATA REVEALS THE ANAEROBIC ELECTRON TRANSPORT CHAIN OF *SHEWANELLA ONEIDENSIS* MR-1

Adapted from: TerAvest and Angenent. In preparation for *Journal of Bacteriology*.

5.1 Abstract

Shewanella oneidensis MR-1 is a model microbe for both bioelectrochemical systems and environmental metal cycling and has been studied using a variety of advanced molecular biology techniques. Whole-transcriptome profiling by microarrays is a common method to analyze changes in gene expression in response to specific conditions. Previous studies have yielded insights into cellular responses to particular conditions but have not been placed in context with other work to gain broader understanding. We compared the transcriptomes (expression data for 3696 loci) of 361 samples of *S. oneidensis* MR-1 from a variety of studies that have been uploaded to the NCBI GEO database and found distinct clustering patterns based on experimental parameters, including the type of microarray used. We utilized machine learning analysis to discover genes important to anode- and Fe(III)-respiration in this organism. This meta-analysis revealed that some putative members of the electron transport chain (ETC), including an NADH dehydrogenase and a cytochrome *c* oxidase, were important for extracellular respiration. Knockout strains of *S. oneidensis* with genes from each of these clusters deleted confirmed their roles in supporting anaerobic respiration with solid electron acceptors. Previous work has found that these genes are not used by *S. oneidensis* under aerobic conditions, indicating that *S. oneidensis* utilizes a specialized ETC to overcome the difficulty in generating proton motive force under anaerobic conditions. Comparison with an ATP synthase knockout strain confirmed this finding.

5.2 Introduction

Shewanella oneidensis MR-1 is a model microbe for studying bioelectrochemical systems, iron cycling in anaerobic sediments, biofilm formation, and other freshwater microbial processes (Thormann, Saville et al. 2004; Thormann, Saville et al. 2005; Marsili, Baron et al. 2008; Pinchuk, Ammons et al. 2008; Rosenbaum, Cotta et al. 2010). *S. oneidensis* is a particularly important model of extracellular respiration because the extracellular electron transport pathway of *S. oneidensis* is well understood compared to other model microbes in bioelectrochemical systems. Multiple studies have confirmed that the MtrCAB electron conduit is necessary and sufficient for electron transfer across the outer membrane (Coursolle, Baron et al. 2010; Coursolle and Gralnick 2010) and accepts respiratory electrons *via* CymA (Shi, Rosso et al. 2012). The function of this pathway has been confirmed by reconstitution of the pathway in *Escherichia coli* (Jensen, Albers et al. 2010). Because of its importance in several research areas and the existing molecular understanding, it has been the subject of research using new, rigorous bioinformatics techniques, including metabolic modeling and gene network analysis (Fredrickson, Romine et al. 2008; Pinchuk, Hill et al. 2010; Torres-Garcia, Brown et al. 2011; Flynn, Hunt et al. 2012). Commonly, whole-genome microarrays (including in-house made chips and Affymetrix GeneChips) have been used to compare transcriptomic profiles of samples of *S. oneidensis* grown under different experimental conditions. The tested conditions include many "typical" culture conditions and introduction of shocks or stressors, such as high and low pH, chromate, and ionizing radiation (Brown, Thompson et al. 2006; Leaphart, Thompson et al. 2006; Qiu, Daly et al. 2006). Multiple time-series experiments have also been performed, wherein the transcriptome was observed at many defined intervals within the same culture (Gao, Yang et al. 2006; Beg, Zampieri et al. 2012). Due to its renowned respiratory versatility, studies on expression profiles of *S. oneidensis* MR-1 respiring a variety of electron acceptors have also

been performed (Beliaev, Thompson et al. 2002; Beliaev, Klingeman et al. 2005; Rosenbaum, Bar et al. 2012).

Two transcriptomic studies have focused on extracellular respiration at anodes, which is an important aspect of *S. oneidensis* physiology that has been exploited for biotechnology research in several areas (Rosenbaum, Bar et al. 2012; Xu, Liu et al. 2012). The first study, by Xu et al. (2012), compared the transcriptomes of two sample groups: one group grown with control anodes and another with modified anodes. The control anodes were plain graphite, while the modified electrodes were coated in Fe-nanoparticles. The study describes improvements in current production caused by the Fe-nanoparticle coating and confirms that the performance enhancement is reflected in changes in gene expression. Several groups of genes known to be important for current production were detected as upregulated in response to the Fe-nanoparticle coating, including *c*-type cytochromes and genes related to biofilm formation. Essentially, this study confirms the involvement of genes previously known to be important to extracellular electron transfer and explains the BES performance on a transcriptional level. However, this information cannot be used to discover additional genes that may be important to anode respiration, particularly those enzymes that are indirectly related to current production or are incorrectly annotated.

In a second study, aimed at gaining a holistic picture of gene expression in anode-respiring cells, Rosenbaum, et al. (2012), compared the transcriptomes of cells respiring with potentiostatically-poised, graphite electrodes with cells respiring with soluble Fe(III)-citrate or oxygen. This study aimed to elucidate overall transcriptional changes caused by electrode respiration beyond outer membrane *c*-type cytochromes and other known extracellular electron transfer functions. Some interesting results were observed, however, high variability and

alteration of multiple variables between the sample sets made it difficult to draw any conclusions from this dataset alone. For example, the electrode-respiring cells were grown as biofilms, while the Fe(III)-citrate- and oxygen-respiring cells were grown planktonically. Further, the electrode-respiring cells were grown in chemostats while the other samples were grown in batch cultures. This caused interference of genes involved in biofilm formation and other functions in comparison between the groups. Several hypotheses were stated, including a role for a cbb_3-type cytochrome oxidase (the Cco complex) in redox sensing, and an electrode-induced transcriptional stress response, but none could be confirmed using only the dataset generated in the study. Placing this dataset in a broader context by comparing it to a wider range of growth conditions could help to strengthen these hypotheses and gain additional insights into the overall transcriptional changes necessary for extracellular respiration.

Genes involved in the electron transport chain (ETC) are particularly important to consider because they may play a supporting role in extracellular electron transfer. Considering the well-known respiratory versatility of *S. oneidensis*, it is not surprising that *S. oneidensis* has a branched ETC, which includes multiple possible paralogs to catalyze each step. However, the specific role of some of these paralogs is unknown. Computational and gene deletion methods show that some of these enzymes are not utilized under aerobic conditions, and inducing conditions are unknown (Pinchuk, Hill et al. 2010). Of particular interest is the Cco cbb_3-type cytochrome oxidase, which was previously detected as differentially expressed between anode- and Fe(III)-respiring conditions (Rosenbaum, Bar et al. 2012). Deletion of Cco activity from *S. oneidensis* did not alter growth under aerobic conditions in one study (Pinchuk, Hill et al. 2010), but significantly decreased aerobic growth in another study (Gao, Barua et al. 2010). Based on homology to enzymes in *Escherichia coli*, this cytochrome oxidase is predicted to translocate

more protons per electron across the cytoplasmic membrane than other complexes found in *S. oneidensis*, yet metabolic modeling indicates that it is not utilized by *S. oneidensis* under aerobic conditions (Pinchuk, Hill et al. 2010). Deletion of this complex also increased the sensitivity of *S. oneidensis* to Cr(VI), indicating that this enzyme is involved in anaerobic respiration or heavy metal detoxification (Gao, Barua et al. 2010).

The multiple NADH dehydrogenases present in the genome of *S. oneidensis* are also important to understanding its overall metabolism. The genome of *S. oneidensis* contains genes that code for two different NADH dehydrogenases: Ndh and Nuo. Based on similarity to complexes in *E.* coli, the Ndh complex is predicted to generate no PMF, while Nuo would translocate 4 H^+ per 2 e^- (Flynn, Hunt et al. 2012). Metabolic models of aerobically-grown *S. oneidensis* match better with experimental data when all electron flux is modeled to go through the Ndh complex, rather than the Nuo complex, even though predicted activity of the Nuo complex would produce higher biomass yields (Pinchuk, Hill et al. 2010). Work by Pinchuk et al. (2010) revealed that only 3 of 20 sequenced *Shewanella* spp. strains contain *nuo* gene clusters, and testing of a subset of these strains indicated that the Nuo complex does not produce any growth advantage under aerobic conditions. Considering this result, it is possible that the Nuo complex of *S. oneidensis* is not functional or has been adapted for a particular anaerobic condition or activity. Use of more efficient proton pumping complexes (e.g., Nuo instead of Ndh) could be an important adaptation for *S. oneidensis* because previous work has indicated that generation of proton motive force (PMF) is difficult under anaerobic conditions, and that ATP is consumed in favor of PMF generation (Hunt, Flynn et al. 2010). Addition of proteorhodopsin (a light-driven proton pump) to *S. oneidensis* confirmed that PMF generation

limits growth and survival of under anaerobic conditions and allowed the modified cells to fully oxidize a larger portion of their substrate pool (Johnson, Baron et al. 2010).

While the extracellular electron transfer machinery of *S. oneidensis* is well-understood, little is known about the anaerobic ETC and other supporting functions. There is already a wealth of data that could be used to elucidate these functions, but to our knowledge, there have not yet been a study that mines previously collected transcriptomic information for this purpose. Many of the published (and some unpublished) transcriptomic studies on *S. oneidensis* provide access to raw expression values through the NCBI Gene Expression Omnibus (GEO database) and much of this data can be synthesized to yield broader analysis of the common traits of *S. oneidensis* grown in similar conditions. This study aims to use this large data set to gain deeper insight into the transcriptional changes associated with electrode respiration in *S. oneidensis* MR-1 and to test hypotheses generated by rigorous bioinformatics meta-analysis using gene knockout studies.

5.3 Materials and methods

5.3.1 Data collection and statistical analysis

All relevant transcriptomic data from the NCBI Gene Expression Omnibus (GEO) database was downloaded as raw intensity values or MAS5 normalized values (data from 14 GSE series were included). Projects that reported only expression ratios between two different conditions were excluded from this study because it was impossible to determine expression values for the individual conditions. Expression was ranked within each sample such that the most abundant transcript was given a value of "1" to normalize between different data collection platforms and produce values that indicate the relative importance of each transcript under the given condition (Folsom, Richards et al. 2010). Ranking was performed using the "rank" function in R to produce a rank for every locus within each sample. Only transcripts that were detected in all

platforms were included in the analysis, resulting in 361 transcriptomic profiles each containing 3696 expression ranks. Sorting and gene exclusion were performed using basic functions in Excel and R. A separate mapping file was generated containing information about each sample, based on the GEO upload pages and journal articles related to the samples. The following information was included in the mapping file: the GEO platform number (which identifies the type of microarray used to collect the data), the GEO series number (an identifier for each group of samples uploaded to GEO, unusually identifying a single project or journal article), the unique GEO sample identification number, the medium in which the sample was grown, the growth substrate, the growth temperature, mutations to the strain, the electron acceptor, the type of growth vessel (e.g., flask or bioreactor), and the time of sampling (e.g., 20 hours or "stationary phase"). Principal component analysis (PCA) was performed in Orange (Demšar, Zupan et al. 2004) and machine learning was performed using the pamR (prediction analysis for microarrays) package for R (Tibshirani, Hastie et al. 2002).

5.3.2 Knockout strains and bioelectrochemical systems

Six strains of *S. oneidensis* were tested for electric current production: wild-type *S. oneidensis* MR-1, Δ*ccoO* (Pinchuk, Hill et al. 2010), Δ*coxB* (Pinchuk, Hill et al. 2010), Δ*atp* (Hunt, Flynn et al. 2010), Δ*nuoN*, and Δ*coxB*Δ*nuoN* (**Table 5.1**). We obtained the first three knockout strains from other research groups, as noted, and produced in-frame deletions of the locus SO_1009, or *nuoN* for the last two strains. This locus was chosen because it is most downstream gene in the putative *nuo* operon, and previous work in *E. coli* has indicated that the complex is non-functional when any single subunit is deleted (Erhardt, Steimle et al. 2012). The deletion was made using the pDS3.0 suicide vector according to previously described methods and confirmed by PCR (Pinchuk, Rodionov et al. 2009). Aerobic growth curves for the WT and single-knockout

strains were generated by inoculating each of 12 wells of a sterile 96 well plate with 2 µL of an overnight culture that was diluted to OD_{600}=0.1 and 200 µL of fresh M4 medium (Rosenbaum, Cotta et al. 2010) and incubating at 30^{o}C with 250 rpm shaking. OD_{600} was measured at several time points using a 96-well plate reader (Synergy 4, BioTek Instruments, Winooski, VT).

Table 5.1. A complete list and description of *S. oneidensis* strains used in this study

strain	deletion	reference
***S. oneidensis* MR-1**	none	(Myers and Nealson 1988)
S. oneidensis* Δ*ccoO	SO_2363	(Pinchuk, Hill et al. 2010)
S. oneidensis* Δ*coxB	SO_4606	(Pinchuk, Hill et al. 2010)
S. oneidensis* Δ*atp	SO_4746-SO_4754	(Hunt, Flynn et al. 2010)
S. oneidensis* Δ*nuoN	SO_1009	this study
S. oneidensis* Δ*coxB*Δ*nuoN	SO_4606 and SO_1009	this study

Current production by *S. oneidensis* knockout strains was tested in potentiostatically-poised, two-chambered, bioelectrochemical systems. The working chamber ("anode") was filled with 250 mL of modified M4 medium, and the counter chamber was filled with PBS (100 mM phosphate buffer, 50 mM NaCl, pH ~7). The two chambers were separated by an anion exchange membrane (Membranes International, Ringwood, NJ). The working electrode was a 9 x 9 cm square of carbon cloth (PANEX ® 30 - PW06, Zoltek Corp, St Louis, MO). Each corner of the cloth was affixed to a carbon rod with carbon cement (CCC Carbon Adhesive, EMS, Hatfield, PA) and small cable ties for connection to the potentiostat. The counter electrode was prepared similarly, with a 2 x 7 x 1 cm carbon block. The working chamber was maintained under anaerobic conditions by sparging with N_2 gas, and was continuously stirred by a magnetic stirbar at ~200 rpm. The working electrode was poised at +400 mV_{SHE} and current was measured by a potentiostat (VSP, BioLogic USA, Knoxville, TN). Turnover cyclic voltammetry analysis was performed once per day. Two scans were taken from -303 to +697 mV_{SHE} and back at a scan rate of 2 mV/s.

The working chambers were inoculated with 2.5 mL of the appropriate culture after 5 h of background electrochemical measurement. Precultures were grown overnight in LB at 30^{o}C, with shaking at 100 rpm, except the Δ*atp* strain, which was grown for 3 days under anaerobic conditions at 25^{o}C in LB + 50 mM sodium fumarate (because of poor growth under aerobic conditions). All cultures were diluted to OD_{600}=0.1 in fresh LB for inoculation. Samples were removed from the working chambers daily. Sample size was always 2 mL to ensure that all reactors maintained equal volumes. pH and OD_{600} were measured and the samples were centrifuged at 10,000 rpm for 8-10 minutes. Cell pellets and supernatants were stored separately at -20^{o}C. HPLC analysis was performed as previously described (TerAvest and Angenent, in preparation).

5.4 Results and discussion

5.4.1 Principal Component Analysis

Initially, we compared the transcriptomes (expression ranks for 3696 loci) of 361 samples of *S. oneidensis* using principal component analysis (PCA) in the Orange software package. These samples were collected in 14 different studies, which are described in **Table A3.1**. The PCA method computes a distance matrix containing the distances between each combination of samples based on the entire transcriptional profile and projects the distance matrix in components which describe the maximal proportion of variation in the data. In this analysis, components 1 and 2 explained 28.5% and 15.2% of the variation, respectively. Coherent clusters were observed in the PCA plots, indicating that our method successfully distinguished between different sample characteristics. We colored the points according to different experimental parameters to determine which factors influenced clustering patterns. Coloring the points by the GEO database platform number (indicating the type of array and method used to collect the expression data) shows that the three largest clusters align well with the three most common

platforms (**Figure 5.1A**). This is surprising, considering that data were ranked in an attempt to rule out this effect. It appears that the platform used has an effect on the relative expression values of genes, which is important to note for future studies. This may have occurred due to artifacts caused by the location of each gene on the chip, differences in dye binding within different probe sets, or other factors (Dobbin, Kawasaki et al. 2005; Yu, Nguyen et al. 2007).

We also colored the points according to the GEO series number and found that samples for each study generally clustered together, even when the study contained multiple different growth conditions (**Figure 5.1B**). Coloring the points by the GEO series number yielded many distinct clusters, indicating that small differences in how workers culture *S. oneidensis* between studies may have very important impacts on transcriptomes. Although clusters related to particular experimental parameters are not immediately clear, some differences can be observed in this initial survey. For example, a time-series of samples from the same culture (GSE25821) shows a cluster of points following a distinct line over time. Also, one study compared cells grown under normal conditions or exposed to hydrogen peroxide (GSE31053) and these samples show a clear divide between the two groups in the PCA plot. Coloring the points according to other variables did not yield as well defined clusters as GEO platform or series identifiers, indicating that samples were clustered mainly by study, and the type of microarray used to make the measurements. Because these results do not reveal much about specific physiological differences between cells grown under different conditions we added a more in-depth statistical analysis on particular conditions of interest.

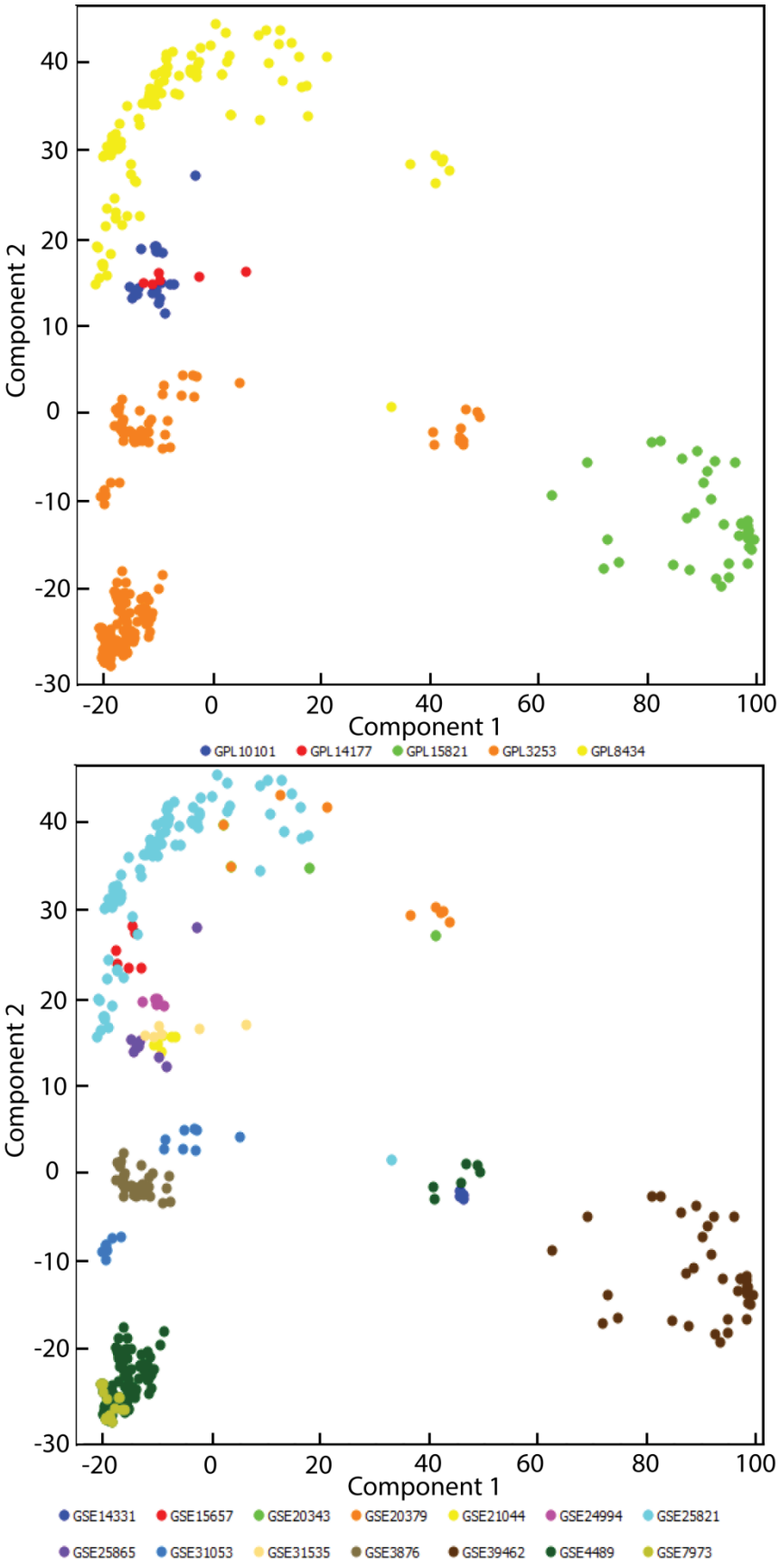

Figure 5.1. A PCA plot with distances between transcriptomes in the 1st and 2nd principal components. Different colors indicate different data series as indicated in the legend. (A) Points are colored by the platform number in the NCBI GEO database, indicating which type of microarray was used to perform transcriptomic analysis. (B) Points are colored by the series number in the NCBI GEO database. More information about each series can be found in Table A3.1.

5.4.2 Machine learning with pamR

Because we were not able to make any specific insights about physiology of anode-respiring cells using PCA, we used machine learning to determine which of the included genes show characteristic differences between conditions of interest. Because this study is focused on extracellular respiration, the samples were classified into four groups based on the electron acceptor used in the experiments: anode (12 samples), Fe(III) (4 samples), fumarate (10 samples), and oxygen (335 samples). The pamR package for R was used to determine genes that have varied expression between conditions and can be used to predict which group a sample belongs to. Using a threshold value of 2.5 gave a confusion matrix with a reasonable error rate for most groups (**Table 5.2**).

Table 5.2. A confusion matrix containing information about the accuracy of sample group predictions based on the pamR training at a threshold of 2.5. The first column indicates the sample group, and the subsequent columns indicate predicted sample group.

	anode	**iron**	**fumarate**	**oxygen**	**error rate**
anode	9	2	0	1	0.25
iron	0	4	0	0	0.00
fumarate	0	2	0	8	1.00
oxygen	6	50	0	279	0.17
overall error rate = 0.19					

The error rate was well below 0.75 (75% incorrect, which would be expected by random prediction) for all groups except fumarate, which could not be predicted correctly. Perhaps this was because fumarate respiration is an anaerobic process, but unlike anode- and Fe(III)-respiration, it occurs in the periplasm and therefore may have some physiological traits similar to each of the other three groups. This may have made it difficult to produce a set of genes which would set fumarate respiration apart from all three of the other groups. This interpretation is consistent with the predictions made by the machine learning algorithm, which placed fumarate samples in the oxygen group 80% of the time and in the Fe(III) group 20% of the time. Although

there is little functional information gained for the fumarate samples, we found that removing them did not affect other parts of the analysis; therefore they were not excluded from the analysis.

At a threshold of 2.5, 280 genes were required to predict the correct group for each sample with the error described by the corresponding confusion matrix (**Table 5.2**). A full list of these genes is given in **Table A3.2**, with annotations. In the analysis, each gene is given a score which indicates whether it was up- or down-regulated in samples from each group. In this case, negative values indicate upregulation because the most highly expressed gene in each sample was given a rank of "1." We annotated the genes according to basic functional groups, and compared the proportion of each group within the genome to the proportion of the same group in the gene list generated by machine learning. Out of 19 groups, we found 7 to have significantly different proportions (**Figure 5.2**; $p<0.05$, hypergeometric distribution). Four groups were enriched in the machine learning results (conserved hypothetical protein, energy metabolism, fatty acid and phospholipid metabolism, and protein synthesis) and 3 groups were less prominent in the machine learning results than in the genome (mobile and extrachromosomal elements, hypothetical protein, and DNA metabolism). Overall, it is clear that different electron acceptors alter energy and protein metabolism, but have little effect on DNA synthesis. The enrichment of protein synthesis is in line with findings by Rosenbaum et al. (2012).

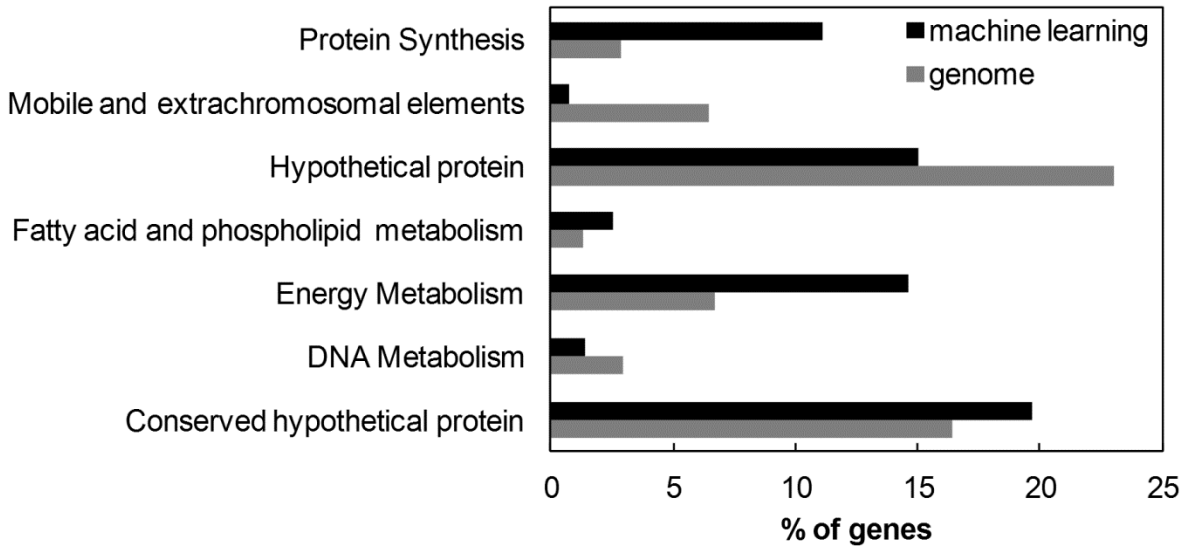

Figure 5.2. Bar chart indicating the percent of the genome or machine learning results that were classified in each of the seven groups found to have significantly different abundances ($p<0.05$, hypergeometric distribution) between the genome and results.

To gain a more detailed picture of the differences between the four sample groups, we probed the machine learning results for clusters of genes that appeared to be specifically involved in extracellular respiration. We found two clusters of genes representing ETC complexes that were predictive for extracellular respiration: the *nuo* cluster, and the *cco* cluster. Of the 5 genes with the most negative scores (indicating increased expression) for the anode group, 3 were *nuoCD*, *nuoE*, and *nuoL*. The *nuoJ* gene also had a negative score for the anode group and *nuoB*, *nuoCD*, and *nuoE* also had negative scores for the Fe(III) respiring group. All of these, and *nuoI* had positive scores for the oxygen group, indicating a strong change in expression of this gene cluster between aerobic and anaerobic conditions. Within the 20 most negative scores for the Fe(III) group is the gene *ccoN*, encoding subunit I of the cbb_3-type cytochrome oxidase. The genes *ccoO* and *ccoP* also had negative scores for the Fe(III) group. Terminal cytochrome *c* oxidases are not known to be part of the extracellular respiration pathway of *S. oneidensis*, which has been well characterized, but this complex has been implicated in

survival of heavy metal stress (Gao, Barua et al. 2010). Rosenbaum et al. (2012) found this gene cluster to be upregulated in anode respiring conditions, relative to Fe(III)-citrate respiring conditions and speculated that the Cco complex may have a role in sensing the redox state of the environment, as seen previously in *Rhodobacter sphaeroides* (Oh and Kaplan 1999). Surprisingly, we did not find that increased expression of the *cco* gene cluster was predictive for anode respiration, but rather Fe(III) respiration. This may indicate that it is an important factor in both conditions, relative to oxygen respiration.

5.4.3 Gene knockout studies

To confirm the importance of the ETC genes discovered by machine learning we obtained or constructed strains of *S. oneidensis* with in-frame deletions of the following genes: *ccoO* (SO_2363), *coxB* (SO_4606), the ATP synthase operon (SO_4746-SO_4754), and *nuoN* (SO_1009) (see **Table 5.1** for a list of strains used in this study). We also tested a double knockout of *coxB* and *nuoN*. We tested Δ*ccoO* and Δ*nuoN* because they were found in the machine learning results, and included the other genes to give deeper insight into their function. Because both the Cco and Nuo complexes are predicted to pump protons within the ETC, we included a strain without ATP synthase to determine whether these complexes contribute to ATP production by generating proton gradients under anaerobic conditions. We included Δ*coxB* because this mutant was readily available, and because the Cox and Cco complexes in *S. oneidensis* are predicted to have the same proton translocation efficiencies and have low fluxes in *S. oneidensis* under aerobic conditions (Pinchuk, Hill et al. 2010).

We tested the performance of these knockout strains in batch-fed, potentiostatically-poised bioelectrochemical systems by measuring maximum current production, coulombic efficiency, and growth (OD_{600}). The Δ*ccoO* strain produced significantly *lower* maximum

current than the wild-type, while the Δ*coxB* and Δ*nuoN* strains produced significantly *higher* maximum current than the wild-type (two tailed t-test, p≤0.05; **Figure 5.3B**). The Δ*coxB* and Δ*nuoN* strains produced very similar current profiles, with a much faster increase to a higher maximal current production, followed by a steep decline (**Figure 5.3A**).

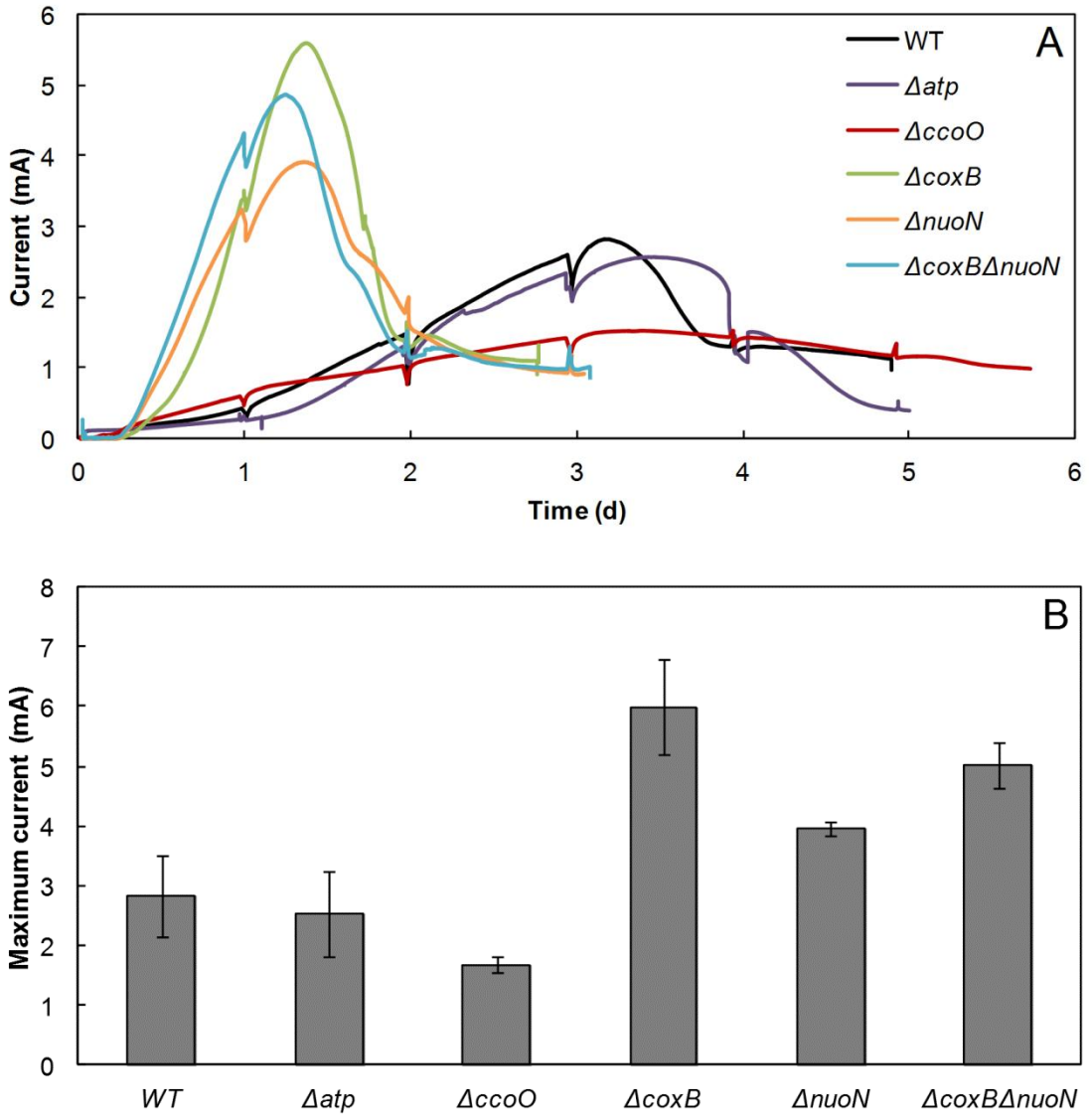

Figure 5.3. Current production from wild-type and knockout strains of *S. oneidensis* in 2-chambered, potentiostatically poised, batch BESs. (A) Current production over time, averaged for 3 biological replicates. (B) Average maximum current production for each strain, error bars represent standard deviation.

The Δ*coxB*Δ*nuoN* double knockout strain had activity very similar to the single-knockouts, indicating that these two complexes function as part of the same pathway, and both are necessary for full activity. Current production by the mutant lacking ATP synthase did not differ significantly from that of the wild-type, in accordance with previous observations that ATP synthase has little activity under anaerobic conditions, and in fact consumes ATP to produce a small amount of PMF (Hunt, Flynn et al. 2010). The phenotype of the Δ*ccoO* strain was opposite that of the other ETC knockout strains, indicating that the Cco complex is not involved in the same pathway as the Cox and Nuo complexes.

Coulombic efficiency of the strains showed a very different trend than maximum current production (**Figure 5.4A**). The ATP synthase knockout was the only strain with very similar coulombic efficiency to the wild-type, which is not surprising, considering that this mutation is expected to have very little impact on the physiology of *S. oneidensis* under these conditions. All other knockouts performed at a lower coulombic efficiency than the wild-type. For the Δ*coxB* and Δ*nuoN* strains, the decrease was statistically significant (two-tailed t-test, $p \leq 0.05$), representing a 57% and 58% decrease compared with WT, respectively. This indicates that the role of these proton pumping complexes is in supporting respiratory efficiency.

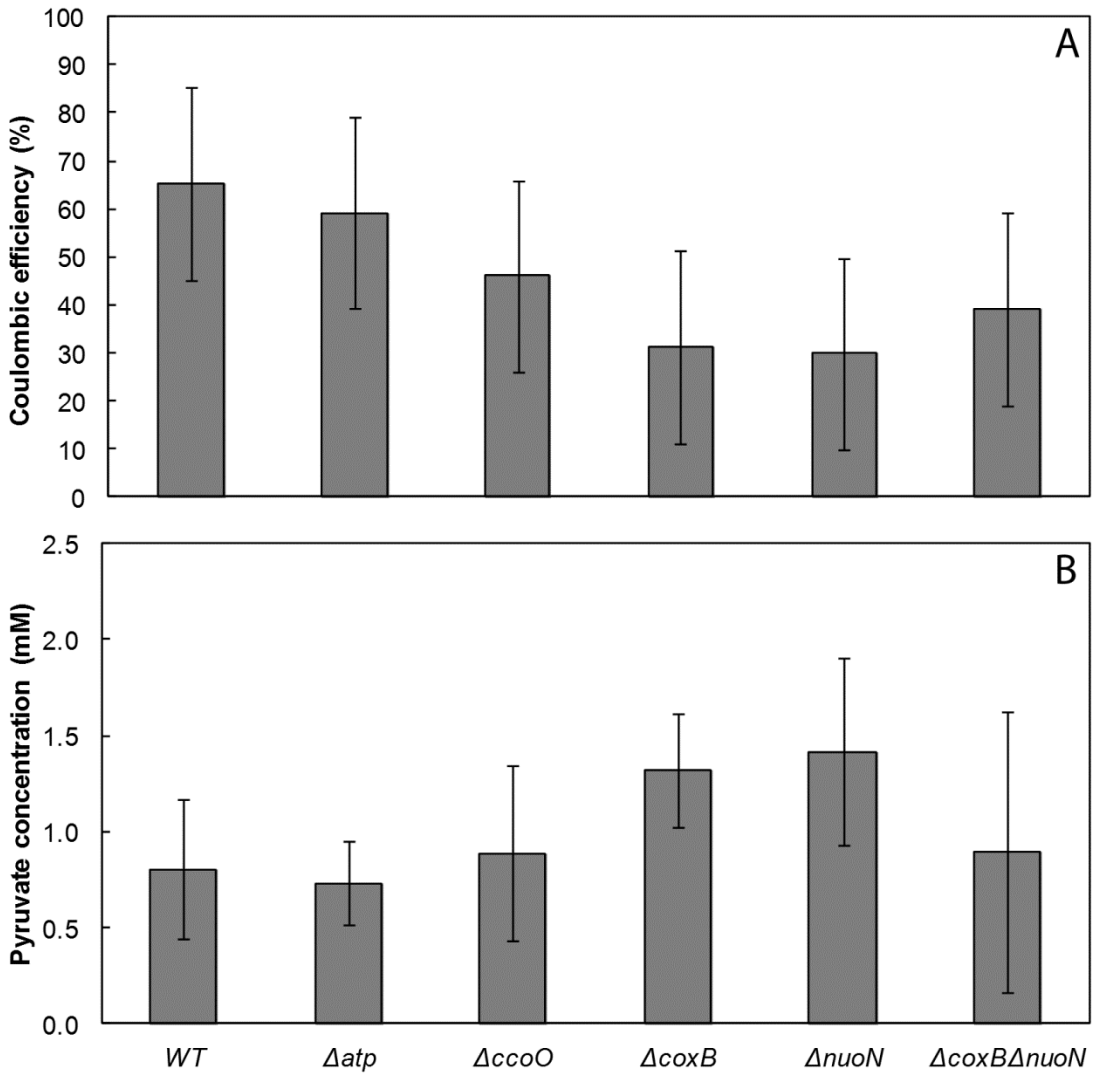

Figure 5.4. Coulombic efficiency for each strain in 2-chambered, batch BESs (A) and pyruvate concentrations at the end of each experiment, measured by HPLC (B). Bars indicate the mean from 3 biological replicates, and error bars represent standard deviation.

Because of the low coulombic efficiencies of the knockout strains, we further investigated the fate of metabolic electrons by quantifying a minor product (pyruvate). Previous work indicated that *S. oneidensis* excretes pyruvate in addition to acetate when PMF generation is low, but converts nearly all lactate to acetate when PMF generation is increased (Johnson, Baron et al. 2010). This may be because a high NADH:NAD^+ ratio in the cytoplasm inhibits further oxidation of pyruvate to acetate (i.e., cells are unable to maintain redox balance). A

similar result was observed when the Nuo complex of *E. coli* was inactivated, yielding it incapable of metabolizing acetate, and forcing it to utilize more reduced substrates (Prüss, Nelms et al. 1994). We found that all strains excreted pyruvate under these conditions, and that the *coxB* and *nuoN* single knockouts produced significantly more pyruvate than the WT, indicating that they, indeed, had a decreased ability to generate PMF, relative to WT (**Figure 5.4B**). This result is consistent with the interpretation that the Cox and Nuo complexes are both members of the anaerobic ETC of *S. oneidensis*. In contrast, the phenotype of the Δ*ccoO* strain was not consistent with the interpretation that it functions as part of the anaerobic ETC of *S. oneidensis*, indicating that it is more likely to be a redox sensor, as previously hypothesized (Rosenbaum, Bar et al. 2012).

Although several other factors differed between some of the strains, growth (measured as maximum OD_{600}) did not differ significantly ($p>0.05$, two-tailed t-test). Although the maximum OD_{600} did not change, we did find that gene knockouts caused changes in growth dynamics, which was reflected in current production (**Figures 5.2**). The Δ*coxB* and Δ*nuoN* strains had a faster initial increase in current production, and reached their maximum cell density and current production sooner. This may be due to the somewhat shortened metabolic pathway of these knockouts; because some of the lactate is converted to pyruvate and excreted, the cells process substrate more quickly and also use up available substrate more quickly.

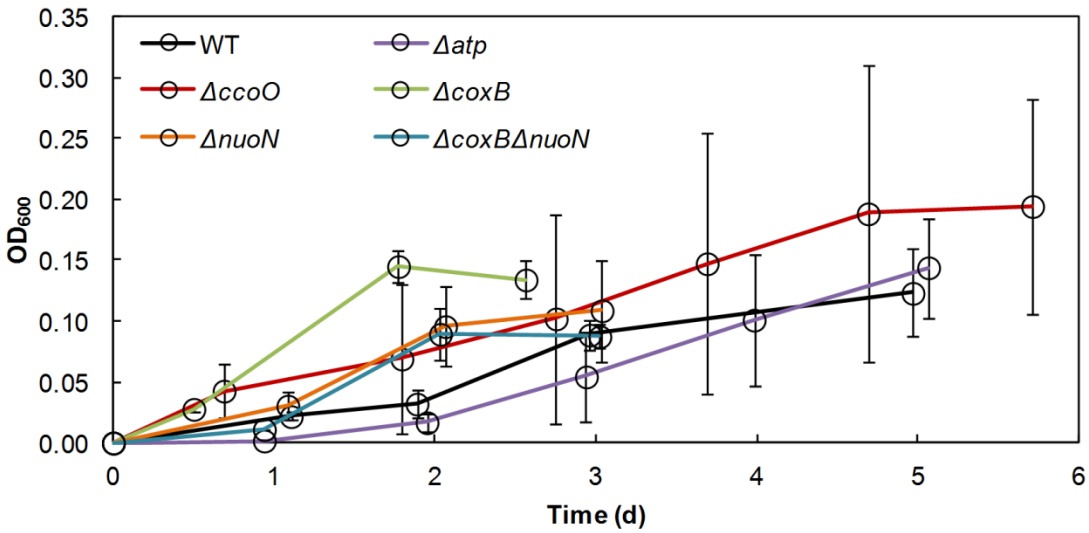

Figure 5.5. A plot of cell density (OD_{600}) over time for each *S. oneidensis* strain grown in batch BESs. OD_{600} was measured with a 1 cm path length. Each point is the average of 3 biological replicates and error bars represent standard deviation.

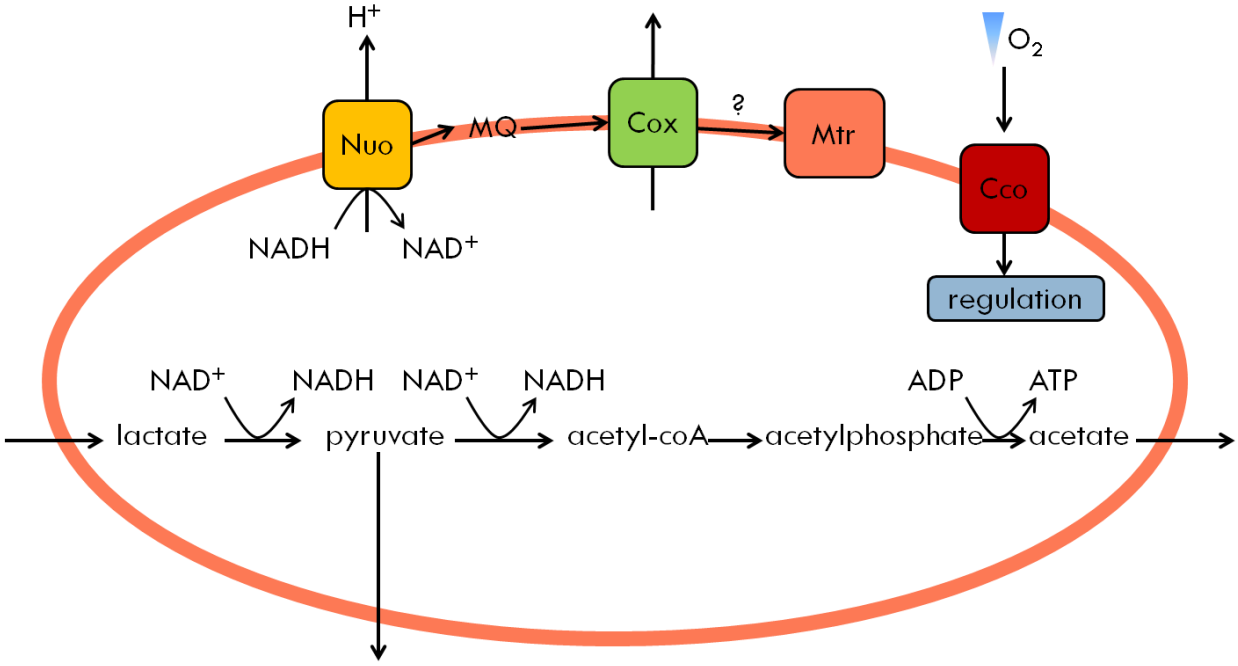

Figure 5.6. A working model of the anaerobic central metabolism and electron transport chain of *S. oneidensis* including the complexes investigated in this study. The pink oval represents the inner membrane of an *S. oneidensis* cell and each complex is denoted by its symbol. (MQ, menaquinone pool).

Together, these observations suggest that these putative ETC complexes function as components of the anaerobic electron transport chain in *S. oneidensis* (**Figure 5.6**). It was

previously suggested that the Nuo and Cox complexes may be more efficient at pumping protons than their counterparts, which may be necessary for *S. oneidensis* under anaerobic conditions because previous work has indicated that maintaining proton motive force is difficult under these conditions (Johnson, Baron et al. 2010). Proton pumping across the cytoplasmic membrane is a particularly important function during extracellular respiration because protons generated by respiration are not consumed by reaction with the terminal electron acceptor when extracellular electron acceptors are used (Mahadevan, Bond et al. 2006). If protons are not pumped out of the cytoplasm, metabolic reactions will cause acidification of the cell. In particular, the Nuo and Cox complexes may be specifically adapted for proton pumping under such conditions because they are not important for aerobic growth. We confirmed this by measuring aerobic growth curves for the Δ*ccoO*, Δ*coxB*, and Δ*nuoN* strains and comparing them with WT (**Figure 5.7**). The growth of both the Δ*coxB* and Δ*nuoN* strains was indistinguishable from WT, while the Δ*ccoO* strain had a slight, but significant growth defect, confirming that the former two are specialized members of the anaerobic electron transport chain, while the latter is likely a redox sensor.

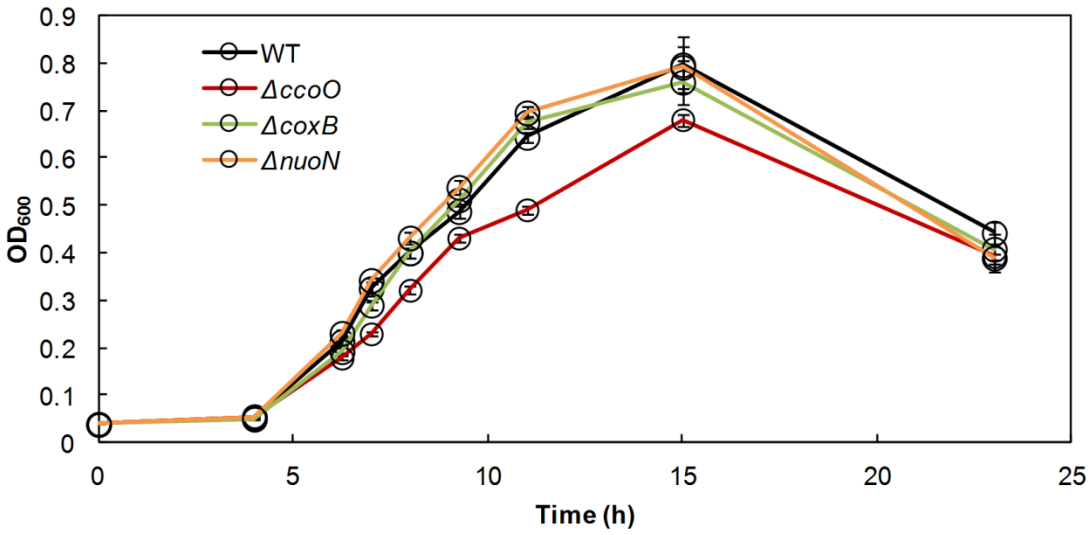

Figure 5.7. Aerobic growth curves for wild-type *S. oneidensis* MR-1 and three single-knockout strains over 24 hours of growth. Each point is the average of 12 measurements and error bars indicate standard error.

5.5 Conclusions

We used meta-analysis of transcriptomes of *S. oneidensis* grown under a variety of conditions to discover genes that support extracellular respiration, and found involvement of two putative members of the ETC, the Cco complex and the Nuo complex. Knockout experiments revealed that the Nuo complex functions as part of an anaerobic ETC in tandem with the Cox complex, while the Cco complex is more likely to be involved in redox sensing. Knockouts of the Nuo and Cox complexes also resulted in faster growth rates and higher maximum current production. At this time, reasons for this are not clear, but may be elucidated by further metabolic characterization of these mutants. When ETC components were knocked out of *S. oneidensis*, it produced current at a lower coulombic efficiency. Likely, this is due to a combination of a switch to less efficient ETC complexes typically associated with aerobic growth in this organism, and less efficient substrate utilization, which we observed as pyruvate accumulation in the medium. These data revealed that *S. oneidensis* uses a specialized electron transport pathway under anaerobic conditions, which is likely to be necessary overcome the difficulty of maintaining a proton gradient across the cytoplasmic membrane and ideal $NADH:NAD^+$ ratios while respiring with extracellular electron acceptors.

5.6 Acknowledgements

We thank Andrew Myers for assisting in data downloading, aggregation, and processing. We thank Jeff Gralnick for providing strains, and Alexander Beliaev and Samantha Reed for providing strains and information on gene deletion strategies for *S. oneidensis* MR-1. This work was supported by the National Science Foundation through CAREER grant no. 0939882 to L.T.A.

CHAPTER 6

SUMMARY AND RECOMMENDATIONS FOR FUTURE WORK

6.1 Summary

Shewanella oneidensis MR-1 produces electric current under a wide variety of conditions in bioelectrochemical systems, however, through this work I have shown that this organism is not ideal for use under certain conditions. Because flavin-mediated electron transfer is a major extracellular electron transfer pathway for this organism, continuously-fed reactor designs reduce its current production by washing out flavins. This can be overcome by adding oxygen to the reactor, which increases biomass and flavin production (Chapter 3). Continuous medium flow is also a disadvantage for *S. oneidensis* because it discourages planktonic growth, and biofilm cells can be damaged by oxidizing electrode potentials. This difficulty may also be overcome by slowing medium flow, or adding oxygen to the system to encourage planktonic growth, because planktonic cells are not negatively affected by electrode potentials (Chapter 4). Meta-analysis of transcriptomic data revealed that *S. oneidensis* uses a specialized electron transport pathway under anaerobic conditions, likely to overcome the difficulty of maintaining a proton gradient across the cytoplasmic membrane and ideal NADH:NAD^+ ratios while respiring with extracellular electron acceptors. This specialized electron transport chain is necessary for *S. oneidensis* to convert substrate into electric current efficiently (Chapter 5). This reveals a metabolic limitation of *S. oneidensis* under anaerobic conditions, providing further evidence that this organism is not appropriate for use in strictly-anaerobic, continuously-fed bioelectrochemical systems.

As the field of bioelectrochemistry expands to include a diversity of applications other than anaerobic wastewater treatment, I expect to see increased utility of *S. oneidensis*. Although

S. oneidensis is not suitable for anaerobic wastewater treatment or other microbial fuel cell-type applications, it has characteristics that make it useful in other BES applications, such as biosensing and biocomputing. Through work with the International Genetically Engineered Machines (iGEM) competition, the Angenent lab has already demonstrated a proof of concept for the use of *S. oneidensis* as a bioelectrochemical actuator in an arsenic sensing system (Webster, TerAvest, et al., manuscript in preparation for *Biosensors and Bioelectronics*). The central component of the biosensor was an *mtrB* deletion strain of *S. oneidensis* with *mtrB* complemented on a plasmid, with expression controlled by an arsenic sensitive promoter (P_{ars}). This resulted in a strain with increased extracellular electron transfer capabilities in the presence of arsenic (as measured by electric current). *S. oneidensis* was the ideal organism for this purpose, because its well-understood extracellular electron transfer pathway provided several possible targets to exogenously regulate current production. Also, its ability to use oxygen provided a way to maintain the cells when arsenic was not present (i.e., when the cells were incapable of using the electrode as an electron acceptor. I expect that development of more advanced genetic engineering tools for *S. oneidensis* will further enhance its utility in biosensing systems in the future.

6.2 Recommendations for future work

The results presented here have provided insight into the physiology of *S. oneidensis* in BESs, however, more work is necessary to understand how the limitations of *S. oneidensis* may be overcome to improve performance. Additional work directly related to Chapters 3, 4, and 5, is outlined here. I also discuss future application of *S. oneidensis* in bioelectrochemical systems designed for biosensing and biocomputing purposes.

The results presented in Chapter 3 clearly show that flavin-mediated electron transfer is stimulated when oxygen is added to continuously-fed bioelectrochemical systems with *S. oneidensis*, however, it was not clear whether flavin production was upregulated by oxygen addition, or whether the increase in electron acceptor availability simply increased growth and thereby increased overall flavin production. Future work on the regulation of the flavin production and export pathway are necessary to elucidate the regulatory pathways that control flavin secretion. This would shed light on the conditions that stimulate *S. oneidensis* to produce flavins and exploit mediated electron transfer in environmental settings. Careful control of oxygen tension would provide insight into the niches in which *S. oneidensis* is most competitive in the environment.

Our results in Chapter 4 indicated damage to *c*-type cytochromes, even at the electrode potential that produced the most electric current. Finer optimization of electrode potentials close to our optimal range may reveal a more favorable potential for *S. oneidensis*. It is also possible that the use of different electrode materials would reduce the damage caused to the cells. This is important future work because many applications with *S. oneidensis* are likely to use potentiostatically-poised electrodes. The high variability in gene expression observed between biological replicates also indicated that future work on gene expression in anaerobic cultures of *S. oneidensis* must be performed with more careful, strictly anaerobic sampling techniques. This would likely decrease variability between replicates and improve the conclusions gained from transcriptional analysis of this organism.

I gained insight into anaerobic respiration of *S. oneidensis* using the data set aggregated in Chapter 5, however, there is much more information that may be gained from this data set. Researchers interested in other aspects of *S. oneidensis* physiology may find his data set useful

for discovery of biofilm processes, general toxicity responses, and other areas. A similar approach to ours could be used with a focus on other aspects, or additional types of analysis (e.g., network analysis) could be used.

As mentioned, I believe that biosensing and biocomputing will be major areas of expansion for application of *S. oneidensis* in bioelectrochemical systems. I have previously described how *S. oneidensis* and other electrochemically active organisms may be used in biocomputing systems in two review articles and a book chapter (TerAvest, Li et al. 2011; TerAvest and Angenent 2012; TerAvest, Li et al. 2012). The extracellular electron transport pathway of *S. oneidensis* provides several targets for regulation by synthetic genetic circuits, which may be programmed to respond in characteristic ways to chemical or physical input signals (e.g., antibiotics, sugars, toxins, or light). Further development in the design of synthetic genetic circuits for complex control of gene expression and tools for genetic manipulation of *S. oneidensis* will increase the speed of progress in this field and lead to application of biosensing and biocomputing systems with electric output generated by *S. oneidensis*.

REFERENCES

Appaix, F., M.-N. Minatchy, et al. (2000). "Rapid spectrophotometric method for quantitation of cytochrome *c* release from isolated mitochondria or permeabilized cells revisited." Biochimica et Biophysica Acta (BBA) - Bioenergetics **1457**(3): 175-181.

Aulenta, F., A. Catervi, et al. (2007). "Electron transfer from a solid-state electrode assisted by methyl viologen sustains efficient microbial reductive dechlorination of TCE." Environmental Science & Technology **41**(7): 2554-2559.

Babauta, J. T., H. D. Nguyen, et al. (2011). "Redox and pH microenvironments within *Shewanella oneidensis* MR-1 biofilms reveal an electron transfer mechanism." Environmental Science & Technology **45**(15): 6654-6660.

Baron, D., E. LaBelle, et al. (2009). "Electrochemical Measurement of Electron Transfer Kinetics by *Shewanella oneidensis* MR-1." Journal of Biological Chemistry **284**(42): 28865-28873.

Beg, Q. K., M. Zampieri, et al. (2012). "Detection of transcriptional triggers in the dynamics of microbial growth: application to the respiratorily versatile bacterium *Shewanella oneidensis*." Nucleic Acids Research **40**(15): 7132-7149.

Beliaev, A. S., D. M. Klingeman, et al. (2005). "Global transcriptome analysis of *Shewanella oneidensis* MR-1 exposed to different terminal electron acceptors." Journal of Bacteriology **187**(20): 7138-7145.

Beliaev, A. S. and D. A. Saffarini (1998). "*Shewanella putrefaciens mtrB* encodes an outer membrane protein required for Fe(III) and Mn(IV) reduction." Journal of Bacteriology **180**(23): 6292-6297.

Beliaev, A. S., D. A. Saffarini, et al. (2001). "MtrC, an outer membrane decahaem *c* cytochrome required for metal reduction in Shewanella putrefaciens MR-1." Molecular Microbiology **39**(3): 722-730.

Beliaev, A. S., D. K. Thompson, et al. (2002). "Gene and protein expression profiles of *Shewanella oneidensis* during anaerobic growth with different electron acceptors." OMICS A Journal of Integrative Biology **6**(1): 39-60.

Bencharit, S. and M. J. Ward (2005). "Chemotactic responses to metals and anaerobic electron acceptors in *Shewanella oneidensis* MR-1." Journal of Bacteriology **187**(14): 5049-5053.

Biffinger, J. C., J. N. Byrd, et al. (2008). "Oxygen exposure promotes fuel diversity for *Shewanella oneidensis* microbial fuel cells." Biosensors and Bioelectronics **23**(6): 820-826.

Biffinger, J. C., J. Pietron, et al. (2007). "A biofilm enhanced miniature microbial fuel cell using *Shewanella oneidensis* DSP10 and oxygen reduction cathodes." Biosensors and Bioelectronics **22**(8): 1672-1679.

Biffinger, J. C., R. Ray, et al. (2009). "Simultaneous analysis of physiological and electrical output changes in an operating microbial fuel cell with *Shewanella oneidensis*." Biotechnology and Bioengineering **103**(3): 524-531.

Borloo, J., L. Desmet, et al. (2011). "Bacterial two-hybrid analysis of the *Shewanella oneidensis* MR-1 multi-component electron transfer pathway." Journal of Integrated OMICS **1**(2): 260-267.

Bouhenni, R. A., G. J. Vora, et al. (2010). "The role of *Shewanella oneidensis* MR-1 outer surface structures in extracellular electron transfer." Electroanalysis **22**(7-8): 856-864.

Bretschger, O., A. Obraztsova, et al. (2007). "Current production and metal oxide reduction by Shewanella oneidensis MR-1 wild type and mutants." Applied and Environmental Microbiology **73**(21): 7003-7012.

Brown, S. D., M. R. Thompson, et al. (2006). "Molecular Dynamics of the *Shewanella oneidensis* Response to Chromate Stress." Molecular & Cellular Proteomics **5**(6): 1054-1071.

Carmona-Martinez, A. A., F. Harnisch, et al. (2011). "Cyclic voltammetric analysis of the electron transfer of *Shewanella oneidensis* MR-1 and nanofilament and cytochrome knock-out mutants." Bioelectrochemistry **81**(2): 74-80.

Carmona-Martínez, A. A., F. Harnisch, et al. (2012). "Electron transfer and biofilm formation of *Shewanella putrefaciens* as function of anode potential." Bioelectrochemistry ***In press.***(0).

Cho, E. J. and A. D. Ellington (2007). "Optimization of the biological component of a bioelectrochemical cell." Bioelectrochemistry **70**(1): 165-172.

Clarke, T. A., M. J. Edwards, et al. (2011). "Structure of a bacterial cell surface decaheme electron conduit." Proceedings of the National Academy of Sciences **108**(23): 9384-9389.

Clauwaert, P., D. van der Ha, et al. (2007). "Open air biocathode enables effective electricity generation with microbial fuel cells." Environmental Science & Technology **41**(21): 7564-7569.

Coursolle, D., D. B. Baron, et al. (2010). "The Mtr respiratory pathway is essential for reducing flavins and electrodes in *Shewanella oneidensis*." Journal of Bacteriology **192**(2): 467-474.

Coursolle, D. and J. A. Gralnick (2010). "Modularity of the Mtr respiratory pathway of *Shewanella oneidensis* strain MR-1." Molecular Microbiology **77**(4): 995-1008.

Covington, E. D., C. B. Gelbmann, et al. (2010). "An essential role for UshA in processing of extracellular flavin electron shuttles by Shewanella oneidensis." Molecular Microbiology **78**(2): 519-532.

Dallas, P., N. Gottardo, et al. (2005). "Gene expression levels assessed by oligonucleotide microarray analysis and quantitative real-time RT-PCR - how well do they correlate?" BMC Genomics **6**(1): 59.

Demšar, J., B. Zupan, et al. (2004). Orange: From experimental machine learning to interactive data mining. Knowledge Discovery in Databases: PKDD 2004. J.-F. Boulicaut, F. Esposito, F. Giannotti and D. Pedreschi, Springer Berlin Heidelberg. **3202:** 537-539.

Dobbin, K. K., E. S. Kawasaki, et al. (2005). "Characterizing dye bias in microarray experiments." Bioinformatics **21**(10): 2430-2437.

El-Naggar, M. Y., G. Wanger, et al. (2010). "Electrical transport along bacterial nanowires from *Shewanella oneidensis* MR-1." Proceedings of the National Academy of Sciences **107**(42): 18127-18131.

Erable, B., L. Etcheverry, et al. (2011). "From microbial fuel cell (MFC) to microbial electrochemical snorkel (MES): maximizing chemical oxygen demand (COD) removal from wastewater." Biofouling **27**(3): 319-326.

Erable, B., I. Vandecandelaere, et al. (2010). "Marine aerobic biofilm as biocathode catalyst." Bioelectrochemistry **78**(1): 51-56.

Erhardt, H., S. Steimle, et al. (2012). "Disruption of individual *nuo*-genes leads to the formation of partially assembled NADH:ubiquinone oxidoreductase (complex I) in *Escherichia coli*." Biochimica et Biophysica Acta (BBA) - Bioenergetics **1817**(6): 863-871.

Fan, Y., H. Hu, et al. (2007). "Enhanced coulombic efficiency and power density of air-cathode microbial fuel cells with an improved cell configuration." Journal of Power Sources **171**(2): 348-354.

Flynn, C. M., K. A. Hunt, et al. (2012). "Construction and elementary mode analysis of a metabolic model for *Shewanella oneidensis* MR-1." BioSystems **107**(2): 120-128.

Foley, J. M., R. A. Rozendal, et al. (2010). "Life cycle assessment of high-rate anaerobic treatment, microbial fuel cells, and microbial electrolysis cells." Environmental Science & Technology **44**(9): 3629-3637.

Folsom, J., L. Richards, et al. (2010). "Physiology of *Pseudomonas aeruginosa* in biofilms as revealed by transcriptome analysis." BMC Microbiology **10**(1): 294.

Fornero, J. J., M. Rosenbaum, et al. (2010). "Electric power generation from municipal, food, and animal wastewaters using microbial fuel cells." Electroanalysis **22**(7-8): 832-843.

Franks, A. E. (2010). "Transcriptional analysis in microbial fuel cells: common pitfalls in global gene expression studies of microbial biofilms." FEMS Microbiology Letters **307**(2): 111-112.

Franks, A. E., N. Malvankar, et al. (2010). "Bacterial biofilms: the powerhouse of a microbial fuel cell." Biofuels **1**(4): 589-604.

Franks, A. E., K. P. Nevin, et al. (2010). "Microtoming coupled to microarray analysis to evaluate the spatial metabolic status of *Geobacter sulfurreducens* biofilms." ISME Journal **4**(4): 509-519.

Franks, A. E., K. P. Nevin, et al. (2009). "Novel strategy for three-dimensional real-time imaging of microbial fuel cell communities: monitoring the inhibitory effects of proton accumulation within the anode biofilm." Energy & Environmental Science **2**(1): 113-119.

Fredrickson, J. K., M. F. Romine, et al. (2008). "Towards environmental systems biology of *Shewanella*." Nature Reviews Microbiology **6**(8): 592-603.

Freguia, S., K. Rabaey, et al. (2008). "Syntrophic processes drive the conversion of glucose in microbial fuel cell anodes." Environmental Science & Technology **42**(21): 7937-7943.

Friedman, E. S., M. A. Rosenbaum, et al. (2012). "A cost-effective and field-ready potentiostat that poises subsurface electrodes to monitor bacterial respiration." Biosensors and Bioelectronics **32**(1): 309-313.

Gao, H., S. Barua, et al. (2010). "Impacts of *Shewanella oneidensis* c-type cytochromes on aerobic and anaerobic respiration." Microbial Biotechnology **3**(4): 455-466.

Gao, H., Z. K. Yang, et al. (2006). "Global transcriptome analysis of the cold shock response of *Shewanella oneidensis* MR-1 and mutational analysis of its classical cold shock proteins." Journal of Bacteriology **188**(12): 4560-4569.

Goldbeck, C. P., H. M. Jensen, et al. (2013). "Tuning promoter strengths for improved synthesis and function of electron conduits in *Escherichia coli*." ACS Synthetic Biology **2**(3): 150-159.

Goldfless, S. J., A. S. Morag, et al. (2006). "DNA repeat rearrangements mediated by DnaK-dependent replication fork repair." Molecular Cell **21**(5): 595-604.

Golitsch, F., C. Bücking, et al. (2013). "Proof of principle for an engineered microbial biosensor based on *Shewanella oneidensis* outer membrane protein complexes." Biosensors and Bioelectronics **47**(0): 285-291.

Gorby, Y., J. McLean, et al. (2008). "Redox-reactive membrane vesicles produced by *Shewanella*." Geobiology **6**(3): 232-241.

Gorby, Y. A., S. Yanina, et al. (2009). "Electrically conductive bacterial nanowires produced by *Shewanella oneidensis* strain MR-1 and other microorganisms." Proceedings of the National Academy of Sciences **106**(23): 9535-9535.

Gottesman, S. (1996). "Proteases and their targets in *Escherichia coli*." Annual Review of Genetics **30**(1): 465-506.

Hamelers, H. V. M., A. t. Heijne, et al. (2010). "New applications and performance of bioelectrochemical systems." Applied Microbiology and Biotechnology **85**(6): 1673-1685.

Harris, H. W., M. Y. El-Naggar, et al. (2010). "Electrokinesis is a microbial behavior that requires extracellular electron transport." Proceedings of the National Academy of Sciences **107**(1): 326-331.

Hartshorne, R., B. Jepson, et al. (2007). "Characterization of *Shewanella oneidensis* MtrC: a cell-surface decaheme cytochrome involved in respiratory electron transport to extracellular electron acceptors." Journal of Biological Inorganic Chemistry **12**(7): 1083-1094.

He, Z. and L. T. Angenent (2006). "Application of bacterial biocathodes in microbial fuel cells." Electroanalysis **18**(19-20): 2009-2015.

He, Z., S. D. Minteer, et al. (2005). "Electricity generation from artificial wastewater using an upflow microbial fuel cell." Environmental Science & Technology **39**(14): 5262-5267.

Hernandez, M. E. and D. K. Newman (2001). "Extracellular electron transfer." Cellular and Molecular Life Sciences **58**(11): 1562-1571.

Holmes, D. E., D. R. Bond, et al. (2004). "Microbial communities associated with electrodes harvesting electricity from a variety of aquatic sediments." Microbial Ecology **48**(2): 178-190.

Hunt, K. A., J. M. Flynn, et al. (2010). "Substrate-level phosphorylation is the primary source of energy conservation during anaerobic respiration of *Shewanella oneidensis* strain MR-1." Journal of Bacteriology **192**(13): 3345-3351.

Ieropoulos, I., C. Melhuish, et al. (2003). Artificial metabolism: towards true energetic autonomy in artificial life. Advances in Artificial Life. W. Banzhaf, J. Ziegler, T. Christaller, P. Dittrich and J. Kim, Springer Berlin / Heidelberg. **2801:** 792-799.

Jensen, H. M., A. E. Albers, et al. (2010). "Engineering of a synthetic electron conduit in living cells." Proceedings of the National Academy of Sciences **107**(45): 19213-19218.

Jeong, J., J. Y. Kim, et al. (2006). "The role of reactive oxygen species in the electrochemical inactivation of microorganisms." Environmental Science & Technology **40**(19): 6117-6122.

Johnson, E. T., D. B. Baron, et al. (2010). "Enhancement of survival and electricity production in an engineered bacterium by light-driven proton pumping." Applied and Environmental Microbiology **76**(13): 4123-4129.

Kim, B.-C., B. L. Postier, et al. (2008). "Insights into genes involved in electricity generation in *Geobacter sulfurreducens* via whole genome microarray analysis of the OmcF-deficient mutant." Bioelectrochemistry **73**(1): 70-75.

Kotloski, N. J. and J. A. Gralnick (2013). "Flavin electron shuttles dominate extracellular electron transfer by *Shewanella oneidensis*." mBio **4**(1).

Lanthier, M., K. B. Gregory, et al. (2008). "Growth with high planktonic biomass in *Shewanella oneidensis* fuel cells." FEMS Microbiology Letters **278**(1): 29-35.

Lazazzera, B. A. (2005). "Lessons from DNA microarray analysis: the gene expression profile of biofilms." Current Opinion in Microbiology **8**(2): 222-227.

Leang, C., X. Qian, et al. (2010). "Alignment of the *c*-type cytochrome OmcS along pili of *Geobacter sulfurreducens*." Applied and Environmental Microbiology **76**(12): 4080-4084.

Leaphart, A. B., D. K. Thompson, et al. (2006). "Transcriptome profiling of *Shewanella oneidensis* gene expression following exposure to acidic and alkaline pH." Journal of Bacteriology **188**(4): 1633-1642.

Li, R., J. M. Tiedje, et al. (2012). "Soluble electron shuttles can mediate energy taxis toward insoluble electron acceptors." Environmental Science & Technology **46**(5): 2813-2820.

Li, S. L., S. Freguia, et al. (2010). "Effects of oxygen on *Shewanella decolorationis* NTOU1 electron transfer to carbon-felt electrodes." Biosensors & Bioelectronics **25**(12): 2651-2656.

Li, Z., X. Zhang, et al. (2010). "Azo dye treatment with simultaneous electricity production in an anaerobic–aerobic sequential reactor and microbial fuel cell coupled system." Bioresource Technology **101**(12): 4440-4445.

Li, Z. J., M. A. Rosenbaum, et al. (2011). "Bacteria-based AND logic gate: a decision-making and self-powered biosensor." Chemical Communications **47**(11): 3060-3062.

Lies, D. P., M. E. Hernandez, et al. (2005). "*Shewanella oneidensis* MR-1 uses overlapping pathways for iron reduction at a distance and by direct contact under conditions relevant for biofilms." Applied and Environmental Microbiology **71**(8): 4414-4426.

Lin, W. C., M. V. Coppi, et al. (2004). "*Geobacter sulfurreducens* can grow with oxygen as a terminal electron acceptor." Applied and Environmental Microbiology **70**(4): 2525-2528.

Liu, H., S. Grot, et al. (2005). "Electrochemically assisted microbial production of hydrogen from acetate." Environmental Science & Technology **39**(11): 4317-4320.

Liu, H. and B. E. Logan (2004). "Electricity generation using an air-cathode single chamber microbial fuel cell in the presence and absence of a proton exchange membrane." Environmental Science & Technology **38**(14): 4040-4046.

Logan, B. E. (2009). "Exoelectrogenic bacteria that power microbial fuel cells." Nature Reviews Microbiology **7**(5): 375-381.

Logan, B. E., D. Call, et al. (2008). "Microbial electrolysis cells for high yield hydrogen gas production from organic matter." Environmental Science & Technology **42**(23): 8630-8640.

Logan, B. E., B. Hamelers, et al. (2006). "Microbial fuel cells: Methodology and technology." Environmental Science & Technology **40**(17): 5181-5192.

Logan, B. E. and K. Rabaey (2012). "Conversion of wastes into bioelectricity and chemicals by using microbial electrochemical technologies." Science **337**(6095): 686-690.

Logan, B. E. and J. M. Regan (2006). "Electricity-producing bacterial communities in microbial fuel cells." Trends in Microbiology **14**(12): 512-518.

Lovley, D. R. (2002). "Dissimilatory metal reduction: from early life to bioremediation." ASM News **68**(5): 231-237.

Lovley, D. R. (2006). "Bug juice: harvesting electricity with microorganisms." Nature Reviews Microbiology **4**(7): 497-508.

Lower, B. H., R. Yongsunthon, et al. (2009). "Antibody-recognition force microscopy shows that outer membrane cytochromes OmcA and MtrC are expressed on the exterior surface of *Shewanella oneidensis* MR-1." Applied and Environmental Microbiology **75**(9): 2931-2935.

Luo, H., G. Liu, et al. (2009). "Phenol degradation in microbial fuel cells." Chemical Engineering Journal **147**(2-3): 259-264.

Mahadevan, R., D. R. Bond, et al. (2006). "Characterization of metabolism in the Fe(III)-reducing organism *Geobacter sulfurreducens* by constraint-based modeling." Applied and Environmental Microbiology **72**(2): 1558-1568.

Malvankar, N. S., M. Vargas, et al. (2011). "Tunable metallic-like conductivity in microbial nanowire networks." Nature Nanotechnology **6**: 573-579.

Marsili, E., D. B. Baron, et al. (2008). "*Shewanella* secretes flavins that mediate extracellular electron transfer." Proceedings of the National Academy of Sciences **105**(10): 3968-3973.

Matsunaga, T., S. Nakasono, et al. (1992). "Electrochemical sterilization of bacteria adsorbed on granular activated carbon." FEMS Microbiology Letters **93**(3): 255-259.

Matsunaga, T., Y. Namba, et al. (1984). "Electrochemical sterilization of microbial cells." Bioelectrochemistry and Bioenergetics **13**(4–6): 393-400.

Mehta, T., M. V. Coppi, et al. (2005). "Outer membrane *c*-type cytochromes required for Fe(III) and Mn(IV) oxide reduction in *Geobacter sulfurreducens*." Applied and Environmental Microbiology **71**(12): 8634-8641.

Meitl, L. A., C. M. Eggleston, et al. (2009). "Electrochemical interaction of *Shewanella oneidensis* MR-1 and its outer membrane cytochromes OmcA and MtrC with hematite electrodes." Geochimica et Cosmochimica Acta **73**(18): 5292-5307.

Methé, B. A., K. E. Nelson, et al. (2003). "Genome of *Geobacter sulfurreducens*: Metal reduction in subsurface environments." Science **302**(5652): 1967-1969.

Meyer, T. E., A. I. Tsapin, et al. (2004). "Identification of 42 possible cytochrome c genes in the Shewanella oneidensis genome and characterization of six soluble cytochromes." OMICS-a Journal of Integrative Biology **8**(1): 57-77.

Miyawaki, O. and L. B. Wingard (1984). "Electrochemical and enzymatic activity of flavin adenine dinucleotide and glucose oxidase immobilized by adsorption on carbon." Biotechnology and Bioengineering **26**(11): 1364-1371.

Morey, J., J. Ryan, et al. (2006). "Microarray validation: factors influencing correlation between oligonucleotide microarrays and real-time PCR." Biological Procedures Online **8**(1): 175-193.

Myers, C. R. and J. M. Myers (1992). "Localization of cytochromes to the outer membrane of anaerobically grown *Shewanella putrefaciens* MR-1." Journal of Bacteriology **174**(11): 3429-3438.

Myers, C. R. and K. H. Nealson (1988). "Bacterial manganese reduction and growth with manganese oxide as the sole electron acceptor." Science **240**(4857): 1319-1321.

Myers, J. M. and C. R. Myers (2001). "Role for outer membrane cytochromes OmcA and OmcB of *Shewanella putrefaciens* MR-1 in reduction of manganese dioxide." Appl. Environ. Microbiol. **67**(1): 260-269.

Nealson, K. H., D. P. Moser, et al. (1995). "Anaerobic electron acceptor chemotaxis in *Shewanella putrefaciens*." Applied and Environmental Microbiology **61**(4): 1551-1554.

Nealson, K. H. and C. R. Myers (1992). "Microbial reduction of manganese and iron - new approaches to carbon cycling." Applied and Environmental Microbiology **58**(2): 439-443.

Nevin, K. P., S. A. Hensley, et al. (2011). "Electrosynthesis of organic compounds from carbon dioxide is catalyzed by a diversity of acetogenic microorganisms." Applied and Environmental Microbiology **77**(9): 2882-2886.

Nevin, K. P., B.-C. Kim, et al. (2009). "Anode biofilm transcriptomics reveals outer surface components essential for high density current production in *Geobacter sulfurreducens* fuel cells." PLoS ONE **4**(5): e5628.

Nevin, K. P., H. Richter, et al. (2008). "Power output and columbic efficiencies from biofilms of *Geobacter sulfurreducens* comparable to mixed community microbial fuel cells." Environmental Microbiology **10**(10): 2505-2514.

Nevin, K. P., T. L. Woodard, et al. (2010). "Microbial electrosynthesis: Feeding microbes electricity to convert carbon dioxide and water to multicarbon extracellular organic compounds." mBio **1**(2).

Oh, J.-I. and S. Kaplan (1999). "The cbb_3 terminal oxidase of *Rhodobacter sphaeroides* 2.4.1: Structural and functional implications for the regulation of spectral complex formation." Biochemistry **38**(9): 2688-2696.

Okamoto, A., R. Nakamura, et al. (2011). "*In-vivo* identification of direct electron transfer from *Shewanella oneidensis* MR-1 to electrodes via outer-membrane OmcA-MtrCAB protein complexes." Electrochimica Acta **56**(16): 5526-5531.

Okamoto, A., R. Nakamura, et al. (2009). "*In vivo* electrochemistry of *c*-type cytochrome-mediated electron-transfer with chemical marking." ChemBioChem **10**(14): 2329-2332.

Palecek, E. and V. Ostatna (2009). "Ionic strength-dependent structural transition of proteins at electrode surfaces." Chemical Communications(13): 1685-1687.

Pant, D., G. Van Bogaert, et al. (2010). "A review of the substrates used in microbial fuel cells (MFCs) for sustainable energy production." Bioresource Technology **101**(6): 1533-1543.

Park, D. H. and J. G. Zeikus (2000). "Electricity generation in microbial fuel cells using neutral red as an electronophore." Applied and Environmental Microbiology **66**(4): 1292-1297.

Pinchuk, G. E., C. Ammons, et al. (2008). "Utilization of DNA as a sole source of phosphorus, carbon, and energy by *Shewanella* spp.: Ecological and physiological implications for dissimilatory metal reduction." Applied and Environmental Microbiology **74**(4): 1198-1208.

Pinchuk, G. E., E. A. Hill, et al. (2010). "Constraint-based model of *Shewanella oneidensis* MR-1 metabolism: a tool for data analysis and hypothesis generation." PLoS Comput Biol **6**(6): e1000822.

Pinchuk, G. E., D. A. Rodionov, et al. (2009). "Genomic reconstruction of *Shewanella oneidensis* MR-1 metabolism reveals a previously uncharacterized machinery for lactate utilization." Proceedings of the National Academy of Sciences **106**(8): 2874-2879.

Pokkuluri, P. R., Y. Y. Londer, et al. (2011). "Structure of a novel dodecaheme cytochrome *c* from *Geobacter sulfurreducens* reveals an extended 12 nm protein with interacting hemes." Journal of Structural Biology **174**(1): 223-233.

Prüss, B. M., J. M. Nelms, et al. (1994). "Mutations in NADH:ubiquinone oxidoreductase of *Escherichia coli* affect growth on mixed amino acids." Journal of Bacteriology **176**(8): 2143-2150.

Qiu, X., M. J. Daly, et al. (2006). "Transcriptome analysis applied to survival of *Shewanella oneidensis* MR-1 exposed to ionizing radiation." Journal of Bacteriology **188**(3): 1199-1204.

Quan, X.-c., Y.-p. Quan, et al. (2012). "Effect of anode aeration on the performance and microbial community of an air–cathode microbial fuel cell." Chemical Engineering Journal **210**(0): 150-156.

Rabaey, K. (2010). Bioelectrochemical systems : from extracellular electron transfer to biotechnological application. London; New York, IWA Publishing.

Rabaey, K., N. Boon, et al. (2005). "Microbial phenazine production enhances electron transfer in biofuel cells." Environmental Science & Technology **39**(9): 3401-3408.

Rabaey, K., N. Boon, et al. (2004). "Biofuel cells select for microbial consortia that self-mediate electron transfer." Applied and Environmental Microbiology **70**(9): 5373-5382.

Rabaey, K., J. Rodriguez, et al. (2007). "Microbial ecology meets electrochemistry: electricity-driven and driving communities." ISME Journal **1**(1): 9-18.

Rabaey, K. and R. A. Rozendal (2010). "Microbial electrosynthesis — revisiting the electrical route for microbial production." Nature Reviews Microbiology **8**(10): 706-716.

Rabaey, K. and W. Verstraete (2005). "Microbial fuel cells: novel biotechnology for energy generation." Trends in Biotechnology **23**(6): 291-298.

Read, S., P. Dutta, et al. (2010). "Initial development and structure of biofilms on microbial fuel cell anodes." BMC Microbiology **10**(1): 98.

Reguera, G., K. D. McCarthy, et al. (2005). "Extracellular electron transfer via microbial nanowires." Nature **435**(7045): 1098-1101.

Reguera, G., K. P. Nevin, et al. (2006). "Biofilm and nanowire production leads to increased current in *Geobacter sulfurreducens* fuel cells." Applied and Environmental Microbiology **72**(11): 7345-7348.

Reguera, G., R. B. Pollina, et al. (2007). "Possible nonconductive role of *Geobacter sulfurreducens* pilus nanowires in biofilm formation." Journal of Bacteriology **189**(5): 2125-2127.

Ringeisen, B. R., E. Henderson, et al. (2006). "High power density from a miniature microbial fuel cell using *Shewanella oneidensis* DSP10." Environmental Science & Technology **40**(8): 2629-2634.

Ringeisen, B. R., R. Ray, et al. (2007). "A miniature microbial fuel cell operating with an aerobic anode chamber." Journal of Power Sources **165**(2): 591-597.

Rosenbaum, M., F. Aulenta, et al. (2011). "Cathodes as electron donors for microbial metabolism: Which extracellular electron transfer mechanisms are involved?" Bioresource Technology **102**(1): 324-333.

Rosenbaum, M., M. A. Cotta, et al. (2010). "Aerated *Shewanella oneidensis* in continuously fed bioelectrochemical systems for power and hydrogen production." Biotechnology and Bioengineering **105**(5): 880-888.

Rosenbaum, M. A., H. Y. Bar, et al. (2011). "*Shewanella oneidensis* in a lactate-fed pure-culture and a glucose-fed co-culture with *Lactococcus lactis* with an electrode as electron acceptor." Bioresource Technology **102**(3): 2623-2628.

Rosenbaum, M. A., H. Y. Bar, et al. (2012). "Transcriptional analysis of *Shewanella oneidensis* MR-1 with an electrode compared to Fe(III)citrate or oxygen as terminal electron acceptor." PLoS ONE **7**(2): e30827.

Ross, D. E., J. M. Flynn, et al. (2011). "Towards Electrosynthesis in *Shewanella*: Energetics of Reversing the Mtr Pathway for Reductive Metabolism." PLoS ONE **6**(2): e16649.

Ross, D. E., S. S. Ruebush, et al. (2007). "Characterization of protein-protein interactions involved in iron reduction by *Shewanella oneidensis* MR-1." Applied and Environmental Microbiology **73**(18): 5797-5808.

Rozen, S. and H. Skaletsky (2000). "Primer3 on the WWW for general users and for biologist programmers." Methods in Molecular Biology **132**: 365-386.

Rozendal, R. A., E. Leone, et al. (2009). "Efficient hydrogen peroxide generation from organic matter in a bioelectrochemical system." Electrochemistry Communications **11**(9): 1752-1755.

Russell, J. B. and G. M. Cook (1995). "Energetics of bacterial growth: balance of anabolic and catabolic reactions." Microbiological Reviews **59**(1): 48-62.

Schmittgen, T. D. and K. J. Livak (2008). "Analyzing real-time PCR data by the comparative C-T method." Nature Protocols **3**(6): 1101-1108.

Schröder, H., T. Langer, et al. (1993). "DnaK, DnaJ and GrpE form a cellular chaperone machinery capable of repairing heat-induced protein damage." EMBO Journal **12**(11): 4137-4144.

Schröder, U. (2007). "Anodic electron transfer mechanisms in microbial fuel cells and their energy efficiency." Physical Chemistry Chemical Physics **9**(21): 2619-2629.

Shi, L., B. Chen, et al. (2006). "Isolation of a high-affinity functional protein complex between OmcA and MtrC: Two outer membrane decaheme *c*-type cytochromes of *Shewanella oneidensis* MR-1." Journal of Bacteriology **188**(13): 4705-4714.

Shi, L., S. Deng, et al. (2008). "Direct involvement of type II secretion system in extracellular translocation of *Shewanella oneidensis* outer membrane cytochromes MtrC and OmcA." Journal of Bacteriology **190**(15): 5512–5516.

Shi, L., K. M. Rosso, et al. (2012). "Molecular underpinnings of Fe(III) oxide reduction by *Shewanella oneidensis* MR-1." Frontiers in Microbiology **3**: 50.

Sun, W. L., J. L. Kong, et al. (1996). "Electrocatalytic activity of riboflavin chemically modified electrode toward dioxygen reduction." Analytical Letters **29**(14): 2425-2439.

Teal, T. K., D. P. Lies, et al. (2006). "Spatiometabolic stratification of *Shewanella oneidensis* biofilms." Applied and Environmental Microbiology **72**(11): 7324-7330.

Tender, L. M., S. A. Gray, et al. (2008). "The first demonstration of a microbial fuel cell as a viable power supply: Powering a meteorological buoy." Journal of Power Sources **179**(2): 571-575.

TerAvest, M. A. and L. T. Angenent (2012). "Engineering bacterial biocomputers using A top-down approach and dynamic genetic circuits." International Journal of Unconventional Computing **8**(5-6): 509-515.

TerAvest, M. A., Z. Li, et al. (2011). "Bacteria-based biocomputing with Cellular Computing Circuits to sense, decide, signal, and act." Energy & Environmental Science **4**(12): 4907-4916.

TerAvest, M. A., Z. Li, et al. (2012). Development of bacteria-based Cellular Computing Circuits for sensing and control in biological systems. Biomolecular information processing: from logic systems to smart sensors and actuators. E. Katz. Weinhem, Germany, Wiley-VCH**:** 265-277.

Thompson, D. K., A. S. Beliaev, et al. (2002). "Transcriptional and proteomic analysis of a ferric uptake regulator (Fur) mutant of *Shewanella oneidensis*: Possible involvement of Fur in energy metabolism, transcriptional regulation, and oxidative stress." Applied and Environmental Microbiology **68**(2): 881-892.

Thormann, K. M., R. M. Saville, et al. (2004). "Initial phases of biofilm formation in *Shewanella oneidensis* MR-1." Journal of Bacteriology **186**(23): 8096-8104.

Thormann, K. M., R. M. Saville, et al. (2005). "Induction of rapid detachment in *Shewanella oneidensis* MR-1 biofilms." Journal of Bacteriology **187**(3): 1014-1021.

Tibshirani, R., T. Hastie, et al. (2002). "Diagnosis of multiple cancer types by shrunken centroids of gene expression." Proceedings of the National Academy of Sciences **99**(10): 6567-6572.

Torres-Garcia, W., S. D. Brown, et al. (2011). "Integrative analysis of transcriptomic and proteomic data of *Shewanella oneidensis*: missing value imputation using temporal datasets." Molecular Biosystems **7**(4): 1093-1104.

Venkataraman, A., M. Rosenbaum, et al. (2010). "Quorum sensing regulates electric current generation of *Pseudomonas aeruginosa* PA14 in bioelectrochemical systems." Electrochemistry Communications **12**(3): 459-462.

Venkataraman, A., M. A. Rosenbaum, et al. (2011). "Metabolite-based mutualism between *Pseudomonas aeruginosa* PA14 and *Enterobacter aerogenes* enhances current generation in bioelectrochemical systems." Energy & Environmental Science **4**(11): 4550-4559.

von Canstein, H., J. Ogawa, et al. (2008). "Secretion of flavins by *Shewanella* species and their role in extracellular electron transfer." Applied and Environmental Microbiology **74**(3): 615-623.

Wilkinson, S. (2000). ""Gastrobots" - Benefits and challenges of microbial fuel cells in food powered robot applications." Autonomous Robots **9**(2): 99-111.

Xiong, Y., B. Chen, et al. (2011). "Targeted protein degradation of outer membrane decaheme cytochrome MtrC metal reductase in *Shewanella oneidensis* MR-1 measured using biarsenical probe CrAsH-EDT_2." Biochemistry **50**(45): 9738-9751.

Xu, S., H. Liu, et al. (2012). "Enhanced performance and mechanism study of microbial electrolysis cells using Fe nanoparticle-decorated anodes." Applied Microbiology and Biotechnology **93**(2): 871-880.

Yu, H., K. Nguyen, et al. (2007). "Positional artifacts in microarrays: experimental verification and construction of COP, an automated detection tool." Nucleic Acids Research **35**(2): e8.

APPENDIX

APPENDIX 1

SUPPLEMENTAL INFORMATION FOR: OXYGEN ALLOWS *SHEWANELLA ONEIDENSIS* MR-1 TO OVERCOME MEDIATOR WASHOUT IN A CONTINUOUSLY-FED BIOELECTROCHEMICAL SYSTEM

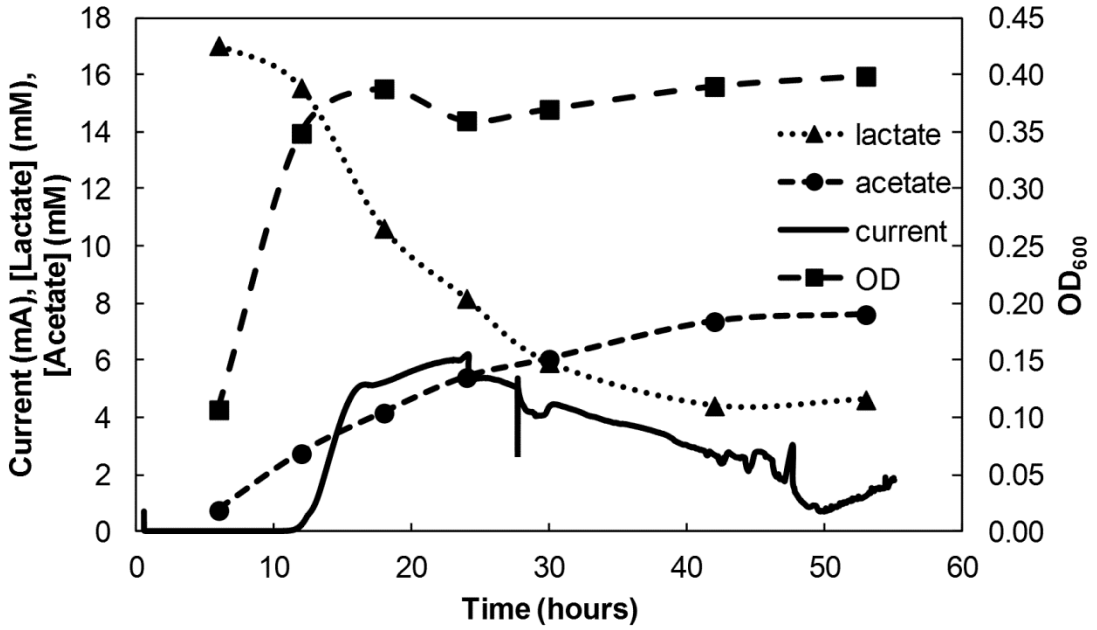

Figure A1.1. Current production, OD_{600}, lactate concentration, and acetate concentration for one experiment with WT *S. oneidensis* grown in a micro-aerobic, continuously-fed BES, for the first 60 h of operation.

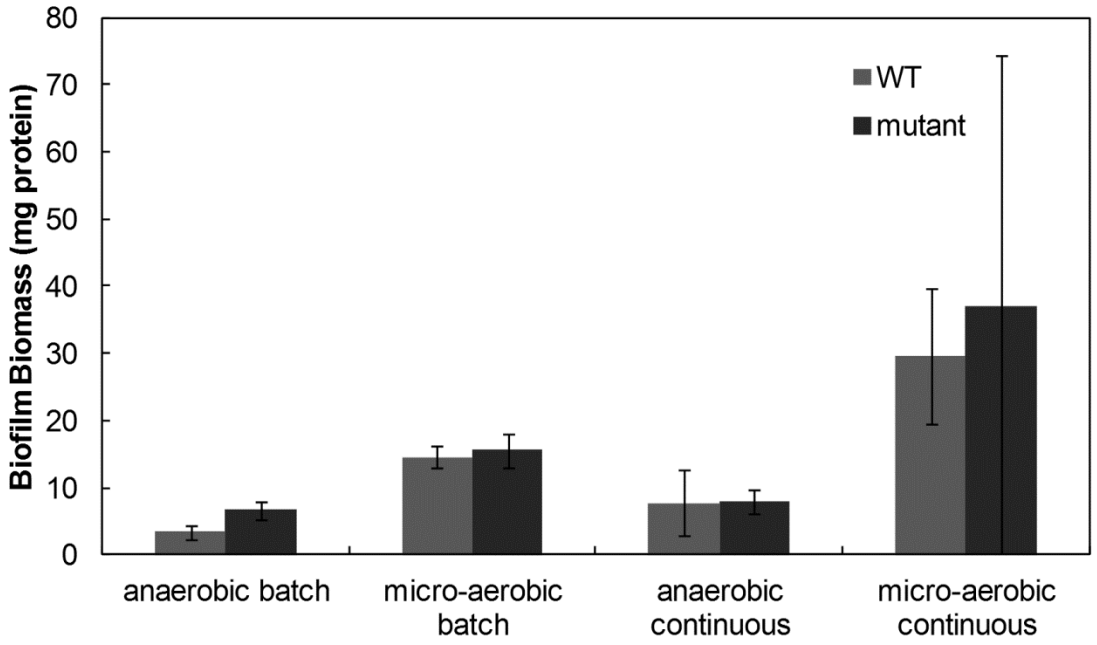

Figure A1.2. Bar chart of average biofilm biomass for each experimental condition (in mg of protein extracted from each electrode at the end of the experiment). Error bars represent standard deviation. The standard deviation was high for the mutant, micro-aerobic, continuous condition because one sample had a very high measurement for unknown reasons.

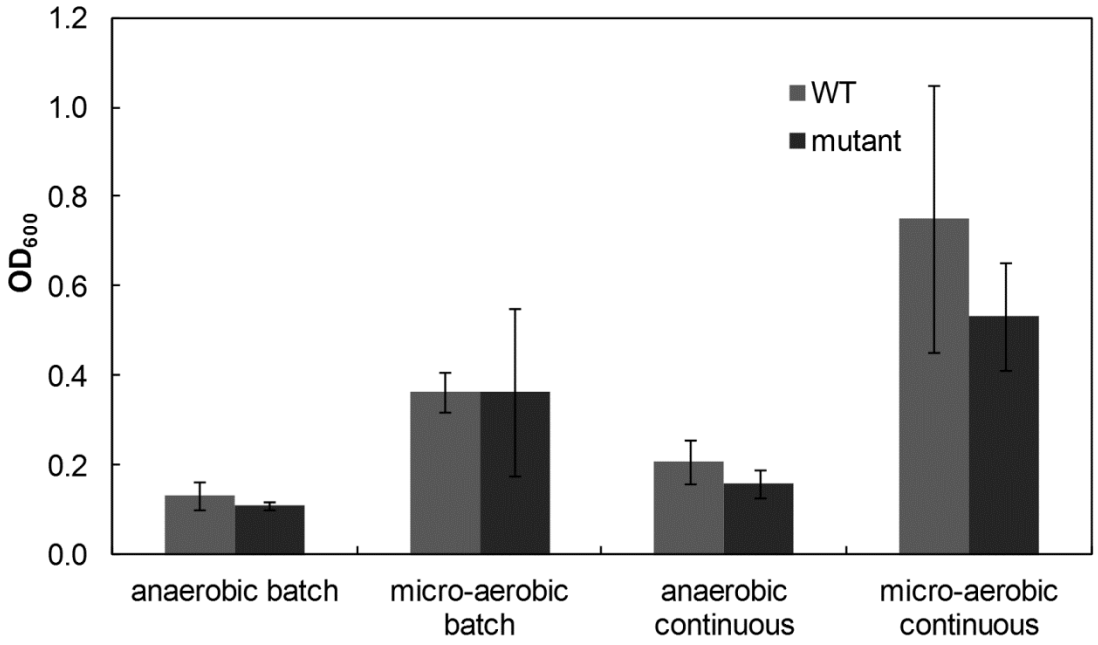

Figure A1.3. Bar chart of OD_{600} for each experimental condition (reported for day 1 for batch experiments and day 7 for continuous experiments). Error bars represent standard deviation.

APPENDIX 2

SUPPLEMENTAL INFORMATION FOR: OXIDIZING ELECTRODE POTENTIALS DECREASE CURRENT PRODUCTION AND COULOMBIC EFFICIENCY THROUGH CYTOCHROME *C* INACTIVATION IN *SHEWANELLA ONEIDENSIS* MR-1

SUPPLEMENTARY INFORMATION

Table A2.1. A list of primers used for qRT-PCR.

locus	forward primer	reverse primer	length (bp)
SO_0220	5'- CCA CGT CCA AAC ACT CAG AA -3'	5'- ATT GAA CGC GCA GTA CCT TC -3'	137
SO_1126	5'- GCA ATG CAA CGT CTG AAA GA -3'	5'- TTG CAT CGG CAG TGA TGT AT -3'	100
SO_1770	5'- AGA AAG CTT AAG CGC ACT CG -3'	5'- CCA TAG ATT GCA CCG TTC CT -3'	125
SO_1779	5'- TCA CGA TTT GCG ATT TGG TA -3'	5'- TCA ACG TTC GCT TGA AAC TG -3'	177
SO_1794	5'- CCT AAT TCG CGC GTT ATG AT -3'	5'- TAC TTC GAG GGG TTG TCC AG -3'	147

APPENDIX 3

SUPPLEMENTAL INFORMATION FOR: META-ANALYSIS OF TRANSCRIPTOMIC DATA REVEALS THE ANAEROBIC ELECTRON TRANSPORT CHAIN OF *SHEWANELLA ONEIDENSIS* MR-1

Table A3.1. A mapping file containing relevant information about *S. oneidensis* growth conditions for each transcriptome sample included in meta-analysis.

GSM number	GEO series	GEO platform	medium	substrate	T °C	mutation	electron acceptor	time
GSM100358cy3	GSE4489	GPL3253	LB	LB	30	none	oxygen	log phase
GSM100358cy5	GSE4489	GPL3253	LB	LB	8	none	oxygen	log phase
GSM100396cy3	GSE4489	GPL3253	LB	LB	30	none	oxygen	log phase
GSM100396cy5	GSE4489	GPL3253	LB	LB	8	none	oxygen	log phase
GSM100397cy3	GSE4489	GPL3253	LB	LB	30	none	oxygen	log phase
GSM100397cy5	GSE4489	GPL3253	LB	LB	8	none	oxygen	log phase
GSM100398cy3	GSE4489	GPL3253	LB	LB	30	none	oxygen	log phase
GSM100398cy5	GSE4489	GPL3253	LB	LB	8	none	oxygen	log phase
GSM100399cy3	GSE4489	GPL3253	LB	LB	30	none	oxygen	log phase
GSM100399cy5	GSE4489	GPL3253	LB	LB	8	none	oxygen	log phase
GSM100400cy3	GSE4489	GPL3253	LB	LB	30	none	oxygen	log phase
GSM100400cy5	GSE4489	GPL3253	LB	LB	8	none	oxygen	log phase
GSM100401cy3	GSE4489	GPL3253	LB	LB	30	none	oxygen	log phase
GSM100401cy5	GSE4489	GPL3253	LB	LB	8	none	oxygen	log phase
GSM100403cy3	GSE4489	GPL3253	LB	LB	30	none	oxygen	log phase
GSM100403cy5	GSE4489	GPL3253	LB	LB	8	none	oxygen	log phase
GSM100405cy3	GSE4489	GPL3253	LB	LB	30	none	oxygen	log phase
GSM100405cy5	GSE4489	GPL3253	LB	LB	8	none	oxygen	log phase
GSM100407cy3	GSE4489	GPL3253	LB	LB	30	none	oxygen	log phase
GSM100407cy5	GSE4489	GPL3253	LB	LB	8	none	oxygen	log phase
GSM100409cy3	GSE4489	GPL3253	LB	LB	30	none	oxygen	log phase
GSM100409cy5	GSE4489	GPL3253	LB	LB	8	none	oxygen	log phase
GSM100411cy3	GSE4489	GPL3253	LB	LB	30	none	oxygen	log phase
GSM100411cy5	GSE4489	GPL3253	LB	LB	8	none	oxygen	log phase
GSM100415cy3	GSE4489	GPL3253	LB	LB	30	none	oxygen	log phase
GSM100415cy5	GSE4489	GPL3253	LB	LB	8	none	oxygen	log phase
GSM100417cy3	GSE4489	GPL3253	LB	LB	30	none	oxygen	log phase
GSM100417cy5	GSE4489	GPL3253	LB	LB	8	none	oxygen	log phase
GSM100421cy3	GSE4489	GPL3253	LB	LB	30	none	oxygen	log phase
GSM100421cy5	GSE4489	GPL3253	LB	LB	8	none	oxygen	log phase
GSM100858cy3	GSE4489	GPL3253	LB	LB	30	none	oxygen	log phase

GSM100858cy5	GSE4489	GPL3253	LB	LB	8	none	oxygen	log phase
GSM100859cy3	GSE4489	GPL3253	LB	LB	30	none	oxygen	log phase
GSM100859cy5	GSE4489	GPL3253	LB	LB	8	none	oxygen	log phase
GSM100860cy3	GSE4489	GPL3253	LB	LB	30	none	oxygen	log phase
GSM100860cy5	GSE4489	GPL3253	LB	LB	8	none	oxygen	log phase
GSM100861cy3	GSE4489	GPL3253	LB	LB	30	none	oxygen	log phase
GSM100861cy5	GSE4489	GPL3253	LB	LB	8	none	oxygen	log phase
GSM100862cy3	GSE4489	GPL3253	LB	LB	30	none	oxygen	log phase
GSM100862cy5	GSE4489	GPL3253	LB	LB	8	none	oxygen	log phase
GSM100863cy3	GSE4489	GPL3253	LB	LB	30	none	oxygen	log phase
GSM100863cy5	GSE4489	GPL3253	LB	LB	8	none	oxygen	log phase
GSM100864cy3	GSE4489	GPL3253	LB	LB	30	none	oxygen	log phase
GSM100864cy5	GSE4489	GPL3253	LB	LB	8	none	oxygen	log phase
GSM100865cy3	GSE4489	GPL3253	LB	LB	30	none	oxygen	log phase
GSM100865cy5	GSE4489	GPL3253	LB	LB	8	none	oxygen	log phase
GSM100866cy3	GSE4489	GPL3253	LB	LB	30	none	oxygen	log phase
GSM100866cy5	GSE4489	GPL3253	LB	LB	8	none	oxygen	log phase
GSM100867cy3	GSE4489	GPL3253	LB	LB	30	none	oxygen	log phase
GSM100867cy5	GSE4489	GPL3253	LB	LB	8	none	oxygen	log phase
GSM100868cy3	GSE4489	GPL3253	LB	LB	30	none	oxygen	log phase
GSM100868cy5	GSE4489	GPL3253	LB	LB	8	none	oxygen	log phase
GSM100869cy3	GSE4489	GPL3253	LB	LB	30	none	oxygen	log phase
GSM100869cy5	GSE4489	GPL3253	LB	LB	8	none	oxygen	log phase
GSM100870cy3	GSE4489	GPL3253	LB	LB	30	none	oxygen	log phase
GSM100870cy5	GSE4489	GPL3253	LB	LB	8	none	oxygen	log phase
GSM100871cy3	GSE4489	GPL3253	LB	LB	30	none	oxygen	log phase
GSM100871cy5	GSE4489	GPL3253	LB	LB	8	none	oxygen	log phase
GSM100872cy3	GSE4489	GPL3253	LB	LB	30	none	oxygen	log phase
GSM100872cy5	GSE4489	GPL3253	LB	LB	15	none	oxygen	log phase
GSM100873cy3	GSE4489	GPL3253	LB	LB	30	none	oxygen	log phase
GSM100873cy5	GSE4489	GPL3253	LB	LB	15	none	oxygen	log phase
GSM100874cy3	GSE4489	GPL3253	LB	LB	30	none	oxygen	log phase
GSM100874cy5	GSE4489	GPL3253	LB	LB	15	none	oxygen	log phase
GSM100875cy3	GSE4489	GPL3253	LB	LB	30	none	oxygen	log phase
GSM100875cy5	GSE4489	GPL3253	LB	LB	15	none	oxygen	log phase
GSM100876cy3	GSE4489	GPL3253	LB	LB	30	none	oxygen	log phase
GSM100876cy5	GSE4489	GPL3253	LB	LB	15	none	oxygen	log phase
GSM100877cy3	GSE4489	GPL3253	LB	LB	30	none	oxygen	log phase
GSM100877cy5	GSE4489	GPL3253	LB	LB	15	none	oxygen	log phase
GSM100878cy3	GSE4489	GPL3253	LB	LB	30	none	oxygen	log phase
GSM100878cy5	GSE4489	GPL3253	LB	LB	15	none	oxygen	log phase

GSM100879cy3	GSE4489	GPL3253	LB	LB	30	none	oxygen	log phase
GSM100879cy5	GSE4489	GPL3253	LB	LB	15	none	oxygen	log phase
GSM100881cy3	GSE4489	GPL3253	LB	LB	30	none	oxygen	log phase
GSM100881cy5	GSE4489	GPL3253	LB	LB	15	none	oxygen	log phase
GSM100882cy3	GSE4489	GPL3253	LB	LB	30	none	oxygen	log phase
GSM100882cy5	GSE4489	GPL3253	LB	LB	15	none	oxygen	log phase
GSM100883cy3	GSE4489	GPL3253	LB	LB	30	none	oxygen	log phase
GSM100883cy5	GSE4489	GPL3253	LB	LB	15	none	oxygen	log phase
GSM100884cy3	GSE4489	GPL3253	LB	LB	30	none	oxygen	log phase
GSM100884cy5	GSE4489	GPL3253	LB	LB	15	none	oxygen	log phase
GSM100885cy3	GSE4489	GPL3253	LB	LB	30	none	oxygen	log phase
GSM100885cy5	GSE4489	GPL3253	LB	LB	15	none	oxygen	log phase
GSM100886cy3	GSE4489	GPL3253	LB	LB	30	none	oxygen	log phase
GSM100886cy5	GSE4489	GPL3253	LB	LB	15	none	oxygen	log phase
GSM100887cy3	GSE4489	GPL3253	LB	LB	30	none	oxygen	log phase
GSM100887cy5	GSE4489	GPL3253	LB	LB	15	none	oxygen	log phase
GSM100904cy3	GSE4489	GPL3253	LB	LB	30	none	oxygen	log phase
GSM100904cy5	GSE4489	GPL3253	LB	LB	15	none	oxygen	log phase
GSM100905cy3	GSE4489	GPL3253	LB	LB	30	none	oxygen	log phase
GSM100905cy5	GSE4489	GPL3253	LB	LB	15	none	oxygen	log phase
GSM100906cy3	GSE4489	GPL3253	LB	LB	30	none	oxygen	log phase
GSM100906cy5	GSE4489	GPL3253	LB	LB	15	none	oxygen	log phase
GSM100907cy3	GSE4489	GPL3253	LB	LB	30	none	oxygen	log phase
GSM100907cy5	GSE4489	GPL3253	LB	LB	15	none	oxygen	log phase
GSM100908cy3	GSE4489	GPL3253	LB	LB	30	none	oxygen	log phase
GSM100908cy5	GSE4489	GPL3253	LB	LB	15	none	oxygen	log phase
GSM100909cy3	GSE4489	GPL3253	LB	LB	30	none	oxygen	log phase
GSM100909cy5	GSE4489	GPL3253	LB	LB	15	none	oxygen	log phase
GSM100910cy3	GSE4489	GPL3253	LB	LB	30	none	oxygen	log phase
GSM100910cy5	GSE4489	GPL3253	LB	LB	15	none	oxygen	log phase
GSM100911cy3	GSE4489	GPL3253	LB	LB	30	none	oxygen	log phase
GSM100911cy5	GSE4489	GPL3253	LB	LB	15	none	oxygen	log phase
GSM100912cy3	GSE4489	GPL3253	LB	LB	30	none	oxygen	log phase
GSM100912cy5	GSE4489	GPL3253	LB	LB	15	none	oxygen	log phase
GSM100913cy3	GSE4489	GPL3253	LB	LB	30	none	oxygen	log phase
GSM100913cy5	GSE4489	GPL3253	LB	LB	15	none	oxygen	log phase
GSM100915cy3	GSE4489	GPL3253	LB	LB	30	none	oxygen	log phase
GSM100915cy5	GSE4489	GPL3253	LB	LB	15	none	oxygen	log phase
GSM100916cy3	GSE4489	GPL3253	LB	LB	30	none	oxygen	log phase
GSM100916cy5	GSE4489	GPL3253	LB	LB	15	none	oxygen	log phase
GSM100917cy3	GSE4489	GPL3253	LB	LB	30	none	oxygen	log phase

GSM100917cy5	GSE4489	GPL3253	LB	LB	15	none	oxygen	log phase
GSM100918cy3	GSE4489	GPL3253	LB	LB	30	none	oxygen	log phase
GSM100918cy5	GSE4489	GPL3253	LB	LB	15	none	oxygen	log phase
GSM100919cy3	GSE4489	GPL3253	LB	LB	30	none	oxygen	log phase
GSM100919cy5	GSE4489	GPL3253	LB	LB	15	none	oxygen	log phase
GSM100921cy3	GSE4489	GPL3253	LB	LB	30	none	oxygen	log phase
GSM100921cy5	GSE4489	GPL3253	LB	LB	8	none	oxygen	log phase
GSM197317cy3	GSE7973	GPL3253	M1	lactate	30	none	oxygen	log phase
GSM197317cy5	GSE7973	GPL3253	M1	lactate	30	arcA	oxygen	log phase
GSM197321cy3	GSE7973	GPL3253	M1	lactate	30	none	oxygen	log phase
GSM197321cy5	GSE7973	GPL3253	M1	lactate	30	arcA	oxygen	log phase
GSM197323cy3	GSE7973	GPL3253	M1	lactate	30	none	oxygen	log phase
GSM197323cy5	GSE7973	GPL3253	M1	lactate	30	arcA	oxygen	log phase
GSM197324cy3	GSE7973	GPL3253	M1	lactate	30	none	oxygen	log phase
GSM197324cy5	GSE7973	GPL3253	M1	lactate	30	arcA	oxygen	log phase
GSM197325cy3	GSE7973	GPL3253	M1	lactate	30	none	fumarate	log phase
GSM197325cy5	GSE7973	GPL3253	M1	lactate	30	arcA	fumarate	log phase
GSM197327cy3	GSE7973	GPL3253	M1	lactate	30	none	fumarate	log phase
GSM197327cy5	GSE7973	GPL3253	M1	lactate	30	arcA	fumarate	log phase
GSM197328cy3	GSE7973	GPL3253	M1	lactate	30	none	fumarate	log phase
GSM197328cy5	GSE7973	GPL3253	M1	lactate	30	arcA	fumarate	log phase
GSM197329cy3	GSE7973	GPL3253	M1	lactate	30	none	fumarate	log phase
GSM197329cy5	GSE7973	GPL3253	M1	lactate	30	arcA	fumarate	log phase
GSM358310cy3	GSE14331	GPL3253	LB	LB	25	none	oxygen	30h
GSM358310cy5	GSE14331	GPL3253	LB	LB	25	none	oxygen	30h
GSM358311cy3	GSE14331	GPL3253	LB	LB	25	none	oxygen	30h
GSM358311cy5	GSE14331	GPL3253	LB	LB	25	none	oxygen	30h
GSM358312cy3	GSE14331	GPL3253	LB	LB	25	none	oxygen	30h
GSM358312cy5	GSE14331	GPL3253	LB	LB	25	none	oxygen	30h
GSM392057	GSE15657	GPL8434	MM	lactate	30	none	oxygen	steady state
GSM392058	GSE15657	GPL8434	MM	lactate	30	none	oxygen	steady state
GSM392059	GSE15657	GPL8434	MM	lactate	30	crp	oxygen	steady state
GSM392060	GSE15657	GPL8434	MM	lactate	30	crp	oxygen	steady state
GSM392061	GSE15657	GPL8434	MM	lactate	30	cyaC	oxygen	steady state
GSM392062	GSE15657	GPL8434	MM	lactate	30	cyaC	oxygen	steady state
GSM509290	GSE20343	GPL8434	M4	lactate	30	none	carbon anode	steady state
GSM509291	GSE20343	GPL8434	M4	lactate	30	none	carbon anode	steady state
GSM509291	GSE20379	GPL8434	M4	lactate	30	none	carbon anode	steady state
GSM509292	GSE20343	GPL8434	M4	lactate	30	none	carbon anode	steady state

GSM509293	GSE20343	GPL8434	M4	lactate	30	none	carbon anode	steady state
GSM509293	GSE20379	GPL8434	M4	lactate	30	none	carbon anode	steady state
GSM509649	GSE20379	GPL8434	M4	lactate	30	none	Fe-citrate	20h
GSM509650	GSE20379	GPL8434	M4	lactate	30	none	Fe-citrate	20h
GSM509651	GSE20379	GPL8434	M4	lactate	30	none	Fe-citrate	20h
GSM509652	GSE20379	GPL8434	M4	lactate	30	none	Fe-citrate	20h
GSM509685	GSE20379	GPL8434	M4	lactate	30	none	oxygen	20h
GSM509686	GSE20379	GPL8434	M4	lactate	30	none	oxygen	20h
GSM509687	GSE20379	GPL8434	M4	lactate	30	none	oxygen	20h
GSM525509	GSE21044	GPL10101	LB	LB	30	none	oxygen	log phase
GSM525510	GSE21044	GPL10101	LB	LB	30	none	oxygen	log phase
GSM525511	GSE21044	GPL10101	LB	LB	30	none	oxygen	log phase
GSM525512	GSE21044	GPL10101	LB	LB	30	arcS	oxygen	log phase
GSM525513	GSE21044	GPL10101	LB	LB	30	arcS	oxygen	log phase
GSM525514	GSE21044	GPL10101	LB	LB	30	arcS	oxygen	log phase
GSM613947	GSE24994	GPL10101	LB	LB	30	none	oxygen	stationary
GSM613948	GSE24994	GPL10101	LB	LB	30	none	oxygen	stationary
GSM613949	GSE24994	GPL10101	LB	LB	30	none	oxygen	stationary
GSM613950	GSE24994	GPL10101	LB	LB	30	uvrY	oxygen	stationary
GSM613951	GSE24994	GPL10101	LB	LB	30	uvrY	oxygen	stationary
GSM613952	GSE24994	GPL10101	LB	LB	30	uvrY	oxygen	stationary
GSM634360	GSE25821	GPL8434	MM	lactate	30	none	oxygen	15h
GSM634361	GSE25821	GPL8434	MM	lactate	30	none	oxygen	15h
GSM634362	GSE25821	GPL8434	MM	lactate	30	none	oxygen	16h
GSM634363	GSE25821	GPL8434	MM	lactate	30	none	oxygen	16h
GSM634364	GSE25821	GPL8434	MM	lactate	30	none	oxygen	18h
GSM634365	GSE25821	GPL8434	MM	lactate	30	none	oxygen	18h
GSM634366	GSE25821	GPL8434	MM	lactate	30	none	oxygen	20h
GSM634367	GSE25821	GPL8434	MM	lactate	30	none	oxygen	20h
GSM634368	GSE25821	GPL8434	MM	lactate	30	none	oxygen	22h
GSM634369	GSE25821	GPL8434	MM	lactate	30	none	oxygen	22h
GSM634370	GSE25821	GPL8434	MM	lactate	30	none	oxygen	24h
GSM634371	GSE25821	GPL8434	MM	lactate	30	none	oxygen	24h
GSM634372	GSE25821	GPL8434	MM	lactate	30	none	oxygen	26h
GSM634373	GSE25821	GPL8434	MM	lactate	30	none	oxygen	26h
GSM634374	GSE25821	GPL8434	MM	lactate	30	none	oxygen	27h
GSM634375	GSE25821	GPL8434	MM	lactate	30	none	oxygen	27h
GSM634376	GSE25821	GPL8434	MM	lactate	30	none	oxygen	28h
GSM634377	GSE25821	GPL8434	MM	lactate	30	none	oxygen	28h
GSM634378	GSE25821	GPL8434	MM	lactate	30	none	oxygen	29h

GSM634379	GSE25821	GPL8434	MM	lactate	30	none	oxygen	29h
GSM634380	GSE25821	GPL8434	MM	lactate	30	none	oxygen	30h
GSM634381	GSE25821	GPL8434	MM	lactate	30	none	oxygen	30h
GSM634382	GSE25821	GPL8434	MM	lactate	30	none	oxygen	31h
GSM634383	GSE25821	GPL8434	MM	lactate	30	none	oxygen	31h
GSM634384	GSE25821	GPL8434	MM	lactate	30	none	oxygen	32h
GSM634385	GSE25821	GPL8434	MM	lactate	30	none	oxygen	32h
GSM634386	GSE25821	GPL8434	MM	lactate	30	none	oxygen	33h
GSM634387	GSE25821	GPL8434	MM	lactate	30	none	oxygen	33h
GSM634388	GSE25821	GPL8434	MM	lactate	30	none	oxygen	34h
GSM634389	GSE25821	GPL8434	MM	lactate	30	none	oxygen	34h
GSM634390	GSE25821	GPL8434	MM	lactate	30	none	oxygen	35h
GSM634391	GSE25821	GPL8434	MM	lactate	30	none	oxygen	35h
GSM634392	GSE25821	GPL8434	MM	lactate	30	none	oxygen	36h
GSM634393	GSE25821	GPL8434	MM	lactate	30	none	oxygen	36h
GSM634394	GSE25821	GPL8434	MM	lactate	30	none	oxygen	48h
GSM634395	GSE25821	GPL8434	MM	lactate	30	none	oxygen	48h
GSM634396	GSE25821	GPL8434	MM	lactate	30	none	oxygen	50h
GSM634397	GSE25821	GPL8434	MM	lactate	30	none	oxygen	50h
GSM634398	GSE25821	GPL8434	LB	LB	30	none	oxygen	1.5h
GSM634399	GSE25821	GPL8434	LB	LB	30	none	oxygen	1.5h
GSM634400	GSE25821	GPL8434	LB	LB	30	none	oxygen	2h
GSM634401	GSE25821	GPL8434	LB	LB	30	none	oxygen	2h
GSM634402	GSE25821	GPL8434	LB	LB	30	none	oxygen	2.5h
GSM634403	GSE25821	GPL8434	LB	LB	30	none	oxygen	2.5h
GSM634404	GSE25821	GPL8434	LB	LB	30	none	oxygen	3h
GSM634405	GSE25821	GPL8434	LB	LB	30	none	oxygen	3h
GSM634406	GSE25821	GPL8434	LB	LB	30	none	oxygen	3.5h
GSM634407	GSE25821	GPL8434	LB	LB	30	none	oxygen	3.5h
GSM634408	GSE25821	GPL8434	LB	LB	30	none	oxygen	4h
GSM634409	GSE25821	GPL8434	LB	LB	30	none	oxygen	4h
GSM634410	GSE25821	GPL8434	LB	LB	30	none	oxygen	4.5h
GSM634411	GSE25821	GPL8434	LB	LB	30	none	oxygen	4.5h
GSM634412	GSE25821	GPL8434	LB	LB	30	none	oxygen	5h
GSM634413	GSE25821	GPL8434	LB	LB	30	none	oxygen	5h
GSM634414	GSE25821	GPL8434	LB	LB	30	none	oxygen	5.5h
GSM634415	GSE25821	GPL8434	LB	LB	30	none	oxygen	5.5h
GSM634416	GSE25821	GPL8434	LB	LB	30	none	oxygen	6h
GSM634417	GSE25821	GPL8434	LB	LB	30	none	oxygen	6h
GSM634418	GSE25821	GPL8434	LB	LB	30	none	oxygen	7h
GSM634419	GSE25821	GPL8434	LB	LB	30	none	oxygen	7h

GSM634420	GSE25821	GPL8434	LB	LB	30	none	oxygen	9h
GSM634421	GSE25821	GPL8434	LB	LB	30	none	oxygen	9h
GSM634422	GSE25821	GPL8434	LB	LB	30	none	oxygen	12h
GSM634423	GSE25821	GPL8434	LB	LB	30	none	oxygen	12h
GSM634424	GSE25821	GPL8434	LB	LB	30	none	oxygen	15h
GSM634425	GSE25821	GPL8434	LB	LB	30	none	oxygen	15h
GSM634426	GSE25821	GPL8434	LB	LB	30	none	oxygen	18h
GSM634427	GSE25821	GPL8434	LB	LB	30	none	oxygen	18h
GSM634428	GSE25821	GPL8434	LB	LB	30	none	oxygen	21h
GSM634429	GSE25821	GPL8434	LB	LB	30	none	oxygen	21h
GSM634430	GSE25821	GPL8434	LB	LB	30	none	oxygen	24h
GSM634431	GSE25821	GPL8434	LB	LB	30	none	oxygen	24h
GSM634432	GSE25821	GPL8434	LB	LB	30	none	oxygen	28h
GSM634433	GSE25821	GPL8434	LB	LB	30	none	oxygen	28h
GSM634434	GSE25821	GPL8434	LB	LB	30	none	oxygen	30h
GSM634435	GSE25821	GPL8434	LB	LB	30	none	oxygen	30h
GSM634436	GSE25821	GPL8434	LB	LB	30	none	oxygen	32h
GSM634437	GSE25821	GPL8434	LB	LB	30	none	oxygen	32h
GSM634438	GSE25821	GPL8434	LB	LB	30	none	oxygen	47h
GSM634439	GSE25821	GPL8434	LB	LB	30	none	oxygen	47h
GSM634440	GSE25821	GPL8434	LB	LB	30	none	oxygen	50h
GSM634441	GSE25821	GPL8434	LB	LB	30	none	oxygen	50h
GSM634442	GSE25821	GPL8434	LB	LB	30	none	oxygen	55h
GSM634443	GSE25821	GPL8434	LB	LB	30	none	oxygen	55h
GSM635111	GSE25865	GPL10101	LM			none	oxygen	
GSM635112	GSE25865	GPL10101	LM			none	oxygen	
GSM635113	GSE25865	GPL10101	LM			none	oxygen	0.25h
GSM635114	GSE25865	GPL10101	LM			none	oxygen	0.25h
GSM635115	GSE25865	GPL10101	LM			none	oxygen	1h
GSM635116	GSE25865	GPL10101	LM			none	oxygen	1h
GSM769226cy3	GSE31053	GPL3253	LB	LB	30	none	oxygen	log phase
GSM769226cy5	GSE31053	GPL3253	LB	LB	30	none	oxygen	log phase
GSM769227cy3	GSE31053	GPL3253	LB	LB	30	none	oxygen	log phase
GSM769227cy5	GSE31053	GPL3253	LB	LB	30	none	oxygen	log phase
GSM769228cy3	GSE31053	GPL3253	LB	LB	30	none	oxygen	log phase
GSM769228cy5	GSE31053	GPL3253	LB	LB	30	none	oxygen	log phase
GSM769229cy3	GSE31053	GPL3253	LB	LB	30	none	oxygen	log phase
GSM769229cy5	GSE31053	GPL3253	LB	LB	30	none	oxygen	log phase
GSM769230cy3	GSE31053	GPL3253	LB	LB	30	arcA	oxygen	log phase
GSM769230cy5	GSE31053	GPL3253	LB	LB	30	arcA	oxygen	log phase
GSM769231cy3	GSE31053	GPL3253	LB	LB	30	arcA	oxygen	log phase

GSM769231cy5	GSE31053	GPL3253	LB	LB	30	arcA	oxygen	log phase
GSM769232cy3	GSE31053	GPL3253	LB	LB	30	arcA	oxygen	log phase
GSM769232cy5	GSE31053	GPL3253	LB	LB	30	arcA	oxygen	log phase
GSM769233cy3	GSE31053	GPL3253	LB	LB	30	arcA	oxygen	log phase
GSM769233cy5	GSE31053	GPL3253	LB	LB	30	arcA	oxygen	log phase
GSM782755	GSE31535	GPL14177	TSB	lactate	30	none	Fe-nano anode	110h
GSM782756	GSE31535	GPL14177	TSB	lactate	30	none	Fe-nano anode	110h
GSM782757	GSE31535	GPL14177	TSB	lactate	30	none	Fe-nano anode	110h
GSM782758	GSE31535	GPL14177	TSB	lactate	30	none	carbon anode	110h
GSM782759	GSE31535	GPL14177	TSB	lactate	30	none	carbon anode	110h
GSM782760	GSE31535	GPL14177	TSB	lactate	30	none	carbon anode	110h
GSM87832cy3	GSE3876	GPL3253	Davis	lactate	30	none	oxygen	log phase
GSM87832cy5	GSE3876	GPL3253	Davis	lactate	30	none	oxygen	log phase
GSM88468cy3	GSE3876	GPL3253	Davis	lactate	30	none	oxygen	log phase
GSM88468cy5	GSE3876	GPL3253	Davis	lactate	30	none	oxygen	log phase
GSM88469cy3	GSE3876	GPL3253	Davis	lactate	30	none	oxygen	log phase
GSM88469cy5	GSE3876	GPL3253	Davis	lactate	30	none	oxygen	log phase
GSM88470cy3	GSE3876	GPL3253	Davis	lactate	30	none	oxygen	log phase
GSM88470cy5	GSE3876	GPL3253	Davis	lactate	30	none	oxygen	log phase
GSM88471cy3	GSE3876	GPL3253	Davis	lactate	30	none	oxygen	log phase
GSM88471cy5	GSE3876	GPL3253	Davis	lactate	30	none	oxygen	log phase
GSM88472cy3	GSE3876	GPL3253	Davis	lactate	30	none	oxygen	log phase
GSM88472cy5	GSE3876	GPL3253	Davis	lactate	30	none	oxygen	log phase
GSM88473cy3	GSE3876	GPL3253	Davis	lactate	30	none	oxygen	log phase
GSM88473cy5	GSE3876	GPL3253	Davis	lactate	30	none	oxygen	log phase
GSM88474cy3	GSE3876	GPL3253	Davis	lactate	30	none	oxygen	log phase
GSM88474cy5	GSE3876	GPL3253	Davis	lactate	30	none	oxygen	log phase
GSM88475cy3	GSE3876	GPL3253	Davis	lactate	30	none	oxygen	log phase
GSM88475cy5	GSE3876	GPL3253	Davis	lactate	30	none	oxygen	log phase
GSM88476cy3	GSE3876	GPL3253	Davis	lactate	30	none	oxygen	log phase
GSM88476cy5	GSE3876	GPL3253	Davis	lactate	30	none	oxygen	log phase
GSM88477cy3	GSE3876	GPL3253	Davis	lactate	30	none	oxygen	log phase
GSM88477cy5	GSE3876	GPL3253	Davis	lactate	30	none	oxygen	log phase
GSM88478cy3	GSE3876	GPL3253	Davis	lactate	30	none	oxygen	log phase
GSM88478cy5	GSE3876	GPL3253	Davis	lactate	30	none	oxygen	log phase
GSM88479cy3	GSE3876	GPL3253	Davis	lactate	30	none	oxygen	log phase
GSM88479cy5	GSE3876	GPL3253	Davis	lactate	30	none	oxygen	log phase
GSM88482cy3	GSE3876	GPL3253	Davis	lactate	30	none	oxygen	log phase

GSM88482cy5	GSE3876	GPL3253	Davis	lactate	30	none	oxygen	log phase
GSM88537cy3	GSE3876	GPL3253	Davis	lactate	30	none	oxygen	log phase
GSM88537cy5	GSE3876	GPL3253	Davis	lactate	30	none	oxygen	log phase
GSM88538cy3	GSE3876	GPL3253	Davis	lactate	30	none	oxygen	log phase
GSM88538cy5	GSE3876	GPL3253	Davis	lactate	30	none	oxygen	log phase
GSM88539cy3	GSE3876	GPL3253	Davis	lactate	30	none	oxygen	log phase
GSM88539cy5	GSE3876	GPL3253	Davis	lactate	30	none	oxygen	log phase
GSM88540cy3	GSE3876	GPL3253	Davis	lactate	30	none	oxygen	log phase
GSM88540cy5	GSE3876	GPL3253	Davis	lactate	30	none	oxygen	log phase
GSM88541cy3	GSE3876	GPL3253	Davis	lactate	30	none	oxygen	log phase
GSM88541cy5	GSE3876	GPL3253	Davis	lactate	30	none	oxygen	log phase
GSM88542cy3	GSE3876	GPL3253	Davis	lactate	30	none	oxygen	log phase
GSM88542cy5	GSE3876	GPL3253	Davis	lactate	30	none	oxygen	log phase
GSM969603	GSE39462	GPL15821	MM	NAG	30	none	oxygen	log phase
GSM969604	GSE39462	GPL15821	MM	Tween-20	30	none	oxygen	log phase
GSM969605	GSE39462	GPL15821	MM	pyruvate	30	none	oxygen	log phase
GSM969606	GSE39462	GPL15821	MM	inosine	31	none	oxygen	log phase
GSM969607	GSE39462	GPL15821	LB	LB	30	none	oxygen	log phase
GSM969608	GSE39462	GPL15821	MM	CAS	30	none	oxygen	log phase
GSM969609	GSE39462	GPL15821	MM	gelatin	30	none	oxygen	log phase
GSM969610	GSE39462	GPL15821	MM	lactate	30	none	oxygen	log phase
GSM969611	GSE39462	GPL15821	MM	acetate	30	none	oxygen	log phase
GSM969612	GSE39462	GPL15821	MM	lactate	30	none	oxygen	log phase
GSM969613	GSE39462	GPL15821	MM	lactate	30	none	fumarate	log phase
GSM969614	GSE39462	GPL15821	MM	NAG	30	none	fumarate	log phase
GSM969615	GSE39462	GPL15821	MM	lactate	30	none	oxygen	log phase
GSM969616	GSE39462	GPL15821	MM	lactate	30	none	oxygen	log phase
GSM969617	GSE39462	GPL15821	MM	lactate	30	none	oxygen	log phase
GSM969618	GSE39462	GPL15821	MM	lactate	30	none	oxygen	20m
GSM969619	GSE39462	GPL15821	MM	lactate	30	none	oxygen	60m
GSM969620	GSE39462	GPL15821	MM	lactate	30	none	oxygen	16h
GSM969621	GSE39462	GPL15821	MM	lactate	30	none	oxygen	17h
GSM969622	GSE39462	GPL15821	MM	lactate	30	none	oxygen	20h
GSM969623	GSE39462	GPL15821	MM	lactate	30	none	oxygen	25h
GSM969624	GSE39462	GPL15821	MM	lactate	30	none	oxygen	27h
GSM969625	GSE39462	GPL15821	MM	NAG	30	none	oxygen	lag
GSM969626	GSE39462	GPL15821	MM	NAG	30	none	oxygen	OD_{600}=0.22
GSM969627	GSE39462	GPL15821	MM	NAG	30	none	oxygen	OD_{600}=0.413
GSM969628	GSE39462	GPL15821	MM	NAG	30	none	oxygen	OD_{600}=0.76
GSM969629	GSE39462	GPL15821	MM	NAG	30	none	oxygen	OD_{600}=1.168

GSM969630	GSE39462	GPL15821	MM	NAG	30	none	oxygen	OD_{600}=1.62
GSM969631	GSE39462	GPL15821	LB	LB	30	none	oxygen	OD_{600}=2.0
GSM969632	GSE39462	GPL15821	LB	LB	30	none	oxygen	20m
GSM969633	GSE39462	GPL15821	LB	LB	30	none	oxygen	60m
GSM969634	GSE39462	GPL15821	LB	LB	30	none	oxygen	120m
GSM969635	GSE39462	GPL15821	LB	LB	30	none	oxygen	150m
GSM969636	GSE39462	GPL15821	LB	LB	30	none	oxygen	250m
GSM969637	GSE39462	GPL15821	LB	LB	30	none	oxygen	360m
GSM969638	GSE39462	GPL15821	LB	LB	30	none	oxygen	540m

Table A3.2. A complete list of results of machine learning analysis (i.e., genes that were predictive for sample groups denoted by terminal electron acceptors) with basic annotation.

Locus	anode-score	Fe-score	fumarate-score	oxygen-score	Symbol	Functional Group
SO_2350	0	-0.0458	0	0	*aspC-1*	Amino acid biosynthesis
SO_2406	0	-0.0808	0	0	*aspC-2*	Amino acid biosynthesis
SO_3070	0	-0.1386	0	0	*asd*	Amino acid biosynthesis
SO_2279	0	-0.2362	0	0.0045	*ilvI*	Amino acid biosynthesis
SO_3262	-0.1077	0	0	0	*ilvB*	Amino acid biosynthesis
SO_2903	0	-0.2916	0	0	*cysK*	Amino acid biosynthesis
SO_0276	0.0503	0	0	0	*argB*	Aminoacid biosynthesis
SO_1792	0	-0.0502	0	0	*folD*	Biosynthesis of cofactors
SO_4254	0	-0.0031	0	0	*folE*	Biosynthesis of cofactors
SO_4702	0	-0.0244	0	0.0019	*gor*	Biosynthesis of cofactors
SO_0777	0	0	0	0.001	*ubiH*	Biosynthesis of cofactors
SO_2264	0	-0.4572	0	0	*iscS*	Biosynthesis of cofactors
SO_3312	0	-0.0036	0	0	*ispG*	Biosynthesis of cofactors
SO_3836	-0.0856	0	0	0	*ispE*	Biosynthesis of cofactors
SO_3638	0	-0.1115	0	0	*pdxA*	Biosynthesis of cofactors
SO_2441	0	0	0	0.002	*thiG*	Biosynthesis of cofactors
SO_3188	0	-0.2389	0	0	*rfbB*	Cell Envelope
SO_1428	0.0217	0	0	-0.0146		Cell Envelope
SO_1605	0.0218	0	0	0		Cell Envelope
SO_1880	0	-0.115	0	0	*nlpB*	Cell Envelope
SO_2375	0	-0.4234	0	0		Cell Envelope
SO_0282	0.001	0	0	0		Cell Envelope
SO_2787	0	-0.012	0	0		Cellular Processes
SO_3105	0	-0.151	0	0	*pspE-1*	Cellular Processes
SO_4215	0	-0.2911	0	0	*ftsZ*	Cellular Processes
SO_1530	0.0644	0	0	0	*pomB*	Cellular Processes
SO_3206	0	-0.139	0	0	*cheB-3*	Cellular Processes
SO_0533	0	0	0	-0.0022		Cellular Processes

SO_3341	0	-0.1438	0	0		Cellular Processes
SO_4625	0	0.035	0	0	*comF*	Cellular Processes
SO_2107	0	-0.0199	0	0	*mdoG-1*	Cellular Processes
SO_0525	0	0.0248	0	0		Cellular Processes
SO_0837	0.1049	0	0	0		Cellular Processes
SO_2749	0.0184	0	0	0	*tolA*	Cellular Processes
SO_3065	-0.0103	0	0	0		Cellular Processes
SO_0482	0	0.2395	0	0	*nrfG*	Central intermediary metabolism
SO_0485	0	0.1544	0	0	*nosL*	Central intermediary metabolism
SO_0830	-0.0164	0	0	0		Central intermediary metabolism
SO_1893	0	0	0	0.0054	*mvaB*	Central intermediary metabolism
SO_0044	0.2725	0	0	0		conserved hypothetical protein
SO_0299	0	0	0	0.0031		conserved hypothetical protein
SO_0309	0.0406	0	0	0		conserved hypothetical protein
SO_0331	0	0.0509	0	0		conserved hypothetical protein
SO_0394	0	-0.2765	0	0		conserved hypothetical protein
SO_0400	0.0249	0	0	0		conserved hypothetical protein
SO_0540	0	0.0466	0	0		conserved hypothetical protein
SO_0665	0	0.0153	0	0		conserved hypothetical protein
SO_0961	0.0463	0	0	0		conserved hypothetical protein
SO_0962	0	0.061	0	0		conserved hypothetical protein
SO_0972	0	0.0794	0	0		conserved hypothetical protein
SO_1047	0.0469	0	0	0		conserved hypothetical protein
SO_1060	0	-0.5957	0	0		conserved hypothetical protein
SO_1069	0.0195	0	0	0		conserved hypothetical protein
SO_1248	0	0	0.0362	0		conserved hypothetical protein
SO_1326	0	0	0	-0.0011		conserved hypothetical protein
SO_1372	-0.0661	0	0	0.0014		conserved hypothetical protein
SO_1392	0	0.0642	0	0		conserved hypothetical protein
SO_1474	0.0896	0	0	0		conserved hypothetical protein
SO_1617	0.0245	0	0	0		conserved hypothetical protein
SO_1736	0	0	0	-0.0018		conserved hypothetical protein
SO_1746	0	0	0	-9.00E-04		conserved hypothetical protein
SO_1816	0	-0.1623	0	0		conserved hypothetical protein
SO_1922	0	0.0863	0	-1.00E-04		conserved hypothetical protein
SO_1988	0	0.0171	0	0		conserved hypothetical protein
SO_2007	0	0	-0.0427	0		conserved hypothetical protein
SO_2110	0.0406	0	0	0		conserved hypothetical protein
SO_2182	0	0	0.0355	0		conserved hypothetical protein
SO_2198	-0.0889	0	0	0		conserved hypothetical protein
SO_2365	0.089	0	0	0		conserved hypothetical protein

SO_2481	0	0	0	-0.0044		conserved hypothetical protein
SO_2593	0	-0.1531	0	0		conserved hypothetical protein
SO_2602	0	-0.1998	0	0		conserved hypothetical protein
SO_2663	0	0.0535	0	0		conserved hypothetical protein
SO_2746	0	-0.1727	0	0		conserved hypothetical protein
SO_2769	0	-0.1392	0	0		conserved hypothetical protein
SO_2863	0.2002	0	0	0		conserved hypothetical protein
SO_2914	-0.3382	-0.1649	0	0.0073		conserved hypothetical protein
SO_2955	-0.0126	0	0	0		conserved hypothetical protein
SO_3076	0.1125	0	0	0		conserved hypothetical protein
SO_3091	-0.1096	-0.004	0	0.0034		conserved hypothetical protein
SO_3319	0.1454	0	0	-7.00E-04		conserved hypothetical protein
SO_3571	-0.0667	0	0	0		conserved hypothetical protein
SO_3580	0	-0.048	0	0		conserved hypothetical protein
SO_3764	0	-0.7241	0	0		conserved hypothetical protein
SO_3795	0	0.0439	0	0		conserved hypothetical protein
SO_3829	0.0248	0	0	0		conserved hypothetical protein
SO_3888	0.0066	0	0	0		conserved hypothetical protein
SO_3907	0	-0.0605	0	0		conserved hypothetical protein
SO_4070	0.1113	0	0	0		conserved hypothetical protein
SO_4143	0	0.0556	0	0		conserved hypothetical protein
SO_4164	-0.135	0	0	0		conserved hypothetical protein
SO_4455	0.1484	0	0	0		conserved hypothetical protein
SO_4554	0.0202	0.0774	0	-0.0021		conserved hypothetical protein
SO_4698	0	0	0	-0.0012		conserved hypothetical protein
SO_2335	0	-0.0247	0	0	*seqA*	DNA Metabolism
SO_2431	-0.1594	0	0	0	*ruvC*	DNA Metabolism
SO_0690	0	0.0888	0	0		DNA Metabolism
SO_4267	0	0.15	0	0	*hsdR-2*	DNA Metabolism
SO_0098	-0.0285	0	0	0	*hutH*	Energy Metabolism
SO_1897	0	0	0	0.0012	*ivd*	Energy Metabolism
SO_2339	0	-0.237	0	0		Energy Metabolism
SO_0396	0.1852	0	0	-0.005	*frdC*	Energy Metabolism
SO_1232	0	0	0.0225	0	*torA*	Energy Metabolism
SO_4357	0	0.0142	0	0	*dmsB-2*	Energy Metabolism
SO_4747	0	-0.2909	0	0	*atpD*	Energy Metabolism
SO_4749	0	-0.6133	0	0	*atpA*	Energy Metabolism
SO_4750	0	-0.0516	0	0	*atpH*	Energy Metabolism
SO_0264	0	-0.198	0	0	*scyA*	Energy Metabolism
SO_0476	0	0.0765	0	0		Energy Metabolism
SO_0939	0	0.0918	0	0		Energy Metabolism

SO_1011	-0.1407	0	0	0.0023	*nuoL*	Energy Metabolism
SO_1013	-0.0771	0	0	0.0113	*nuoJ*	Energy Metabolism
SO_1014	0	0	0	0.0036	*nuoI*	Energy Metabolism
SO_1018	-0.1642	-0.025	0	0.0141	*nuoE*	Energy Metabolism
SO_1019	-0.169	-0.0185	0	0.0046	*nuoCD*	Energy Metabolism
SO_1020	0	-0.2231	0	0.0072	*nuoB*	Energy Metabolism
SO_1233	0	0	0.0173	0	*torC*	Energy Metabolism
SO_2361	0	-0.1438	0	0	*ccoP*	Energy Metabolism
SO_2363	0	-0.1982	0	0	*ccoO*	Energy Metabolism
SO_2364	0	-0.4662	0	0	*ccoN*	Energy Metabolism
SO_3920	0	0	0	-0.001	*hydA*	Energy Metabolism
SO_3921	0	0	0.0157	0	*hydB*	Energy Metabolism
SO_4061	0	0	0.2049	0	*psrB*	Energy Metabolism
SO_0344	0	0	0	1.00E-04	*prpC*	Energy Metabolism
SO_0345	0	0	0	0.0098	*prpB*	Energy Metabolism
SO_0401	0.4235	0	0	-0.0093		Energy Metabolism
SO_2345	0	-0.7296	0	0	*gapA-2*	Energy Metabolism
SO_2347	0	-0.3169	0	0	*gapA-3*	Energy Metabolism
SO_3547	0	-0.0098	0	0	*pgi*	Energy Metabolism
SO_0083	0	0	0	-2.00E-04		Energy Metabolism
SO_1891	-0.0174	0	0	0.0086		Energy Metabolism
SO_0810	-0.0272	0	0	0	*rbsK*	Energy Metabolism
SO_1664	0	-0.0555	0	0	*galE*	Energy Metabolism
SO_4458	0.0907	0	0	0		Energy Metabolism
SO_0432	0	-0.0309	0	0	*acnB*	Energy Metabolism
SO_1928	0	-0.1631	0	0.0038	*sdhA*	Energy Metabolism
SO_1929	0	-0.293	0	0.0109	*sdhB*	Energy Metabolism
SO_1931	0	-0.1823	0	0.0088	*sucB*	Energy Metabolism
SO_1933	0	-0.2274	0	0	*sucD*	Energy Metabolism
SO_3072	0	-0.1918	0	0	*fabB*	Fatty acid and phospholipid metabolism
SO_4380	-0.0334	0	0	0		Fatty acid and phospholipid metabolism
SO_4381	-0.0697	0	0	0		Fatty acid and phospholipid metabolism
SO_1679	0	0	-0.0658	0.0109		Fatty acid and phospholipid metabolism
SO_2772	0.1239	0	0	0		Fatty acid and phospholipid metabolism
SO_3463	0.0436	0	0	0	*pgpA*	Fatty acid and phospholipid metabolism
SO_4335	0	0	0.0286	0		Fatty acid and phospholipid metabolism
SO_0068	0	0.0796	0	0		hypothetical protein
SO_0377	0	0.1186	0	0		hypothetical protein

SO_0391	0	0.2505	0	0		hypothetical protein
SO_0515	0.0181	0	0	0		hypothetical protein
SO_0552	0	-0.0319	0	0		hypothetical protein
SO_0655	0	0	0	5.00E-04		hypothetical protein
SO_0786	0	0.1229	0	0		hypothetical protein
SO_0787	0	0.0747	0	0		hypothetical protein
SO_0844	0	0.1325	0	0		hypothetical protein
SO_0912	0	0.1751	0	0		hypothetical protein
SO_0971	0	0.0248	0	0		hypothetical protein
SO_1027	0.1663	0.1241	0	-0.0014		hypothetical protein
SO_1078	0	0.1327	0	0		hypothetical protein
SO_1081	0	0.1694	0	0		hypothetical protein
SO_1318	-0.0978	0	0	0		hypothetical protein
SO_1382	0	0.0313	0	0		hypothetical protein
SO_1489	0	-0.1951	0	0		hypothetical protein
SO_1532	0.2087	0	0	0		hypothetical protein
SO_1854	0	-0.0191	0	0		hypothetical protein
SO_1864	-0.0623	0	0	0		hypothetical protein
SO_2181	0.016	0	0	0		hypothetical protein
SO_2480	-0.1013	0	0	0		hypothetical protein
SO_2515	0.0742	0	0	0		hypothetical protein
SO_2517	-0.0076	0	0	0.0019		hypothetical protein
SO_2691	0	0.0335	0	0		hypothetical protein
SO_2854	0.0823	0	0	0		hypothetical protein
SO_2929	0	-0.0746	0	0		hypothetical protein
SO_3100	0	0.1858	0	0		hypothetical protein
SO_3131	0	0.0026	0	0		hypothetical protein
SO_3234	0	-0.2704	0	0		hypothetical protein
SO_3527	0.0175	0	0	0		hypothetical protein
SO_3615	-0.0432	0	0	0		hypothetical protein
SO_3693	0	0.0517	0	0		hypothetical protein
SO_3886	0	0.0138	0	0		hypothetical protein
SO_4006	-0.0899	0	0	0		hypothetical protein
SO_4177	0.0849	0	0	0		hypothetical protein
SO_4276	0	0.0539	0	0		hypothetical protein
SO_4482	0.1729	0	0	0		hypothetical protein
SO_4490	0	0.0361	0	0		hypothetical protein
SO_4528	0	0.0885	0	0		hypothetical protein
SO_4621	0	0.0305	0	0		hypothetical protein
SO_4694	0	0	0.0236	0		hypothetical protein
SO_2652	0	-0.008	0	0		Mobile and extrachromosomal elements

SO_2941	0	0.0253	0	0		Mobile and extrachromosomal elements
SO_0605	0	-0.0651	0	0	*hflK*	Protein Fate
SO_1795	0	-0.3607	0	0	*clpX*	Protein Fate
SO_2601	0	-0.3487	0	0		Protein Fate
SO_0481	0	0.0506	0	0		Protein Fate
SO_1139	0	-0.3231	0	0	*fklB*	Protein Fate
SO_1627	0	-0.3173	0	0	*map*	Protein Fate
SO_3870	0	0.0203	0	0		Protein Fate
SO_0220	0	-0.088	0	0	*rplK*	Protein Synthesis
SO_0222	0	-0.0904	0	0	*rplJ*	Protein Synthesis
SO_0226	0	-0.8792	0	0	*rpsL*	Protein Synthesis
SO_0231	0	-0.6349	0	0	*rplC*	Protein Synthesis
SO_0232	0	-0.0994	0	0	*rplD*	Protein Synthesis
SO_0235	0	-0.0482	0	0	*rpsS*	Protein Synthesis
SO_0241	0	-0.4225	0	0	*rplN*	Protein Synthesis
SO_0244	0	-0.0281	0	0	*rpsN*	Protein Synthesis
SO_0245	0	-0.4908	0	0	*rpsH*	Protein Synthesis
SO_0247	0	-0.2558	0	0	*rplR*	Protein Synthesis
SO_0253	0	-0.2918	0	0	*rpsM*	Protein Synthesis
SO_0254	0	-0.4632	0	0	*rpsK*	Protein Synthesis
SO_0255	0	-0.7838	0	0	*rpsD*	Protein Synthesis
SO_1357	0	-0.3172	0	0	*rpsP*	Protein Synthesis
SO_1629	0	-0.2936	0	0	*rpsB*	Protein Synthesis
SO_2112	0	-0.3747	0	0	*rplY*	Protein Synthesis
SO_2270	0	0	0	-6.00E-04	*rimK-2*	Protein Synthesis
SO_2402	0	-0.0705	0	0	*rpsA*	Protein Synthesis
SO_3652	0	-0.5149	0	0	*rplU*	Protein Synthesis
SO_3939	0	-0.6705	0	0	*rpsI*	Protein Synthesis
SO_3940	0	-0.829	0	0	*rplM*	Protein Synthesis
SO_4247	0	-0.2573	0	0	*rpmB*	Protein Synthesis
SO_0217	0.0669	0	0	0	*tufB*	Protein Synthesis
SO_0842	0	-0.4326	0	0	*fusA-2*	Protein Synthesis
SO_3962	0	-0.3264	0	0.0095	*yfiA-3*	Protein Synthesis
SO_0015	0	-0.1137	0	0	*glyQ*	Protein Synthesis
SO_2310	0	-0.2549	0	0	*serS*	Protein Synthesis
SO_2619	0	-0.1138	0	0	*metG*	Protein Synthesis
SO_3424	0	-0.0353	0	0	*valS*	Protein Synthesis
SO_1575	-0.0505	0	0	0		Protein Synthesis
SO_3113	0	-0.0027	0	0	*tgt*	Protein Synthesis
SO_2018	0	-0.2523	0	0	*adk*	Purines
SO_2403	0	-0.6086	0	0	*cmk*	Purines

SO_3937	0	-0.0193	0	0	*purA*	Purines
SO_2592	-0.0319	0	0	0	*pyrD*	Purines
SO_2791	0	-0.1057	0	0	*cdd*	Purines
SO_0532	0.025	0.0056	0	0	*arsR*	Regulatory Functions
SO_1469	0	0.2038	0	0		Regulatory Functions
SO_2193	0.1467	0	0	0		Regulatory Functions
SO_2490	0	-0.1482	0	0		Regulatory Functions
SO_2640	0.2641	0	0	0		Regulatory Functions
SO_3385	0.0039	0	0	0		Regulatory Functions
SO_4477	0	0	0	-7.00E-04	*cpxR*	Regulatory Functions
SO_4623	0	0	0	-0.0021		Regulatory Functions
SO_1935	0	0	0	2.00E-04	*rnk*	Regulatory Functions
SO_0437	0	0.0746	0	0		Regulatory Functions
SO_3963	0	-0.1114	0	0	*ptsN*	Signal Transduction
SO_0545	-0.0146	0	0	0		Signal Transduction
SO_2889	0	0	0.1247	0		Signal Transduction
SO_4471	-0.0048	0	0	0	*ntrB*	Signal Transduction
SO_0947	0	-0.301	0	0	*srmB*	Transcription
SO_4034	0	-0.022	0	0	*deaD*	Transcription
SO_4631	-0.025	0	0	0	*greB*	Transcription
SO_0986	0	0.2528	0	0		Transport and Binding Proteins
SO_3134	-0.0213	0	0	0	*dctP*	Transport and Binding Proteins
SO_1825	0	-0.9491	0	0		Transport and Binding Proteins
SO_0857	0	0	-0.0018	0		Transport and Binding Proteins
SO_2713	-0.0525	0	0	6.00E-04		Transport and Binding Proteins
SO_3779	-0.0944	0	0	0	*cydC*	Transport and Binding Proteins
SO_4029	0	0	0	-0.0013		Transport and Binding Proteins
SO_0157	0	0.1213	0	0		Transport and Binding Proteins
SO_1270	0	-0.4446	0	0		Transport and Binding Proteins
SO_2865	0.0253	0	0	0		Transport and Binding Proteins
SO_1827	0	-0.8453	0	0	*exbD2*	Transport and Binding Proteins
SO_1828	0	-0.5066	0	0	*tonB2*	Transport and Binding Proteins
SO_1821	0	-0.0274	0	0		Transport and Binding Proteins
SO_0386	0	0.0106	0	0		Unknown Function
SO_0536	0.1039	0	0	0		Unknown Function
SO_0698	0.2062	0	0	-8.00E-04	*fsxA*	Unknown Function
SO_1346	0	-0.1193	0	0	*lepA*	Unknown Function
SO_1387	0	0.014	0	0		Unknown Function
SO_1581	0	-0.0322	0	0	*phnA*	Unknown Function
SO_2118	0	0.1318	0	0		Unknown Function
SO_2265	0	-0.1315	0	0		Unknown Function

SO_2380	0	0	0.0524	0		Unknown Function
SO_2674	0	0.0986	0	0		Unknown Function
SO_2907	0	-0.3721	0	0		Unknown Function
SO_3017	-0.1306	0	0	0.0113		Unknown Function
SO_3093	-0.1166	0	0	0		Unknown Function
SO_3949	-0.1306	0	0	0.0063		Unknown Function
SO_4207	-0.0103	0	0	0		Unknown Function
SO_4378	-0.0461	0	0	0		Unknown Function
SO_4660	0	0.0727	0	0		Unknown Function

APPENDIX 4

REGULATED EXPRESSION OF POLYSACCHARIDE UTILIZATION AND CAPSULAR BIOSYNTHESIS LOCI IN BIOFILM AND PLANKTONIC *BACTEROIDES THETAIOTAOMICRON* DURING GROWTH IN CHEMOSTATS

Adapted from TerAvest , He, Rosenbaum, Martens, Cotta, Gordon, and Angenent. Accepted for publication in *Biotechnology and Bioengineering, July 2013.**

* Please see the original publication for supplementary information

A4.1 Abstract

Bacteroides thetaiotaomicron is a prominent member of the human distal gut microbiota that specializes in breaking down diet and host-derived polysaccharides. While polysaccharide utilization has been well studied in *B. thetaiotaomicron,* other aspects of its behavior are less well characterized, including the factors that allow it to maintain itself in the gut. Biofilm formation may be a mechanism for bacterial retention in the gut. Therefore, we used custom GeneChips to compare the transcriptomes of biofilm and planktonic *B. thetaiotaomicron* during growth in mono-colonized chemostats. We identified 1154 genes with a fold-change greater than 2, with confidence greater than or equal to 95%. Among the prominent changes observed in biofilm populations were: (i) greater expression of genes in polysaccharide utilization loci that are involved in foraging of O-glycans normally found in the gut mucosa; and (ii) regulated expression of capsular polysaccharide biosynthesis loci. Hierarchical clustering of the data with different datasets, which were obtained during growth under a range of conditions in minimal media and in intestinal tracts of gnotobiotic mice, revealed that within this group of differentially expressed genes, biofilm communities were more similar to the *in vivo* samples than to planktonic cells and exhibited features of substrate limitation. The current study also validates the use of chemostats as an *in vitro* ‘gnotobiotic’ model to study gene expression of attached

populations of this bacterium. This is important to gut microbiota research, because bacterial attachment and the consequences of disruptions in attachment are difficult to study *in vivo.*

A4.2 Introduction

The adult human gut microbiota is composed of members of all three domains of life and their viruses. This community is dominated by Bacteria, and specifically by members of two bacterial phyla, the Bacteroidetes and Firmicutes. *Bacteroides thetaiotaomicron* is prominently represented among the Bacteroidetes in the distal gut, where it ferments chemically diverse, complex dietary glycans to short chain fatty acids that can be absorbed by the host (Koropatkin et al. 2012; Martens et al. 2011). *B. thetaiotaomicron* is also able to utilize host mucus glycans, such as mucin, including mucin O-glycans, as nutrient substrates when polysaccharides are absent from the host diet, giving it a competitive advantage over other, less versatile, simple sugar-fermenting bacteria (Benjdia et al. 2011; Martens et al. 2008; Martens et al. 2011; Sonnenburg et al. 2005).

The saccharolytic capabilities of *B. thetaiotaomicron* are reflected in its genome. The type strain (VPI-5482) has 88 polysaccharide utilization loci (PULs), composed of 866 genes that comprise 18% of its genome (Martens et al. 2008). Each PUL characterized to date encodes a group of cell envelope-associated proteins collectively known as a Sus-like system, which endows the bacterium with the ability to metabolize a glycan or group of related glycans. Each of *B. thetaiotaomicron* Sus-like systems contains: (i) a homolog of SusC, which is a TonB-dependent receptor that spans the outer membrane and transports oligosaccharides in an energy dependent manner; and (ii) a homolog of SusD, which is an outer membrane lipoprotein that binds specific glycans and participates in delivering oligosaccharides to the SusC transporter (Koropatkin et al. 2008; Reeves et al. 1996; Reeves et al. 1997). In addition to SusC- and SusD-

like proteins, a PUL can include other outer membrane glycan binding proteins, as well as various glycoside hydrolases, polysaccharide lyases, and/or carbohydrate esterases (Koropatkin and Smith 2010). Whole genome transcriptional profiling, targeted gene disruption, characterization of purified Sus proteins, and assays of growth *in vitro* on glycan arrays (a high-throughput method to directly measure functional interactions with polysaccharides (Blixt et al. 2004; Padler-Karavani et al. 2012; Stevens et al. 2006)) have helped define the carbohydrate recognition and utilization capabilities of *B. thetaiotaomicron* and the carbohydrate specificities of its PULs (Kitamura et al. 2008; Koropatkin et al. 2009; Koropatkin and Smith 2010). The repertoire of PULs present in the genome, and their patterns of gene expression help define the niches of *B. thetaiotaomicron* and of other members of Bacteroides *in vivo* (Martens et al. 2011; Sonnenburg et al. 2010).

A major challenge for members of the gut microbiota is to prevent washout from the gut habitat. The ability to form 'attached' populations would provide a competitive advantage to a gut symbiont by increasing retention time, providing access to solid state plant- and human-derived nutrient substrates, and facilitating development of syntrophic (nutrient-sharing) relationships with other members of the microbiota (Sonnenburg et al. 2004). The formation of extracellular matrices composed principally of polysaccharides and other biological polymers with bound/embedded microbes provides an important mechanism for microbes to adhere to each other and to living or non-living surfaces, such as food particles. The intestine is lined by mucus that serves as a microhabitat for members of the microbiota, supplying attachment sites (e.g., O-glycans) and nutrients (Ambort et al. 2012; Ambort et al. 2011; Lindén et al. 2008a; Lindén et al. 2008b; McGuckin et al. 2011). Biofilm formation affects the motility of microbes and also their response to nutrient limitation and other stresses (Beloin and Ghigo 2005;

Lazazzera 2005). However, investigation of gut biofilms has been difficult because of the challenges associated with accessing this community *in vivo,* or replicating the gut environment *in vitro* (Marzorati et al. 2011).

Studies have shown that *B. thetaiotaomicron* is prominently represented on the surfaces of mixed food particles isolated from human feces (Macfarlane and Dillon 2007; Macfarlane and Macfarlane 2006), and undigested plant material in the gut lumen and within the mucus layer of gnotobiotic mice colonized by *B. thetaiotaomicron* and fed simple-sugar or polysaccharide-rich diets (Sonnenburg et al. 2005). Because both plant materials and host-derived mucus can serve as carbon and energy sources for *B. thetaiotaomicron*, attachment is likely to be mediated, at least in part, by Sus-like proteins involved in nutrient binding (Shipman et al. 2000). When cells bind to a nutrient that is part of a solid surface they, in essence, attach to that surface. However, *B. thetaiotaomicron* also attaches to glass surfaces, indicating that nutrient binding is not its only attachment mechanism (Macfarlane et al. 2005). One study demonstrated that attachment of this bacterial species to glass was regulated by the availability of soluble substrate (i.e., it occurred only under conditions where glucose concentrations were high), indicating that nutrient binding and attachment are tightly linked in this organism (Macfarlane et al. 2005).

In the present study, we use GeneChip-based whole genome transcriptional profiling to explore how biofilm formation impacts gene expression in *B. thetaiotaomicron.* To do so, we sampled mono-colonized chemostats, examining biofilm as well as planktonic populations. The results are compared to the transcriptional profiles of *B. thetaiotaomicron* obtained in monocolonized gnotobiotic mice as well as during *in vitro* culture as planktonic cells under defined limiting and non-limiting nutrient conditions. Specifically, we investigated the links between attachment, nutrient binding and uptake, and capsule formation to generate hypotheses

on how attachment of this organism may affect human health, and to compare biofilm and planktonic populations as *in vitro* models of gene expression *in vivo*.

A4.3 Results and discussion

Growth in chemostats and differential expression analysis

The sequenced type strain, *B. thetaiotaomicron* VPI-5482, was inoculated into six sterile chemostats and fed continuously with sterile TYG (tryptone, yeast extract, glucose) medium. Growth proceeded at 37^{o}C under an atmosphere of N_2 and CO_2 (80%/20%). Each chemostat contained a carbon paper growth surface to allow for biofilm formation. During the first 24 h, dense planktonic growth occurred (OD_{600} ~ 0.6). Biofilm was not detected by scanning electron microscopy (SEM) of the carbon paper surface at 8 h but was clearly visible by the naked eye and SEM at 8 d (**Figure A4.1A-D**).

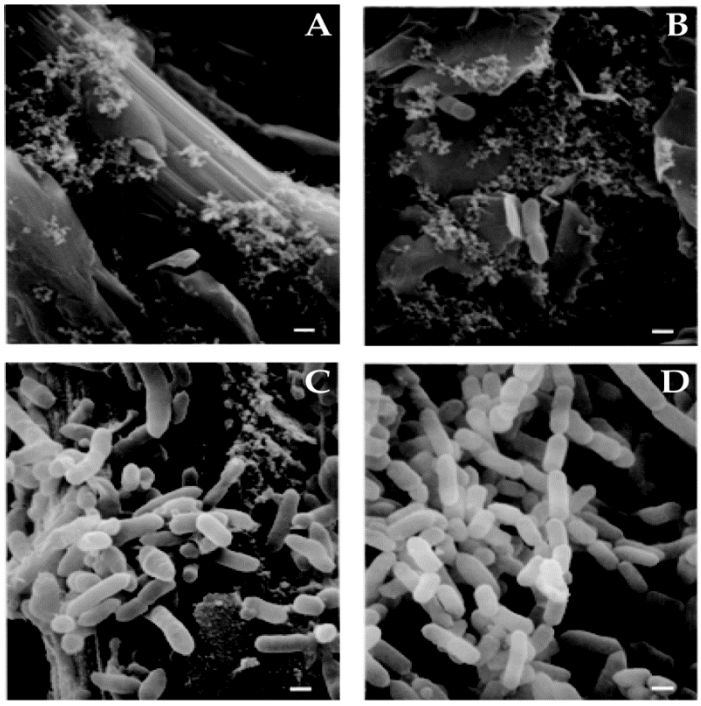

FIGURE A4.1. Scanning electron micrographs of the growth surface sampled at 8 h (panels A and B) and 8 days (panels C and D) after inoculation. Few bacteria are shown in panels A and B, illustrating the rarity of their association with the growth surface at this early time point. Bars, 0.5 µm.

RNA was extracted from planktonic cells harvested from the chemostats after 8 h of growth. Biofilm cells were removed from the carbon paper surface after 8 days of growth. Because the experiments were performed in chemostats, both samples were in a steady-state growth phase, not in stationary phase, even though the sampling times were long. The samples were harvested at different times and HRTs to ensure that the planktonic sample was not contaminated with biofilm cells and *vice versa*. Gene expression was compared for biofilm (n=6) and planktonic (n=6) samples using the LEMMA (Laplace EM Microarray Analysis) method implemented as a package in R (Bar et al. 2010). Using a false discovery rate of 0.05, 1584 genes were detected as differentially expressed between the two groups. Of these, we defined 1145 genes as "differentially expressed" for the rest of the study (base 2 logarithm of the fold-change in their expression was greater than 1, i.e. fold-change was greater than 2). Transcripts were categorized based on a variety of annotation schemes: COG category, KEGG orthology group (KO) (KEGG database), KEGG enzyme commission (EC) number, carbohydrate active enzyme (CAZyme) family (CAZy database), and peptidase family (MEROPS database). The results are provided in **Table S1**. Using these annotations, we determined which functional groups were significantly enriched within the differentially expressed genes compared to the genome (determined using the hypergeometric distribution; $p<0.05$) (see **Table S2)**. This analysis indicates that groups that are significantly enriched within the differentially expressed genes are specifically involved in changes between biofilm and planktonic samples, but does not take into account up- or down-regulation. Further functional insights about the significance of these observed differences in gene expression came from a follow-up analysis that placed them in the context of *B. thetaiotaomicron's* PULs.

Substrate acquisition and utilization

As noted in the Introduction, *B. thetaiotaomicron* VPI-5482 has 88 PULs, containing a total of 866 genes. Two hundred seventy eight of these genes were differentially expressed in the biofilm cells, with 80 PULs being represented (although not all genes in each of these 80 PULs were differentially expressed). Among the 866 PUL genes are 209 *susC*/*susD* homologs, 93 of which (51 SusC homologs and 42 SusD homologs) were differentially expressed. With the exception of two *susC* homologs and two *susD* homologs from 3 different PULs all of the differentially expressed *susC/susD* homologs showed increased expression in the biofilm compared to planktonic populations. **Table S3** provides: (i) a rank ordering of PULs based on the magnitude of the average difference in expression of their constituent genes between biofilm *versus* planktonic populations; and (ii) includes information about the differences in expression of their other genes (e.g., CAZyme family members, hypothetical proteins). **Figure A4.2** shows the change in expression for all genes in the 5 PULs with the largest differences (ranking based on their *susC/susD* responses) and annotation of the genes that comprise these PULs. Interestingly, two of these 5 PULs, *BT4294-4300*, and *BT2802-2809* are known to be induced in response to host-derived glycans (Sonnenburg et al. 2005) and five sulfatases, including a mucin-degrading sulfatase, were expressed at significantly higher levels in biofilm compared to planktonic cell populations (**Table S3**). One possible reason for this is that starvation during biofilm growth causes the cell to upregulate Sus-like systems to "surveillance levels" that prime the cell to gather any nutrients that are available. Alternatively, attachment *per se* may prime *B. thetaiotaomicron* cells for degradation of host mucins. Mono- and co-colonization studies in gnotobiotic mice have established that sulfatases are important fitness factors for *B.*

thetaiotaomicron, especially when the mice were fed a simple sugar diet that requires adaptive foraging on host glycans (Benjdia et al. 2011).

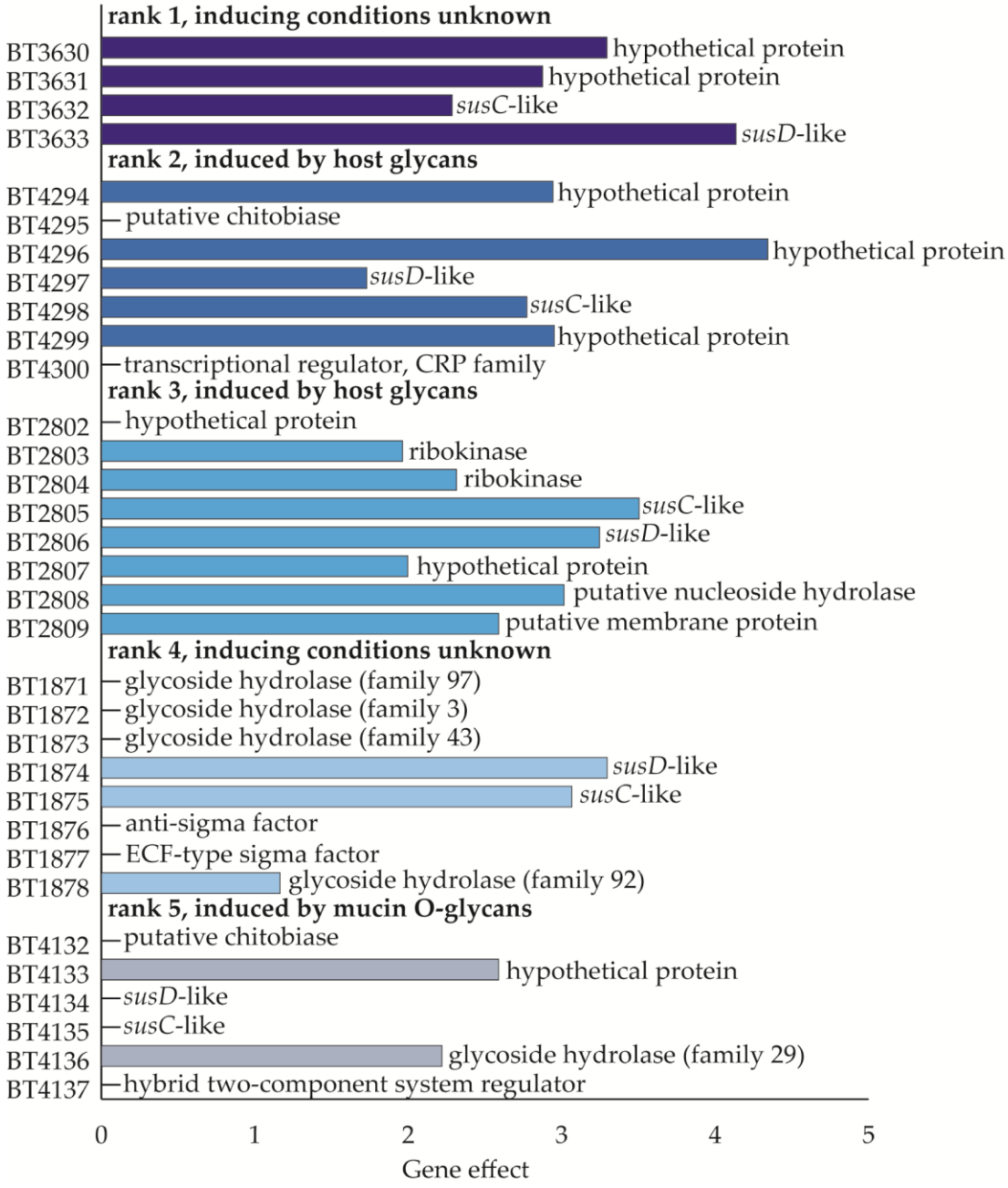

Figure A4.2. Gene effect (base 2 logarithm of the fold expression change) of each gene within the 5 most differentially expressed PULs (based on change in *susC*/*susD* expression) and annotations for each gene. Bars are not shown for genes that were not detected as differentially expressed. Inducing conditions for each PUL were determined in reference (3).

The *B. thetaiotaomicron* genome contains 8 capsular polysaccharide synthesis (*CPS*) loci, each comprised of 15-32 genes (Martens et al. 2009). A total of 74 genes, distributed among all 8 *CPS* loci, exhibited significant differences in their expression between biofilm and planktonic communities, including 13 genes that were upregulated in *CPS* locus 8 (*BT0037-68*), and 24 genes that were downregulated in *CPS* locus 1 (*BT0375-402*). This indicates that specific changes in the capsule are required for attachment or life in the biofilm (see **Table S4** for a complete list of the genes present in each *CPS* locus and the magnitude of their differential expression in biofilm *versus* planktonic populations). Our findings show that attachment to a carbon surface in a chemostat not only regulates expression of PULs involved in adaptive foraging of mucus glycans *in vivo* but also regulates expression of capsular biosynthetic loci. We have not defined how these changes impact capsular glycan composition. It is possible that changes in the capsule are involved in interactions between biofilm community members, whether at the level of attachment or nutrient sharing/harvest.

Comparison of transcriptional profiles of the biofilm community to profiles obtained in vitro *under defined growth conditions and in gnotobiotic mice*

To gain additional perspective about the response of *B. thetaiotaomicron* to attachment and biofilm community formation, we compared the GeneChip datasets we generated in other studies to the datasets from biofilm and planktonic communities in our chemostats. We previously used the custom *B. thetaiotaomicron* GeneChip employed in the present study to characterize the transcriptome of this organism under a variety of conditions, including during *in vitro* growth in defined minimal medium containing a range of potential substrates, and *in vivo* in mono-associated gnotobiotic mice consuming a plant polysaccharide-rich diet, or a diet devoid of complex polysaccharides and rich in simple sugars (see **Table S5** for an annotated list of these

5 datasets and their GEO accession numbers). The 6 datasets were subjected to unsupervised hierarchical clustering analysis with the dist and hclust functions in R. The results of this analysis were visualized as a dendrogram, which was labeled with relevant experimental information, as well as the dataset of origin (**Figure A4.3**).

When all genes were used in the clustering analysis, the biofilm and planktonic cells clustered together. However, when the differentially expressed genes identified by the chemostat experiment were used to perform the clustering analysis, the first branch point showed a clear division based on 'substrate availability' (where available substrate is defined as sugars or polysaccharides given within the previous 6 h of growth). Using only the differentially expressed genes highlighted differences between biofilm and planktonic samples and allowed us to interpret these differences in terms of other growth conditions. Within the substrate limited cluster, there was a division between cultures grown *in vitro versus* those harvested from the distal gut (cecum) of mono-colonized gnotobiotic mice fed various diets (**Figure A4.3**). Non-limited samples broke into two groups depending on whether complex or simple sugars were fed (**Figure A4.3**). Thus, overall, samples could be classified into four major groups based on this clustering pattern: (i) substrate limited, grown in mouse (LM); (ii) substrate limited, grown in glass or tube (LG); (iii) non-limited with complex sugars (NC); and (iv) non-limited with simple sugars (NS).

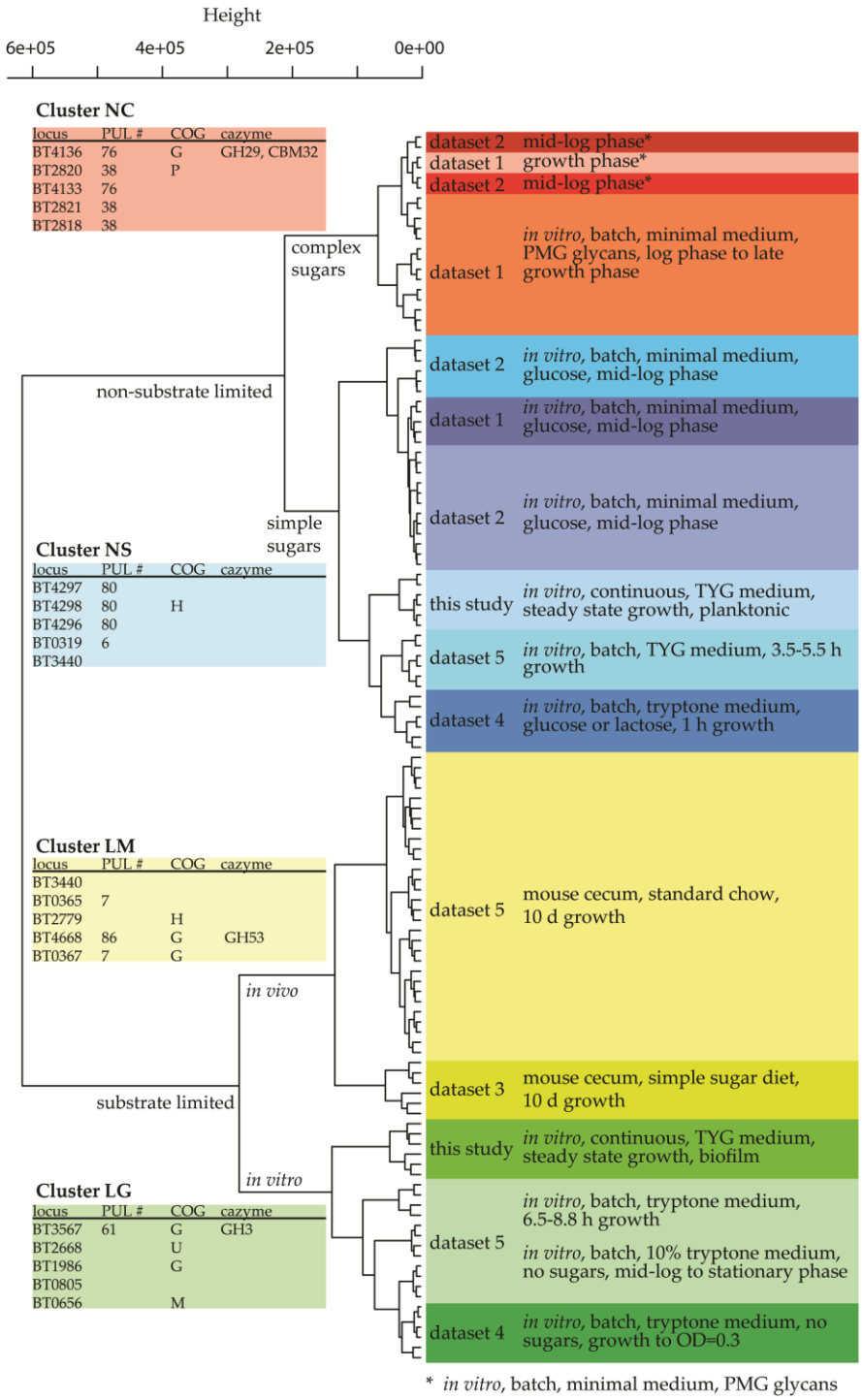

Figure A4.3. The analysis is based on genes that are differentially expressed between biofilm and planktonic samples. Their expression under other environmental conditions was used to perform the unsupervised clustering shown, using the hclust function in R. Color code: red labels, 'non-limited with complex sugars' (NC) cluster; blue, 'non-limited with simple sugars' (NS) cluster; yellow, 'substrate limited grown in mouse' (LM) cluster; green, the 'substrate limited grown in glass or tube' (LG) cluster. Labels on the right indicate the datasets, and essential information describing them. Tables on the left show loci and annotations for the five most discriminatory genes for each cluster. (PMG, porcine gastric mucin)

To observe which of the genes used in the clustering analysis were predictive for the sample cluster, we used a machine learning approach implemented in the PAMr package for R (Tibshirani et al. 2002). With a threshold of 5.0, 278 "key clustering genes" were required to accurately predict which of the four major clusters each sample belonged to (**Table S6**). These genes represent the core transcriptomic changes among the four groups and their potential phenotypic differences. The key clustering genes were enriched in 5 COG functional categories compared to the genome and the differentially expressed genes: (i) cell envelope biogenesis, outer membrane (M); (ii) inorganic ion transport and metabolism (P); (iii) carbohydrate transport and metabolism (G); (iv) amino acid transport and metabolism (E); and (v) coenzyme metabolism (H), with the largest enrichment in categories M and G. When combining the annotated dendrogram with the machine learning results, it becomes clear that the essential differences between the four sample groups lie in carbohydrate uptake and utilization; dendrogram clustering occurred mainly on the basis of substrate type and availability and the key clustering genes were enriched in carbohydrate utilization functions (**Table S6**). This indicates that there were widespread differences in carbohydrate utilization function between the biofilm and planktonic groups, although both were grown under the same experimental conditions, suggesting further that biofilm formation changes carbohydrate binding, uptake and utilization in *B. thetaiotaomicron* (**Figure A4.4**).

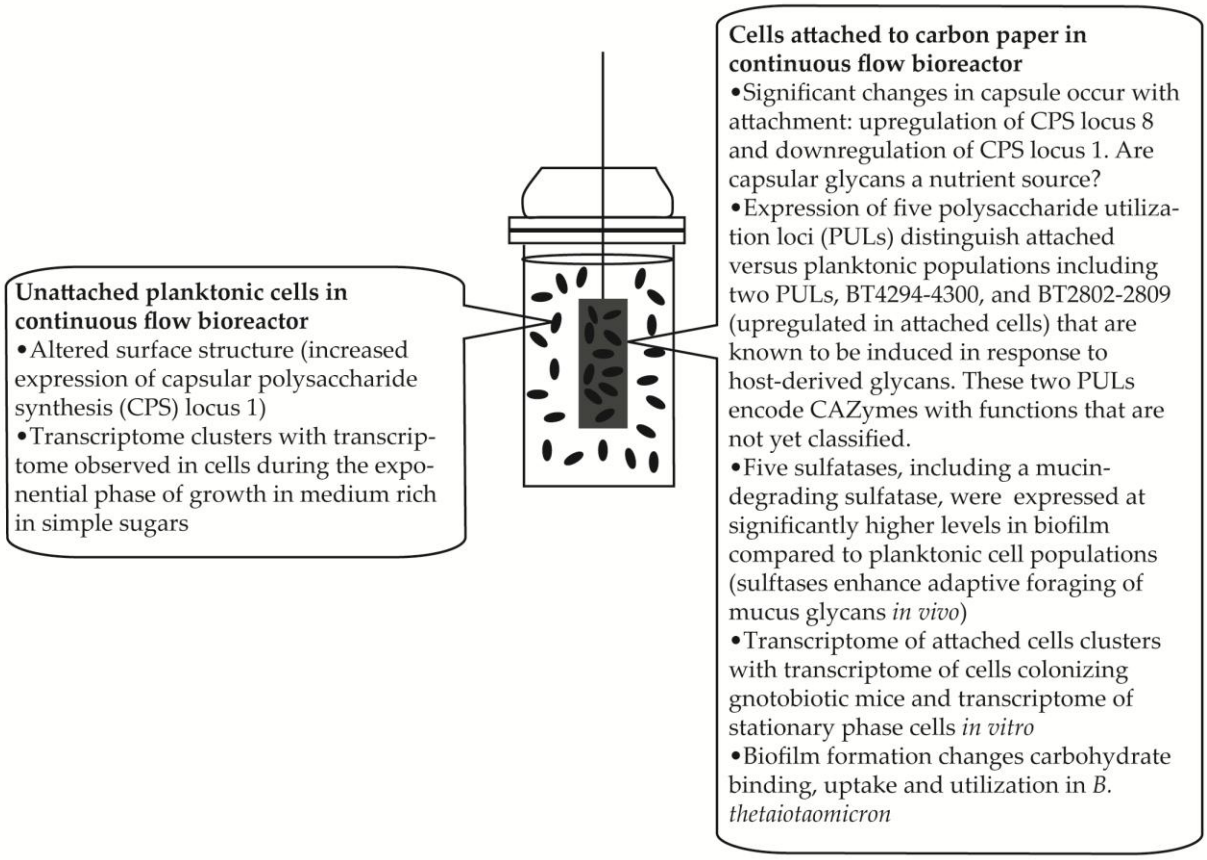

Figure A4.4. Summary of major transcriptional differences that distinguish the expressed functional features of biofilm and planktonic *B. thetaiotaomicron* populations present in the chemostat.

Prospectus

Mechanisms that mediate and regulate attachment of gut bacteria to various living and non-living surfaces represent a key area that needs further investigation. Attachment is likely key to harvesting nutrients present in partially digested food. Direct attachment to other bacterial cells and/or gaining proximity to these cells via attachment to common nutrient platforms could be an important step in establishing syntrophic relationships, as in water columns within aquatic ecosystems. Bacterial attachment and the consequences of 'attachment disorders' are difficult to study *in vivo*, but the current study shows that chemostats can be used as an *in vitro* 'gnotobiotic' model to study how a prominent human saccharolytic bacterium attaches to a defined surface and

its response to attachment. In terms of gene expression, chemostat-grown cells were more similar *in vivo*-grown cells than cells grown in batch-fed conditions were, making chemostats a good choice for *in vitro* experiments with this organism. In this system, we see that biofilm formation occurs in a reproducible fashion and that attachment to a carbon surface 'primes' the organism to induce expression of polysaccharide utilization loci (PULs) involved degradation of mucus glycans while also affecting the expression of capsular polysaccharide biosynthetic genes involved in decorating the surface of the bacterial cell with carbohydrates. Both types of responses will change the interactions of this organism with nutrient foundations, including those derived from the host or capsular glycans of other attached cells.

Hierarchical clustering of transcriptional profiles of *B. thetaiotaomicron* populations studied under a wide variety of environmental conditions indicate that populations in the gut of mono-colonized gnotobiotic mice fed various diets, and biofilm communities elicit transcriptional responses resembling those seen under nutrient limiting conditions, making them more similar to each other than to high-nutrient growth conditions. This study suggests that future genetic and biochemical/metabolic analyses of *B. thetaiotaomicron* during its assembly into biofilm communities within continuous flow chemostats may provide new ways for defining and testing hypotheses about how this mutualist attaches to various surfaces present in the gut, acquires and processes various nutrients in an attached state, and how it adjusts to various perturbations.

A4.4 Materials and methods

Bacterial Strains and Culture Conditions

B. thetaiotaomicron strain VPI-5482 (ATCC 29148) was used in all experiments. Tryptone, yeast extract, glucose (TYG) medium was used for bacterial growth in the chemostats,

containing (per liter deionized water): tryptone, 10 g; yeast extract, 5 g; glucose, 4 g; L-cysteine, 0.5 g; KH_2PO_4, 4 g; K_2HPO_4, 9 g; TYG salt solution, 40 mL; $CaCl_2 \cdot 2H_2O$, 8 mg; $FeSO_4$, 0.4 mg; hematin, 1.2 mg. TYG salt solution consists of (per liter deionized water): $MgSO_4 \cdot 7H_2O$, 0.5 g; $NaHCO_3$, 10 g; NaCl, 2 g. All chemicals were used as purchased. Prior to inoculation, the bacterial culture was pre-grown in TYG medium overnight. Pre-cultures were inoculated directly from frozen stocks prior to each experiment.

Chemostat Design and Operation

Two identical chemostats were constructed from glass with a ~210 mL liquid volume. A water jacket around each chemostat maintained an operating temperature of 37ºC. A 54 cm^2 carbon paper growth surface for biofilm attachment was inserted into each chemostat, (P50, Ballard Material Products, Lowel, MA, USA). Before operation, the chemostats, medium storage tanks, and all connections/pump tubing were autoclaved at 121ºC for 60 min. Glucose and hematin solutions were filter-sterilized (0.22-µm pore diameter), and added to the medium storage tank after autoclaving. To inoculate, 3 mL of overnight-grown *B. thetaiotaomicron* culture (~ 6×10^9 CFU) were injected into the chemostats. The chemostats were continuously fed with TYG medium at a hydraulic retention time (HRT) of 13 h (unless stated otherwise). A N_2/CO_2 (80%/20%) gas mixture was constantly sparged into the working chamber to remove the potential oxygen flux from the feeding solution and to compensate for the pressure loss due to the difference of flow rates between influent and effluent. Cell density was obtained by measuring optical density of 100 µL aliquots of the culture at a wavelength of 600 nm (Synergy HT microplate reader; Bio-TEK Instruments Inc., Winooski, VT, USA).

Sample Collection and RNA Extraction

Planktonic cells were harvested during the exponential growth phase (optical density of 0.50 – 0.55 at 600 nm, 8 h after inoculation). A sample of the working chamber culture was collected in RNAprotect bacteria reagent (Qiagen Inc., Valencia, CA, USA) at a volumetric ratio of 1:2. After being centrifuged at 5000 × g for 30 min, the supernatant was decanted and the cells were stored at -80ºC prior to extraction of total RNA using an RNeasy kit (Qiagen).

Biofilm samples were collected after an 8-day operating period. During the last two days of the operating period, the HRT was shortened gradually until it was ~ 30 min. In this way, planktonic cells were largely removed by fast replacement of the medium. To minimize RNA degradation in the biofilm during sampling, the growth surface was immediately frozen in liquid nitrogen after its removal from the chemostat. The growth surface was cut into small pieces with sterile scissors and distributed into 2 mL centrifuge vials containing 500 µL of extraction buffer (200 mM Tris, pH 8.0 / 200 mM NaCl/ 20 mM EDTA), 210 µL of 20% SDS, 500 µL of phenol:chloroform:isoamyl alcohol (125:24:1, pH 4.5, Ambion, Foster City, CA, USA) and 150 µL of 0.1-mm silica beads. Biofilm and planktonic samples were mechanically disrupted with a mini-beadbeater (BioSpec Products Inc., Bartlesville, OK, USA) on instrument setting “high” for 5 min at room temperature. After centrifugation at 10,000 × g for 3 min, the supernatant was extracted once more with phenol:chloroform:isoamyl alcohol and RNA was precipitated by adding 60 µL of sodium acetate (3 M) and 600 µL of ethanol (-20ºC). The extracted RNA was stored in 100 µL of water at -80 ºC.

GeneChip Analysis

Total cellular RNA was purified using a Qiagen RNA Easy mini kit according to the manufacturer's directions. Following extraction of RNA, samples were treated with DNAse I (Ambion) and purified again with a Qiagen RNA Easy column. Due to the large initial

concentration of contaminating DNA, biofilm samples were subjected to an additional DNAse I treatment and purification. All samples were monitored for DNA contamination by PCR using primers specific for *B. thetaiotaomicron* genes. cDNA targets were prepared as previously described according to a standard Affymetrix protocol (Santa Clara, CA, USA) and applied to custom *B. thetaiotaomicron* GeneChips (Sonnenburg et al. 2005). These GeneChips contain probe pairs derived from 4719 of the 4779 predicted *B. thetaiotaomicron* genes. GeneChip data was processed using Microarray Suite 5 (Affymetrix). Each array was normalized to an arbitrary mean value of 500. The data generated for this study have been deposited in NCBI's Gene Expression Omnibus and are accessible through GEO Series accession number GSE38534 (http://www.ncbi.nlm.nih.gov/geo/query/acc.cgi?acc=GSE38534) (Edgar et al. 2002).

Statistical Analysis

Differential expression analysis was performed using the LEMMA package for R, with a false discovery rate of 0.05 (Bar et al. 2010). Expression values were normalized using the quantile normalization function in R prior to the differential expression analysis. Genes with a gene effect (base 2 logarithm of the fold expression change) less than 1 were not considered. Hierarchical clustering was also performed in R, using the dist function with the Euclidean method to calculate the distance matrix and the hclust function with the Ward method to generate the tree. Plots were drawn using the plotColoredClusters function in the ClassDiscovery package, which is part of the Object-Oriented Microarray and Proteomic Analysis (OOMPA) suite (http://bioinformatics.mdanderson.org/Software/OOMPA). GeneChip data for *B. thetaiotaomicron* grown under different conditions used in hierarchical clustering analyses was downloaded from the NCBI Gene Expression Omnibus (GEO) database. These datasets consisted of publicly available data collected from a variety of previous studies on *B.*

thetaiotaomicron grown under widely varying conditions. In general, all samples were grown either in standard culture flasks with minimal or standard rich media (e.g. TYG), or in mono-colonized gnotobiotic mice, and sampled at defined time points for RNA extraction. More details are given in **Table S5**, and more information about each study can be found by looking up the relevant GEO accession number at http://www.ncbi.nlm.nih.gov/geo/. All data were ranked prior to analysis to normalize between different experiments (Folsom et al. 2010). The significance of the enrichment of different gene groups in the differentially expressed genes was checked using the hypergeometric distribution using the dhyper function in R, and a p-value cutoff of 0.05. Machine learning to determine key genes in the clustering analysis was performed using the PAMr package for R, with a threshold value of 5.0 (Tibshirani et al. 2002).

Scanning Electron Microscopy

Small pieces of the carbon paper were fixed overnight in a solution containing 2% glutaraldehyde at 4ºC, followed by washing with deionized water for 10-20 min. Secondary fixation was conducted in 1% osmium tetroxide at 4ºC for 2 h. The carbon paper pieces were washed with deionized water for 10-20 min, dehydrated in a series of ethanol solutions (50, 70, 90, and 100%), and critical point dried in CO_2. The samples were coated with gold and viewed using a scanning electron microscope (Hitachi S-450, Hitachi Ltd., Tokyo, Japan). To examine biofilm formation during the exponential growth phase (at 8 h, when planktonic cells were harvested for RNA extraction), the growth surface was gently rinsed with sterile phosphate buffer to remove any adsorbed planktonic cells.

A4.5 Acknowledgements

This work was funded by the National Science Foundation (CAREER grant 0939882 to LTA) and the NIH (DK30292 to JIG).

A4.6 References

Ambort D, Johansson MEV, Gustafsson JK, Nilsson HE, Ermund A, Johansson BR, Koeck PJB, Hebert H, Hansson GC. 2012. Calcium and pH-dependent packing and release of the gel-forming MUC2 mucin. Proceedings of the National Academy of Sciences of the United States of America 109(15):5645-5650.

Ambort D, van der Post S, Johansson MEV, MacKenzie J, Thomsson E, Krengel U, Hansson GC. 2011. Function of the CysD domain of the gel-forming MUC2 mucin. Biochemical Journal 436:61-70.

Bar H, Booth J, Schifano E, Wells MT. 2010. Laplace Approximated EM Microarray Analysis: An empirical Bayes approach for comparative microarray experiments. Statistical Science 25(3):388-407.

Beloin C, Ghigo J-M. 2005. Finding gene-expression patterns in bacterial biofilms. Trends in Microbiology 13(1):16-19.

Benjdia A, Martens EC, Gordon JI, Berteau O. 2011. Sulfatases and a radical S-Adenosyl-l-methionine (AdoMet) enzyme are key for mucosal foraging and fitness of the prominent human gut symbiont, *Bacteroides thetaiotaomicron*. Journal of Biological Chemistry 286(29):25973-25982.

Blixt O, Head S, Mondala T, Scanlan C, Huflejt ME, Alvarez R, Bryan MC, Fazio F, Calarese D, Stevens J and others. 2004. Printed covalent glycan array for ligand profiling of diverse glycan binding proteins. Proceedings of the National Academy of Sciences of the United States of America 101(49):17033-17038.

Edgar R, Domrachev M, Lash AE. 2002. Gene Expression Omnibus: NCBI gene expression and hybridization array data repository. Nucleic Acids Research 30(1):207-210.

Folsom J, Richards L, Pitts B, Roe F, Ehrlich G, Parker A, Mazurie A, Stewart P. 2010. Physiology of *Pseudomonas aeruginosa* in biofilms as revealed by transcriptome analysis. BMC Microbiology 10(1):294.

Kitamura M, Okuyama M, Tanzawa F, Mori H, Kitago Y, Watanabe N, Kimura A, Tanaka I, Yao M. 2008. Structural and Functional Analysis of a Glycoside Hydrolase Family 97 Enzyme from Bacteroides thetaiotaomicron. Journal of Biological Chemistry 283(52):36328-36337.

Koropatkin N, Martens EC, Gordon JI, Smith TJ. 2009. Structure of a SusD Homologue, BT1043, Involved in Mucin O-Glycan Utilization in a Prominent Human Gut Symbiont. Biochemistry 48(7):1532-1542.

Koropatkin NM, Cameron EA, Martens EC. 2012. How glycan metabolism shapes the human gut microbiota. Nature Reviews Microbiology 10(5):323-335.

Koropatkin NM, Martens EC, Gordon JI, Smith TJ. 2008. Starch catabolism by a prominent human gut symbiont is directed by the recognition of amylose helices. Structure 16(7):1105-1115.

Koropatkin NM, Smith TJ. 2010. SusG: A unique cell-membrane-associated α-amylase from a prominent human gut symbiont targets complex starch molecules. Structure 18(2):200-215.

Lazazzera BA. 2005. Lessons from DNA microarray analysis: the gene expression profile of biofilms. Current Opinion in Microbiology 8(2):222-227.

Lindén SK, Florin THJ, McGuckin MA. 2008a. Mucin dynamics in intestinal bacterial infection. PLoS ONE 3(12):e3952.

Lindén SK, Sutton P, Karlsson NG, Korolik V, McGuckin MA. 2008b. Mucins in the mucosal barrier to infection. Mucosal Immunology 1(3):183-197.

Macfarlane S, Dillon JF. 2007. Microbial biofilms in the human gastrointestinal tract. Journal of Applied Microbiology 102(5):1187-1196.

Macfarlane S, Macfarlane GT. 2006. Composition and metabolic activities of bacterial biofilms colonizing food residues in the human gut. Applied and Environmental Microbiology 72(9):6204-6211.

Macfarlane S, Woodmansey EJ, Macfarlane GT. 2005. Colonization of mucin by human intestinal bacteria and establishment of biofilm communities in a two-stage continuous culture system. Applied and Environmental Microbiology 71(11):7483-7492.

Martens EC, Chiang HC, Gordon JI. 2008. Mucosal glycan foraging enhances fitness and transmission of a saccharolytic human gut bacterial symbiont. Cell Host & Microbe 4(5):447-457.
Martens EC, Lowe EC, Chiang H, Pudlo NA, Wu M, McNulty NP, Abbott DW, Henrissat B, Gilbert HJ, Bolam DN and others. 2011. Recognition and degradation of plant cell wall polysaccharides by two human gut symbionts. PLoS Biology 9(12):e1001221.
Martens EC, Roth R, Heuser JE, Gordon JI. 2009. Coordinate regulation of glycan degradation and polysaccharide capsule biosynthesis by a prominent human gut symbiont. Journal of Biological Chemistry 284(27):18445-18457.
Marzorati M, Van den Abbeele P, Possemiers S, Benner J, Verstraete W, Van de Wiele T. 2011. Studying the host-microbiota interaction in the human gastrointestinal tract: basic concepts and *in vitro* approaches. Annals of Microbiology 61(4):709-715.
McGuckin MA, Lindén SK, Sutton P, Florin TH. 2011. Mucin dynamics and enteric pathogens. Nature Reviews Microbiology 9(4):265-278.
Padler-Karavani V, Song XZ, Yu H, Hurtado-Ziola N, Huang SS, Muthana S, Chokhawala HA, Cheng JS, Verhagen A, Langereis MA and others. 2012. Cross-comparison of protein recognition of sialic acid diversity on two novel sialoglycan microarrays. Journal of Biological Chemistry 287(27):22593-22608.
Reeves AR, D'Elia JN, Frias J, Salyers AA. 1996. A *Bacteroides thetaiotaomicron* outer membrane protein that is essential for utilization of maltooligosaccharides and starch. Journal of Bacteriology 178(3):823-30.
Reeves AR, Wang GR, Salyers AA. 1997. Characterization of four outer membrane proteins that play a role in utilization of starch by *Bacteroides thetaiotaomicron*. Journal of Bacteriology 179(3):643-9.
Shipman JA, Berleman JE, Salyers AA. 2000. Characterization of four outer membrane proteins involved in binding starch to the cell surface of *Bacteroides thetaiotaomicron*. Journal of Bacteriology 182(19):5365-5372.
Sonnenburg ED, Zheng H, Joglekar P, Higginbottom SK, Firbank SJ, Bolam DN, Sonnenburg JL. 2010. Specificity of polysaccharide use in intestinal bacteroides species determines diet-induced microbiota alterations. Cell 141(7):1241-1252.
Sonnenburg JL, Xu J, Leipi DD, Chen C-H, Westover BP, Weatherford J, Buhler JD, Gordon JI. 2005. Glycan foraging *in vivo* by an intestine-adapted bacterial symbiont. Science 307(5717):1955-9.
Stevens J, Blixt O, Glaser L, Taubenberger JK, Palese P, Paulson JC, Wilson IA. 2006. Glycan microarray analysis of the hemagglutinins from modern and pandemic influenza viruses reveals different receptor specificities. Journal of Molecular Biology 355(5):1143-1155.
Tibshirani R, Hastie T, Narasimhan B, Chu G. 2002. Diagnosis of multiple cancer types by shrunken centroids of gene expression. Proceedings of the National Academy of Sciences of the United States of America 99(10):6567-6572.

APPENDIX 5

PROTOCOLS

A5.1. Preparation of working electrodes for electrochemical tests

Materials:
graphite rods (fine, <0.5 cm diameter, >10 cm length)
carbon cloth (PANEX ® 30 - PW06, Zoltek Corp) or graphite paper(AvCarb 250, FuelCellStore)
carbon cement (Leit-C, conductive carbon cement, Electron microscopy sciences)
pipette tips of 1 mL pipettor, nonsterile

Procedure:

To prepare cloth electrodes:

1. Clean the graphite rods thoroughly and sand off a thin layer with sand paper. Rinse and dry.
2. Cut carbon cloth into 9 cm x 9 cm squares.
3. IN A FUME HOOD: dip the end of the graphite rod (~1 cm) in carbon cement and affix 2 corners of the carbon cloth to the cemented area using a small cable tie.
4. Apply additional carbon cement above the cable tie (using the pipette tip to scrape it on) and affix the other two corners using another cable tie.
5. Leave the electrode in the fume hood for a minimum of 2 hours to allow the carbon cement to dry (the xylene solvent is harmful if inhaled).
6. Remove the dry electrode from the fume hood and cut off excess ends of the cable ties.
7. Test the resistance from the end of the graphite rod to one edge of the carbon cloth using a multimeter. The reading should be stable and <3 Ω.

To prepare paper electrodes:

1. Clean the graphite rods thoroughly and sand off a thin layer with sand paper. Rinse and dry.
2. Use the graphite saw to cut a slit in one end of the graphite rod, centered and ~1 cm deep.
3. Cut graphite paper to desired size (8 cm x 3 cm).
4. IN A FUME HOOD: insert the paper into the slit in the carbon rod. Coat the connection in carbon cement on both sides, using a pipette tip.
5. Lay the electrode horizontally to dry for at least 2 hours.
6. Remove from the fume hood, and check resistance as above.

A5.2. Preparation of Ag/AgCl/sat'd KCl reference electrodes for electrochemical tests

Materials:
glass reference electrode bodies with magnesia frits (made by Dave Wise, Cornell glassblower)
silver (Ag^0) wire
rubber stopper (proper size to fit tightly in glass body)
DI water
potassium chloride (KCl)
bacteriological agar
hotplate/stirrer
magnetic stirbar
10 mL syringe with long needle
parafilm

Procedure:

For 3-6 reference electrodes:

1. Add 50 mL of DI water, 0.75 g of agar, and a sitrbar to a small beaker.
2. Heat with stirring on the hotplate, and gently boil until all agar has melted.
3. In the meantime, cut a ~ 3 cm piece of silver wire and insert through the center of the rubber stopper so that most of it will hang inside the body of the electrode and a small piece sticks out for connection to the potentiostat.
4. Oxidize the silver wire using the Prep_RE program on the potentiostat (VSP). The silver wire should be the working electrode, a graphite rode the counter electrode, and another Ag/AgCL reference electrode the reference electrode. Place all electrodes in a dilute KCl solution in DI water and run the program.
5. After the agar has melted, add KCl to the solution until it is saturated (continue heating and stirring), and excess KCl sits on the bottom of the beaker.
6. Pour agar/KCl solution into the glass body until it is half full. Remove bubbles from the thin area using the syringe to aspirate/detach bubbles. Fill the body the rest of the way.
7. Cap the body with the rubber stopper containing the oxidized silver wire. Thoroughly clean the junction between the glass and the stopper with DI water, and cover with a strip of parafilm to prevent evaporation.

Note: if a reference electrode is not available for oxidizing silver wires, one wire may be oxidized by soaking in a 10% bleach solution for 10 minutes.

Note 2: If the reference electrode will be in the reactor, the reference electrode must be poured after autoclaving, because the agar will re-melt in the autoclave.

A5.3. HPLC analysis for lactate, acetate, and pyruvate

Materials:
1 mL HPLC vials, compatible with Waters autosampler
Waters HPLC (600 Controller, 717plus autosampler with 100 sample carousel, 410 refractive index detector)
Aminex HPX-87H column
5 mM sulfuric acid (HPLC grade) in Milli-Q water

Procedure:

1. Turn on autosampler and detector. Wait for them to initialize.
2. Turn on controller.
3. Set sparging to 100 (make sure Helium is on and bubbling).
4. Set oven temp to 65^{o}C.
5. Turn on temp control in autosampler, set to 4^{o}C (2nd config page).
6. Turn on computer if not already on.
7. Open Peak385-32bit and load control file 302CON.
8. Allow Helium sparging for 30 minutes.
9. During setup load samples into carousel and note their order. Load carousel into autosampler.
10. Turn sparging down to 20.
11. Clear bubbles from the pumps by opening the silver valve and flushing at 1 mL/min for 10 minutes. Lower flow to 0.1 and close valve.
12. Slowly ramp the flow rate up to 0.6 using the direct control screen.
13. When pressure is stable continue.
14. Check settings in program table. Settings should be 0.6 mL/min, 100% A
15. Program method- Enter the correct vial range, 30 uL injection volume, and 25 minutes for the run.
16. In Peak simple, click the 1234 button and click postrun for channel 4. Set up file saving scheme. Check details and make sure the run ends at 23 min.
17. On the controller push operate method, wait for initialization and press start run.
18. Watch a run or two and make sure it's working properly.

A5.4. RNA sample preparation from S. oneidensis on graphite paper electrodes

Materials:

MoBio PowerBiofilm RNA extraction kit
sterile petri dishes
RNAprotect Bacterial Reagent
sterile razor blades
sterile tweezers
sterile, 10 mL serological pipette
pipette bulb
sterile 15 mL plastic test tubes (Falcon tubes)

Procedure:

1. Place 5 mL of RNAprotect in a sterile petri dish for each electrode to be processed.
2. In a biosafety cabinet, and as quickly as possible, remove the electrode from the bioreactor and place immediately into the petri dish, ensuring that it becomes covered in RNAprotect.
3. Separate the paper from the graphite rod by twisting the rod back and forth to break the paper at the junction.
4. Close the petri dish and seal with tape. Store the plates with the electrodes at -80^{o}C until extraction.
5. Thaw the electrodes.
6. Slice the graphite paper into thin strips and transfer them to a sterile tube. Transfer all RNAprotect solution to the same tube.
7. Use a serological pipette to crush the graphite paper as thoroughly as possible. Use a pipette bulb to push solids and solution out of the pipette periodically.
8. Close the tube and vortex at maximum speed for ~30 s.
9. Centrifuge the tube at 7,000 x g for 10 min, and remove the RNAprotect solution.
10. Use the entire pellet as the starting material for the PowerBiofilm RNA extraction kit. Follow the manufacturer's instructions, and elute RNA in 50 µL of RNAse-free water.
11. Aliquot the RNA in PCR tubes, in 8 µL volumes and store at -80^{o}C.

A5.5. DNAse treatment of RNA samples

Materials:
RNAse-free DNAse I (Ambion)
10X DNAse buffer (Ambion)
RNAse-free PCR tubes
0.5 M RNAse-free EDTA
RNAse-free water
RNA samples

Procedure:
1. Combine the following in a PCR tube:
    a. 22 µL of RNA sample
    b. 2.5 µL 10X buffer
    c. 0.5 µL DNAse I
2. Mix well by pipetting up and down.
3. Incubate at 37^{o}C for 30 min in a thermal cycler.
4. Add 0.25 µL of EDTA solution to each tube. Mix well by pipetting up and down.
5. Incubate at 75^{o}C for 10 min in a thermal cycler.
6. Check for DNA contamination using a standard PCR protocol that would amplify residual DNA in the sample. If bands are visible on an agarose gel, there is still DNA contamination in the sample.
7. If DNA remains, dilute the treated sample 1:5 in RNAse-free water and repeat steps 1-6.

A5.6. qRT-PCR analysis with Invitrogen SuperScript 1-step SYBR green kit w/ ROX

Materials:

Invitrogen SuperScript 1-step SYBR green kit w/ ROX
Applied Biosystems MicroAmp Optical 96 well plate
Applied Biosystems MicroAmp Optical Sealing Film
RNAse-free water
PCR-clean, RNAse-free, sterile pipette tips w/ filters (1 mL, 200 µL, and 10 µL sizes)
RNAseZAP
RNA samples

Procedure:

1. Turn on blower in the laminar flow hood, and clean all surfaces and pipettor barrels with 70% ethanol. Let dry.
2. Wipe work surface and pipettor barrels with RNAseZAP, wipe again with a small amount of DI water.
3. Place all RNA samples on ice to thaw while preparing mastermix.
4. Prepare mastermix as follows (for 60, 25 µL reactions)
    a. 750 µL 2X reaction mix
    b. 600 µL RNAse free water
    c. 30 µL forward primer (10 µM stock)
    d. 30 µL reverse primer (10 µM stock)
    e. 30 µL RT/Taq enzyme mix
5. Place a MicroAmp plate on a 96-well ice rack and distribute 24 µL of mastermix into each of 60 wells.
6. Distribute 1 µL of the correct template or control into each well.
7. Seal with MicroAmp Optical film. Use the sealing tool to ensure that each well is sealed.
8. Centrifuge the plate for a short time to ensure that all liquid is at the bottom of the wells. Load the plate into the RT-PCR instrument.
9. Run the PCR and collect data using an ABI 7000 RT-PCR system using the following cycling conditions:
    a. 50^{o}C for 3 min (cDNA synthesis)
    b. 95^{o}C for 5 min
    c. 40 cycles of:
        i. 95^{o}C for 15 s
        ii. 60^{o}C for 30 s
    d. 40^{o}C for 1 minute
    e. "Add dissociation step" using the instrument software
10. Ensure that the reaction volume is set at 25 µL, and data collection occurs during the 60^{o}C step.
11. Save the SDS file and press Start.
12. After the run has finished, use the software to pick a C_t threshold, and export the C_t value for each well.

A5.7. Generation of in-frame deletion mutants of S. oneidensis MR-1

Follow the detailed protocol for generating knockouts in *S. oneidensis* MR-1, found at the following link:

https://www.google.com/url?sa=t&rct=j&q=&esrc=s&source=web&cd=1&ved=0CC8QFjAA&url=http%3A%2F%2Fwww.protocol-online.org%2Fforums%2Findex.php%3Fapp%3Dcore%26module%3Dattach%26section%3Dattach%26attach_id%3D4552&ei=l1j5UZPWLOqg4APz_oDQCg&usg=AFQjCNFGpIednlCQoGV9374hyIWI1iyNQA&sig2=icBFMLRD3E_fmhMjtvYfYQ&bvm=bv.49967636,d.dmg

The following modifications should be made to the protocol:

1. Use pDS3.0 instead of pDS3.1 if the insert does not contain internal *SmaI* restriction sites.
2. pDS3.0 can be transformed directly into *E. coli* WM3064 by electroporation.
3. Conjugation can be performed without the conjugation step.
    a. Grow overnight cultures of the *E. coli* donor strain and *S. oneidensis* recipient at appropriate conditions.
    b. Use a centrifuge to pellet 250 µL of the *E. coli* culture. Wash with 500 µL LB, pellet again, and resuspend in 150 µL of the *S. oneidensis* culture.
    c. Pipette the resuspension onto an LB agar plate with 300 µM DAP (do not spread). Allow to dry in a sterile environment, and incubate at 30^{o}C for 8 hours.
    d. Scrape a large amount of cells from this plate and restreak for single colonies onto an LB plate with the appropriate antibiotic and without DAP.
    e. Incubate overnight at 30^{o}C and confirm conjugation of resulting *S. oneidensis* colonies by PCR screening and/or sequencing.

A5.8. Preparation of electrocompetent Escherichia coli WM3064

Materials:
Escherichia coli WM3064
diaminopimelic acid (DAP)
lysogeny broth (LB)

Procedure:
Day1:
1. Grow an overnight culture in 20 mL LB + 300 µM DAP in a 250ml flask at 37°C with shaking.
3. Autoclave at least 100 mL of 10% glycerol and store at 4°C.
Day 2:
1. Inoculate 500 mL of fresh LB medium in a 1 L flask with 2.5 mL of fresh overnight culture and
grow cells at 37°C, shaking at 200 rpm. Grow culture to an OD600 of 0.15.
2. When cells reach desired OD600, place flasks on ice. Incubate cells on ice for at least one hour. In the meantime, turn the centrifuge on so that it will be cold (4°C) when spinning down the cells, and chill ten 50 mL centrifuge tubes on ice (per 500 mL subculture volume) along with 15-20 eppendorf tubes for final 50 µL aliquots of competent cells.
3. Transfer entire volume of subculture to chilled 50 mL centrifuge tubes, and centrifuge @ 3200rpm
for 20 min at 4°C.
4. Decant about 3/4 of the supernatant from each tube. Remove the rest of the supernatant using a
pipette, being careful not to suck up the cells.
5. Gently resuspend the pellets in 1 mL of cold, sterile 10% glycerol (per 50 mL of original subculture) and pool the entire volume of resuspended cells into a single 50 mL centrifuge tube.
6. Add more 10% glycerol. Use 15 mL of 10% glycerol per 500 mL cell culture. Centrifuge at 3200
rpm for 15 min at 4°C.
7. Perform two additional washes with 15 mL 10% glycerol.
8. Remove the supernatant from the final wash.
9. Mix up and down gently to resuspend pellet in 750 µL cold 10% glycerol.
10. Transfer 50 µL aliquots of cells into the chilled tubes and store at -80°C.

A5.9. Electroporation of E. coli *WM3064*

Materials:
electrocompetent *E. coli* WM3064
electroporation cuvette (1 mm gap)
Super Optimal Broth with Catabolite Repression (SOC)
diaminopimelic acid (DAP)
lysogeny broth (LB) and LB agar plates (1.5% agar)
BioRad electroporator

Procedure:
1. Thaw an electroporation stock of WM3064 on ice.
2. Add 2 µL of purified plasmid to the bacteria.
3. Transfer bacteria to electroporation cuvette, on ice.
4. Place cuvette in the holder of the electroporator and ZAP! 1.8 kV, 200 Ω, 25 µF.
5. Add 900 µL SOC+DAP (300 µM) to the cuvette, mix, transfer to sterile microcentrifuge tube.
6. Recover at 37°C for 1.5 hours.
7. Pellet the cells and resuspend in a small volume of supernatant. Plate entire volume on an LB agar plate with the appropriate antibiotic and 300 µM DAP.
8. Grow overnight at 37°C.
9. PCR screen and sequence resulting colonies to check for correct insert.